Authors’ Response to ACP MS No.: acp-2019-669

We thank the reviewer for their comments and suggestions. In the text below, we outline our responses in blue. Line numbers refer to the revised manuscript.

Anonymous Referee #1

Winton et al report observations of the nitrogen isotopic composition of nitrate in Antarctic (DML) in the atmosphere, snow “skin layer”, and depth profiles in snow pits. They use these observations combined with a snow chemistry model to understand what controls the variability in the nitrogen isotopes and nitrate concentrations and to assess the utility of such observations in ice cores as a proxy for past surface UV radiation. They conclude that although photolytic driven recycling and loss of reactive nitrogen is what determines the nitrate isotopes and abundances at this location, that variability in parameters such as snow accumulation rate have a large enough impact on the nitrogen isotopes so as to preclude the influence of variability in surface UV in determining the nitrogen isotopic composition of snow nitrate.

We agree that variability in the snow accumulation rate precludes the use of using the $\delta^{15}N$-NO_3^- composition as a surface UV proxy in the short-term. However, longer-term UV trends may be inferred from ice cores at the site taking into account or constraining factors masking the UV-impact such as e-folding depth and accumulation rate.

The observations and model-based interpretation are robust and important as it would be useful to have a paleo-UV proxy. As the authors state, it is important to assess the sensitivity of nitrogen isotopes at particular locations in order to determine its usefulness as a proxy for any given process. Unfortunately, the paper is frustrating to read because it is it so repetitive and spends so much time on introductory material throughout the manuscript that it is hard to find the actual interpretation of the results. It is as if the authors are afraid to state their interpretation. I suggest moving (and condensing) the introductory material that is spread throughout the manuscript (especially in section 4) to the introduction and making sure that the actual interpretation is presented up front instead of hidden. Because of this, it’s sometimes hard to determine if the results support their conclusions. The paper as is reads as a first or second draft, not a final manuscript ready for submission for publication. This is particularly evident in the conclusions, which is not even written in paragraph form.

We agree with the reviewer that too much background information is spread throughout the discussion rather than the introduction. We have condensed and moved the most relevant material to the introduction. Overall, we have revised the manuscript to provide better clarity on our interpretation of the results and conclusions.

Additional comments:

I find the concept of the number of times nitrate is recycled difficult to wrap my head around. Does this mean that each molecule of nitrate is recycled on average three times before being archived? Is this averaged over the depth of the photic zone? I would imagine some molecules (like those that are close to the surface in summer) are recycled more than others, so that there is actually some distribution of recycling events on a molecule per molecule basis so as to average around the number 3. Is this interpretation correct? I suggest elaborating on this in the methods section.

The number of recylings is the “average number of recyclings” undergone by the archived nitrate, i.e., below the zone of active photochemistry. Recycling includes the following processes: the combination of NOx production from nitrate photolysis in snow, venting to the air above the snowpack and subsequent atmospheric re-oxidation of NO_x to form atmospheric nitrate, the deposition (dry and/or wet) of a fraction of the product, and the export of another fraction (Erbland et al., 2015). In TRANSITS, there is a tracer/counter called CYCL, which, in a given box (snow layer or atmosphere), represents the average number of recyclings undergone by nitrate in that box. The CYCL value for primary nitrate is set to 0, and CYCL variables in the boxes are incremented by 1 each time NO_2 molecules cross the air-snow interface. The average number of recyclings is calculated as a mass weighted average of the CYCL values of the 52 snow layers (representing one week of snowfall) which are archived below 1 m over the course of 1 year, in order to average out any seasonal variability.

The average number of recyclings undergone by the archived nitrate at our study site in Dronning Maud Land (DML) is 2 for the last layer before leaving the photic zone, which means that, on average, the archived nitrate at DML has undergone 2 recyclings (i.e., loss, local re-oxidation, deposition). Erbland et al. (2015) notes that this number of recyclings represents an average value for the archived nitrate. Considering individual ions in the archived nitrate, the number of recyclings could be variable as some ions may have travelled through the entire snowpack zone of active photochemistry without being recycled, while some underwent many recyclings.

We have expanded the explanation of the number of recycling’s in the methodology (lines 337-345) as follows:

Modified text: “TRANSITS calculates the average number of recyclings undergone by the archived NO_3^-, i.e., below the zone of active photochemistry. In TRANSITS, the average number of recyclings undergone by NO_3^- in a given box (snow layer or atmosphere) is represented by a tracer (or counter) called CYCL. The CYCL value for primary NO_3^- is set to 0, and CYCL variables in the boxes are incremented by 1 each time NO_2 molecules cross the air-snow interface. The average number of recyclings is calculated as a mass weighted average of the CYCL values of the 52 snow layers (representing one week of snowfall) which are archived below 1 m over the course of 1 year, in order to average out any seasonal variability. Erbland et al. (2015) notes that the number of recyclings represents an average value for the archived NO_3^-, i.e., considering individual ions in the archived NO_3^-, the number of recyclings could be variable as some ions may have travelled through the entire snowpack zone of active photochemistry without being recycled, while some underwent many recyclings.”

Second paragraph of the introduction: It seems strange to say that the primary sources of nitrate are transport of nitrate from the stratosphere and transport of alkyl nitrates in the troposphere without mentioning transport of inorganic nitrate in the troposphere. Where is the evidence that inorganic nitrate is not transported in the troposphere to Antarctica? A model study suggests that it is certainly possible (Lee et al., 2014). Also, soil NOx should be mentioned as a NOx source in the troposphere.

We have added the transport of inorganic nitrate (fossil fuel combustion, soil, and lightning) and referenced Lee et al. (2014) in lines 53-56 as follows:

Modified text: "Primary sources of reactive nitrogen species to the Antarctic lower atmosphere and snow pack include the sedimentation of polar stratospheric clouds (PSC) in late winter (Savarino et al., 2007) and, to a minor extent, advection of oceanic methyl nitrate (CH_3NO_3) and peroxyacyl nitrates (PAN) (Jacobi et al., 2000;Jones et al., 1999;Beyersdorf et al., 2010), in addition to tropospheric transport of inorganic NO_3^- from lightning, biomass burning and soil emissions (Lee et al., 2014)."

Page 2 lines 61 – 62: Reprase to: "Model results from Zatko et al. (2016) suggest that…"

Done

Page 4 line 116: Are you referring to skin layer nitrate here? Since you are measuring nitrate in three different locations, you should always be specific about which location you are talking about and not just say "nitrate".

No, we are referring to ice core nitrate as mentioned in the sentence. We have added "ice core nitrate" for clarity.

Page 4 line 128: Perhaps you should say that you are referring to the e-folding depth of the snow photic zone, UV radiation, or something less vague.

Done

Page 5 line 157: If you remove the word "While" from the beginning of this sentence it will be grammatically correct.

Done

Page 8 line 259: By "lower" do you mean "shallower"? Lower could also mean deeper, so it would be better to use words like deeper and shallower when referring to the depth in the snow beneath the surface.

"Lower" has been replaced with "shallower".

Section 2.7: It seems quite important to state what value you assume for the N-isotopic composition of primary nitrate, before it is impacted by photolysis.

The $\delta^{15}N-NO_3^-$ value of primary nitrate is set to 19 ‰ as estimated by Savarino et al. (2007). This value is reported in Table S3.

Page 12 line 371: "values" of what? Concentration? Isotopes? Both? Since you measured more than one thing you need to be specific.

We have added $\delta^{15}N-NO_3^-$ values to this sentence.

Page 13 Section 3.5: You should probably note that gas phase HNO3 and particulate nitrate have different dry deposition rates.

Agreed, we have noted this in lines 418-419 as follows:

Modified text: "Although gas phase HNO_3 and particulate NO_3^- have different dry deposition rates…"

Section 3.6: I think you should elaborate on the difference between the actual (from photolysis) and apparent fraction factor. The latter is lower than the actual due to recycling. Also, related to this, can the difference between the actual and apparent fractionation factor be used to calculate fractional loss?

We have discussed the difference in lines 88-91. We found that the single loss Raleigh model does not work well at sites with an annual signal in $\delta^{15}N-NO_3^-$, and therefore suggest that at DML it is not useful for calculating fractional loss. The text was modified as follows:

Modified text: "As this approach may oversimplify the processes occurring at the air-snow interface, Erbland et al. (2013) referred to the quantity as an "apparent" fractionation constant ($^{15}\varepsilon_{app}$). Thus, the apparent fractionation constant represents the integrated isotopic effect of the processes involving NO_3^- in the surface of the snow pack and in the lower atmosphere."

Page 15 line 455: Is this at DML?

Yes, the Weller et al. (2004) study is at DML. We have added "at DML" for clarity.

Page 15 line 459: Which results? Concentration? Isotopes? Both?

Both. We have added "NO_3^- mass concentrations and $\delta^{15}N-NO_3^-$" to the sentence.

Page 15 lines 472 – 473: Does the model simulate the influence of hoar frost and diamond dust on nitrate deposition? The way this sentence is written it seems that it does, but this is surprising to me as I didn't think the model was a meteorological/snow model that calculated such things. It seems that you are saying that diamond dust and hoar frost explain the difference between the model and the observations, and that the model has these things but they didn't happen in reality.

No, the model does not simulate the influence of hoar frost and diamond dust on nitrate deposition. We suggest that the difference between the simulated and observed nitrate concentrations in the skin layer is due to a sampling artefact where we are diluting the high nitrate concentrations of diamond dust and hoar frost observed in new deposition. We have modified the sentence in lines 564-566 as follows:

Modified text: "Here, extremely high concentrations of NO_3^- from new deposition from diamond dust and hoar frost are also found. In summary, it is likely that we do not measure such high NO_3^- mass concentrations in hoar frost and diamond dust in the skin layer because of sampling artefacts or blowing snow, which can dilute or remove the diamond dust and hoar frost."

Section 4.2: This is a perfect example of the section 4 having lots of introductory material without any results. The entire first paragraph reads like an introduction except for the very last sentence. However, the very last sentence of the first paragraph is not specifically supported by your observations. By the time I finished the 5 pages of section 4.2, I have no idea what you learned or what you are concluding from your new observations.

Section 4.2 has been condensed to 2 pages and the interpretation of results clarified.

Section 4.1: Again, I have no idea what you are concluding in this section.

We conclude that overall our nitrate conclusion measurements agree well with the literature and that the simulated results from TRANISTS match our observations with the exception of the skin layer concentrations. We provide possible reasons for this difference, and have modified Section 4.1 for clarity.

Page 17 line 540: “is no exception” to what?

We have deleted “is no exception”.

Page 18 lines 547 – 551: It seems that if you are collecting both gas and particulate phase nitrate that you cannot conclude that sea salt promotes conversion of HNO3 to nitrate. I’m sure that it does, however, I don’t see how your observations provide evidence of this.

We agree and have removed this section.

Page 18 lines 558-559: I suggest rephrasing this as “…Dome C where the underlying snowpack is the dominant… skin layer via photolytic recycling and redeposition.

Done

First paragraph of section 4.3: Need a reference for this statement.

Section of text has been removed.

Page 20 line 617: It could also be transported away as nitrate, not just NO2.

We have added nitrate to the sentence.

Page 21 line 648: “The contribution to what? of natural sources”

The “contribution of nitrate from natural sources” has been added to the sentence.

Page 21 lines 659-660: If you say that denitrification causes O-isotopes to increase, then you need cite a paper that provides evidence of this. However, I would delete this sentence since this paper does not address O-isotopes.

Agreed, we have delete the sentence.

Page 22 line 690: How was the apparent fractionation factor calculate? There should be an equation for this in the methods section.

Please see equation 7 in the methods in section 3.6.

Page 22 line 706: are these FNO2 values a daily mean, a daily maximum?

The model estimates are mean values for the 1-14 January 2017 period as stated in line 465.

Page 24 lines 742 – 746: What is the difference between the grain size and impurity concentrations at these two locations? The N-isotopes may be sensitive to something, but if that something shows no significant difference between these two locations than it won’t be able to explain the differences in Nisotopes.

As far as we are aware, at Dome C and DML, there are only published values of major ions in the snow pack in the top 30 cm which is the depth relevant for influencing the e-folding depth. For example, in the top 30 cm of the snow pack nitrate concentrations at Dome C are ~75 ppb (Frey et al., 2009) while they are ~55 ppb at DML (this study). Insoluble dust concentrations are higher at DML than Dome C in the Holocene (Delmonte et al., 2019), while no black carbon data is available at DML for comparison. There is considerate variability in the snow grain size across Antarctica (Brucker et al., 2010). In particular, wind crust layers which occur in the snowpack have larger grain sizes and these have been observed at Dome C (France et al., 2011).

Based on the available data, we don't have a clear understanding of why the e-folding depth is lower at DML. Station pollution is less than at Dome C (Helmig et al., 2020), thus it is unlikely related to black carbon. However, other impurities are deposited in DML snow due to the closer proximity to marine sources. Snow grain sizes may be smaller, which will increase scattering, at DML than Dome C (Brucker et al., 2010). The larger e-folding depth at Dome C is in part due the presence of windcrust layers which comprise larger grain sizes. Sensitivity studies show that nitrate impurities have only a small contribution on the e-folding depth compared to scattering by snow grains which dominate (Chan et al., 2015;France et al., 2011;Zatko et al., 2013). Further work is required to determine why the e-folding depth is lower at DML. We have discussed this in lines 692-700 as follows:

Modified text: "The e-folding depth depends on the density and grain size of snow crystals, and the concentration of impurities. In terms of published values, impurity concentrations are generally higher at DML, for example dust and major ion concentrations (Delmonte et al., 2019;Legrand and Delmas, 1988), due to proximity to marine sources. Yet station pollution is greater at Dome C (Helmig et al., 2020), and thus the lower e-folding depth is unrelated to black carbon concentrations. Furthermore, there is considerate variability in snow grain size across Antarctica. The larger e-folding depth in windcrust layers at Dome C is due to larger grain sizes in those layers (France et al., 2011). Snow grain size may be smaller at DML, which will increase scattering (Brucker et al., 2010), but further work is required to confirm if this is the dominate factor influencing the lower e-folding depth at DML. Sensitivity studies show that NO_3^- impurities make a small contribution to the e-folding depth compared to scattering by snow grains which dominate (France et al., 2011;Chan et al., 2015;Zatko et al., 2013)."

Page 25 lines 786-787: The e-folding depth is 20 years yet the nitrate is archived after 5-6 years. This seems conflicting. Why is nitrate archived when it is still in the photic zone?

Weller et al. (2004) determine archived nitrate as the typical mean concentrations representative for the last 100 years. We have deleted the e-folding time of 20 years from sentence.

Page 25 lines 792 and 796: Are you referring to observed or modeled values here?

Observed values. We have added "observed" sentence.

Page 25 line 807: Snow optical properties are part of what determines the depth of the photic zone, so it seems weird to mention these two things separately here as if they aren't related.

We have deleted snow optical properties.

Page 26 Line 821: "lower" than what?

Lower than the base case profile. We have added "base case" to the sentence.

Page 28, last sentence of section 4.5.3: Explicitly state here why the sensitivity is greater at Dome C than at DML.

Done

Page 28 line 899: What would cause a change in the e-folding depth?

The e-folding depth could change due to a change in dust or black carbon concentrations (which are light absorbing impurities) or a change in the snow morphology in a particular snow layer. This has been added to lines 843-844 as follows:

Modified text: “The e-folding depth could change over time due to higher or lower dust or black carbon concentrations or a change in the snow grain size in a particular snow layer.”

Page 29 line 919: What does “unpicking” mean in this context? Perhaps choose a better word.

Unpicking been replaced with disentangling.

Page 29 line 931: This is percent. Should it be permil?

Yes, percent symbols have been changed to permil symbols.

Figure 1 caption: State the difference between HiVol 2 and 3.

Done.

Figure 2: The boxes in this figure are totally unclear to me. What are the gray boxes trying to convey?

The box a) is in insert of the Kohnen Station and boxes b) and c) our inserts of our two sampling sites at the station. We have edited the caption to make this clearer.

Figure 4: Mark the seasons (e.g., shade winter) in c) and f). It’s hard to see the seasonal cycles.

We have shaded the seasons in panel c) and updated the caption. The snow pit in Frey et al. (2009) was not dated and thus we cannot shade the seasons for Dome C.

Figure 4: Why does the x-axis scales to all the way to 1500 and 300 when the observations are much lower than this? The axes should be scaled by the range of the data.

We deliberately chose to keep the x-axis the same for each plot rather than scaling by the range of the data. This is so the reader can see the difference in concentration and isotopic values between the atmosphere, skin layer and snowpack profiles and between the two sites. In particular, we wanted to highlight the denitrification of the snowpack from enriched values in the snow pits to depleted values in the atmosphere.

Figure 5: Why is “recycling factor” listed as a process occurring below the snow photic zone? How is “tropospheric input” different from “net lateral advection”?

We have moved recycling to encompass the atmosphere and snow boxes. We have renamed net lateral advection to tropospheric input.

Figure 7: Why are these values for accumulation rates chosen as sensitivity studies in the model? What is the base case that you are changing each parameter around?

The justification for the range of accumulation rates used in the sensitivity study can be found in section 4.5.1.

The base case is explained in section 4.5 and in the caption, we refer the reader to that section.

Figure 8: This is showing the change in TCO around what value?

We used present day TCO values that were used in all our calculations. These values vary weekly and can be found the supplement (Table S3). For each week, a constant amount of ozone (e.g. 100 DU) was added or subtracted from these values. We have added this information to the caption and text in lines 816-817 as follows:

Modified text: “For each week, a constant amount of ozone (e.g. 100 DU) was added or subtracted from these present day values.”

References

Brucker, L., Picard, G., and Fily, M.: Snow grain-size profiles deduced from microwave snow emissivities in Antarctica, Journal of Glaciology, 56, 514-526, 2010.

Chan, H., King, M., and Frey, M.: The impact of parameterising light penetration into snow on the photochemical production of NOx and OH radicals in snow, Atmos. Chem. Phys, 15, 7913-7927, 2015.

Delmonte, B., Winton, H., Baroni, M., Baccolo, G., Hansson, M., Andersson, P., Baroni, C., Salvatore, M. C., Lanci, L., and Maggi, V.: Holocene dust in East Antarctica: Provenance and variability in time and space, The Holocene, 0959683619875188, 2019.

Erbland, J., Savarino, J., Morin, S., France, J., Frey, M., and King, M.: Air–snow transfer of nitrate on the East Antarctic Plateau–Part 2: An isotopic model for the interpretation of deep ice-core records, Atmospheric Chemistry and Physics, 15, 12079-12113, 2015.

France, J., King, M., Frey, M., Erbland, J., Picard, G., Preunkert, S., MacArthur, A., and Savarino, J.: Snow optical properties at Dome C (Concordia), Antarctica; implications for snow emissions and snow chemistry of reactive nitrogen, Atmospheric Chemistry and Physics, 11, 9787-9801, 2011.

Frey, M. M., Savarino, J., Morin, S., Erbland, J., and Martins, J.: Photolysis imprint in the nitrate stable isotope signal in snow and atmosphere of East Antarctica and implications for reactive nitrogen cycling, Atmospheric Chemistry and Physics, 9, 8681-8696, 2009.

Helmig, D., Liptzin, D., Hueber, J., and Savarino, J.: Impact of exhaust emissions on chemical snowpack composition at Concordia Station, Antarctica, The Cryosphere, 14, 199-209, 2020.

Legrand, M. R., and Delmas, R. J.: Soluble impurities in four Antarctic ice cores over the last 30 000 years, Annals of Glaciology, 10, 116-120, 1988.

Weller, R., Traufetter, F., Fischer, H., Oerter, H., Piel, C., and Miller, H.: Postdepositional losses of methane sulfonate, nitrate, and chloride at the European Project for Ice Coring in Antarctica deep-drilling site in Dronning Maud Land, Antarctica, Journal of Geophysical Research: Atmospheres, 109, 2004.

Zatko, M. C., Grenfell, T. C., Alexander, B., Doherty, S. J., Thomas, J. L., and Yang, X.: The influence of snow grain size and impurities on the vertical profiles of actinic flux and associated NO x emissions on the Antarctic and Greenland ice sheets, Atmospheric Chemistry and Physics, 13, 3547-3567, 2013.

Authors' Response to ACP MS No.: acp-2019-669

We thank the reviewer for the comments and suggestions. In the text below, we outline our responses in blue. Line numbers refer to the revised manuscript.

Anonymous Referee #2

This work present new observations of the isotopic composition of nitrate in atmospheric, skin layer, surface snow and snowpit samples from Dronning Maud Land, Antarctica. The goal of the work is to understand the primary driver(s) of post-depositional processing of nitrate in this environment, based upon a snowpack box model, and determine whether it would be possible to uncover a d15N-nitrate signal that is dependent upon total column ozone. A great deal of work has been done on interpreting the d15N-nitrate in surface snow and the atmosphere at Dome C, and this work seeks to expand the application of similar tools to another site with different environmental conditions (i.e. accumulation rate, snowfall timing, and e-folding depth).

While the data and methods in this work appear sound, and the results are interesting, the manuscript reads as a first draft. With so many authors on this paper, and several who have led work at Dome C, it is surprising how disorganized and filled with typos this work is. Overall, it is difficult to connect the results with the interpretation. Much of the discussion section reads as introduction, and the introduction itself is overly repetitive.

We agree with reviewer, and have reorganised and edited the entire manuscript with particular focus on the introduction and discussion. Please also see our response to referee #1's main comment.

Most critically on the interpretation front, is that the authors must first consider the efolding depth results THEN the results considering changes in the snow accumulation, timing, etc. The model (shown in Figure 7) is simply not at all good enough to draw the conclusions the authors are drawing UNTIL it is shown that with the reduced e-folding depth the model can actually reproduce the observations. This is done as a final step and negates all of the previous discussion that suggests that the model output is robust, and therefore negates the conclusions being drawn.

We agree with the reviewer that the e-folding depth results need to be accounted for before suggesting that the model output fits the observations. We reran TRANISTS with a 5 cm e-folding depth scenario as suggested by reviewer #2. First, we modified the methods section to include a 5 cm e-folding depth scenario (section 2.7 Air-snow transfer modelling). Second, we have added a section on the e-folding depth in the results section (section 3.8 Light attenuation through the snow pack) so the reader can see the observed results of a lower measured e-folding depth at DML upfront. We have also compared the new 5 cm e-folding depth case to the base case in section 3.9 Simulated nitrate mass concentrations and isotopic ratios from TRANSITS modelling. Third, we compare the lower e-folding depth to Dome C and discuss the impact of the lower e-folding depth on post-depositional processes (section 4.3.2.2 Nitrate recycling). Fourth, we have rerun the snow accumulation rate and snowfall timing sensitivity tests with an e-folding depth of 5 cm and modified Figs. 6, 7 and 8 and Table 2 with the new sensitivity test results. An observed e-folding depth of 5 cm was used as it has good fit with observations down to 30 cm depth. In light of the new sensitivity results from TRANSITS, we have reorganised section "4.5 Sensitivity of $\delta^{15}N\text{-}NO_3^-$ to deposition parameters and implications for interpreting ice core records of $\delta^{15}N-NO_3^-$ at DML". Here, we discuss the TRANSITS modelling results by first showing that the base case scenario cannot reproduce the observations and that a reduced e-folding depth is required. Next, we discuss the sensitivity results of a variable snow accumulation rate and snowfall timing with an e-folding depth of 5 cm. With an e-folding depth of 5 cm we are able to reproduce the observations and thus our original conclusions that TRANSITS does a good job are valid.

In section 4.2.3, confidence is built in that TRANSITS can reproduce the seasonal cycle, not at the site here that we are comparing with, but at other sites in Antarctica? This makes no sense.

There are no year-round measurements of atmospheric or skin layer $\delta^{15}N-NO_3^-$ at DML to compare to the TRANSITS seasonality simulations. This section has been rewritten to show that of the available year-round observations and seasonality simulations of atmospheric and skin layer $\delta^{15}N-NO_3^-$ and nitrate mass concentrations in Antarctica, the seasonal pattern is the same at all Antarctic sites. The section has been renamed 4.2.2 Temporal variability of nitrate deposition.

The introduction should be rewritten to better frame where the paper is headed, after the discussion section is reorganized and edited.

Done.

It is well established that photolysis is a major driver of nitrate loss across East Antarctica, between the vast literature at Dome, Erbland's work and Shi's work. At this point, this should be a starting point, not something that is derived step-wise in the manuscript. Furthermore, it would help tighten up and shorten the manuscript. Finally, take a closer look at and include Shi et al., Investigation of post-depositional processing of nitrate in East Antarctic snow: isotopic constraints on photolytic loss, re-oxidation, and source inputs, Atmos. Chem. Phys., 15, 9435–9453, 2015, https://doi.org/10.5194/acp-15-9435-2015.

We agree, and this is reflected in the revised introduction and discussion. In addition, we have cited the Shi et al. (2015) reference in the appropriate places throughout the manuscript, and added the key findings of the paper in lines 137-140 as follows:

Modified text: "Erbland et al. (2013) suggest that NO_3^- loss at the coast reflects both photolysis and evaporation processes, while Shi et al. (2015) proposes that NO_3^- loss at the coast cannot be fully explained by local post-deposition processes and that seasonal cycles in the snowpack reflect stratospheric and troposphere NO_3^- sources during the cold and warm seasons respectively."

The evaporation (volatilization) of nitrate needs more discussion in the introduction. It is stated that that is negligible several times and then, finally, it is explained at lines 680-685 that this is temperature dependent process and THEREFORE not important AT THIS SITE. This should be detailed much earlier on.

As part of the revised introduction, the evaporation of nitrate is discussed in lines 86-98 as follows:

Modified text: "Fractionation constants, which assume a Rayleigh single loss and irreversible process of NO_3^- removal from the snow between phases during evaporation-condensation processes, have been calculated to separate the isotopic signature of evaporation and photolysis processes. As this approach may oversimplify the processes occurring at the air-snow interface, Erbland et al. (2013) referred to the quantity as an "apparent" fractionation constant ($^{15}\varepsilon_{app}$). Thus, the apparent fractionation constant represents the integrated isotopic effect of the processes involving NO_3^- in the surface of the snow pack and in the lower atmosphere. Nitrate evaporation from the snow pack has a $^{15}\varepsilon_{app}$ of ~0 as determined by two independent studies (Erbland et al., 2013;Shi et al., 2019). This indicates that during NO_3^- evaporation, the air above the snow is not replenished and thus there is only a small NO_3^- mass loss. In comparison, fractionation constants associated with laboratory studies and field observations of NO_3^- photolysis are large: $^{15}\varepsilon_{app}$ = -34 ‰ (Berhanu et al., 2014;Meusinger et al., 2014) and -54 < $^{15}\varepsilon_{app}$ < -60 ‰ (Frey et al., 2009;Erbland et al., 2013), respectively. The negative fractionation constant obtained from photolysis implies that the remaining NO_3^- in the skin layer snow is enriched in $\delta^{15}N\text{-}NO_3^-$. In turn, the atmosphere is left with the source of NO_x that is highly depleted in $\delta^{15}N\text{-}NO_3^-$. It follows that evaporation of NO_3^- is negligible on high-elevation Antarctic sites (Erbland et al., 2013;Shi et al., 2019)."

More evidence should be provided that the collection method is robust for representing the isotopic composition of nitrate in the air. The authors state that is "assumed that the atmospheric NO3- collected on glass fibre filters represents the sum of atmospheric particulate NO3- and HNO3 (gas phase)" and then says this is described in Frey et al. (2009). Except Frey et al. makes this exact same ASSUMPTION without providing any evidence that this is the case. Later in this manuscript it is suggested that differences found from earlier work by Weller and Wagenbach may be because different filters were used (Teflon) – which filters are robust? Might the Weller and Wagenbach filters only represent one phase? and if so the authors should understand what the implications of this is for the data comparison.

The glass fiber filters used in this study were employed and tested previously at Dome C, i.e., Frey et al. (2009) do not state an assumption but report evidence from tests with second stage filters. Accordingly, the atmospheric nitrate collected on glass fiber filters represents the sum of atmospheric particulate nitrate ($p\text{-}NO_3^-$) and gaseous nitric acid (HNO_3). The bulk of HNO_3 present in the gas phase adsorbed most likely to aerosols on the filter. This is supported by the observation that second-stage filters (Whatman 41), known to trap HNO_3 quantitatively (Morin et al., 2007), showed either very low nitrate concentrations or none at all.

In section 3.5 and in figure 5, it is never explained what scenario 1 vs scenario 2 is, and where does the 296 for wet deposition come from?

The value for wet deposition (296 pg m^{-2} s^{-1}) in scenario two is calculated using equations 3-5 (total deposition – dry deposition). Scenario one and scenario two are now described in the caption of Fig. 5 and lines 429-443 as follows:

Modified text: "Taking this simple mass balance approach, a schematic of NO_3^- mass fluxes for two scenarios are illustrated in Fig. 5. Scenario 1 is an average annual budget for DML (Fig. 5a). As the atmospheric campaign did not cover an entire annual cycle, we use estimates of atmospheric NO3- fluxes at DML reported by Pasteris et al. (2014) and Weller and Wagenbach (2007) of 43 and 45 pg m^{-2} s^{-1}, respectively, as year round dry deposition fluxes. Due to the linear relationship of ice core NO_3^- mass concentrations with the inverse accumulation, the authors assume that the magnitude of the dry deposition flux is homogenous over the DML region. Mean annual mass concentrations of NO_3^- in our snow pits suggest a total NO_3^- deposition mass flux of 110 pg m^{-2} s^{-1} and therefore a wet deposition mass flux of 65 pg m^{-2} s^{-1}.

However, at relatively low snow accumulation sites where photolysis drives the fractionation of NO_3^- from the surface snow to atmosphere (Frey et al., 2009), it is necessary to take into account the skin layer in the NO_3^- flux budget as this air-snow interface is where air-snow transfer of NO_3^- takes place. In scenario 2, we utilise the available NO_3^- mass concentrations measured in aerosol, skin layer, and snow pits from the ISOL-ICE campaign to estimate the mass flux budget for January 2017 (Fig. 5b). The dry deposition mass flux of atmospheric NO_3^- during January 2017 at DML averages 64 ± 38 pg m^{-2} s^{-1} (Table S5). The NO_3^- mass flux to the skin layer is 360 pg m^{-2} s^{-1}, however only 110 pg m^{-2} s^{-1} of NO_3^- is archived. Considering the active skin layer, only 30 % of deposited NO_3^- is archived in the snow pack while 250 pg m^{-2} s^{-1} is re-emitted to the overlaying atmosphere."

The authors make a claim regarding d18O-NO3- data late in the manuscript (line 660) – this is inappropriate given that none of that data is shown. Further, the claim is that the d18O rises due to denitrification, but there is not previous validity to this statement in the literature.

We have deleted this sentence as this manuscript does not address O-isotopes.

It is stated that the poorly constrained "quantum yield of NO3- photolysis in natural snow" yields a flux of NOx that is 50 times too high. Can this not be tested in TRANSITS? And shouldn't this affect the TRANSITS results as well and not just the estimated calculations here?

We agree that it would be useful to further test the sensitivity of NO_x fluxes to quantum yield in TRANSITS given the large uncertainty of this quantity. However, this has been done previously and we therefore refer to the literature and clarify the statement in lines 471-487 as follows:

Modified text: "It should be borne in mind that the above simple model estimates (Eq. (8)) may significantly underestimate the real emission flux. Previous comparisons of F_{NO2} computed with Eq. (8) and F_{NOx} measured at Dome C showed that observations can exceed model predictions by up to a factor 50 (Frey et al., 2015;Frey et al., 2013). While NO_3^- mass concentrations in snow, the surface actinic flux and e-folding depth were measured at the DML field site, quantum yield of NO_3^- photolysis in surface snow (ΦNO_3^-) was not, but introduces significant uncertainty in the model estimates. Previous lab measurements on natural snow samples collected at Dome C showed ΦNO_3^- to vary between 0.003 and 0.05 (Meusinger et al., 2014). As described above (section 2.6) JNO_3^- used in Eq. (8) was calculated with ΦNO_3^- at -30 ºC (= 2 x 10^{-3}) after Chu and Anastasio (2003), which is near the lower end of the observed range. Thus, up to half of the mismatch between Eq. (8) and Dome C observations can be explained by adjusting ΦNO_3^-. Another factor contributing to larger fluxes and not included in Eq. (8) is forced ventilation.

In the more sophisticated TRANSITS model, Erbland et al. (2015) found that the photolytic quantum yield was one of the major controls on archived flux and primary input flux at Dome C. Erbland et al. (2015) initially used a quantum yield of 2.1 x 10^{-3} at 246 K (France et al., 2011) but it underestimated NO_3^- recycling and overestimated primary NO_3^- trapped in snow. Adjusting the quantum yield to 0.026, within the range observed in the lab (Meusinger et al., 2014), gave more realistic archived $\delta^{15}N$-NO_3^- values. However, at Dome C TRANSITS simulated F_{NO2} fluxes were about a factor of 9 - 18 higher than observed F_{NOx}. Erbland et al.

(2015) suggested that the discrepancy could result from the simplifications made in the TRANSITS model regarding the fate of NO_3^- photolysis products."

Finally, consider better comparing with Zatko et al., 2016 throughout the discussion – the equations used here are very similar to that paper and that work does in fact quantify the recycling despite the line later that only two studies have done so and then Zatko's work is compared with.

What we meant to say is that there are only two methods in the literature to quantify the number of recyclings (Erbland et al., 2015;Davis et al., 2008). Zatko et al. (2016) uses the Davis approach. We have edited the section on recycling, stating there are in fact three studies and have included the Zatko et al. (2016) paper in our comparison in lines 671-672 as follows:

Modified text: "Only three studies have attempted to quantify the degree of NO_3^- recycling between the air and snow (Davis et al., 2008;Erbland et al., 2015;Zatko et al., 2016)."

Also Zatko's earlier work (2013) on impurities should be better considered. Later it is attributed to Geng et al. for some reason. Can impurities in the snow not help account for some of the difference in the photolysis results? i.e. difference in impurities in the snow at DML and Dome C could help to account for the significantly lower photolysis rates at DML.

The impact of impurities on e-folding depth is addressed in section 4.3.2.2. Please see response to referee #1 concerning the impact of grain size and impurities on e-folding depth.

The timing and rate of snowfall CANNOT explain the misalignment between the observations and model results (Line 845). The e-folding depth is critical to right FIRST, then test the sensitivity of these other parameters to determine how to make the fit better. Literally none of the model results presented in Figure 7 before the e-folding depth results come close to overlapping with the observations. Also, you should consider having the model results on a different x-axis so that the depth profile, especially for d15N, can be seen. At this point, the idea of seasonality and the possibility of interannual interpretation is difficult to see.

We agree and thank the reviewer for the valuable comment to improve the manuscript. Please see our response to the e-folding depth comment above. We carried out the TRANISTS runs as suggested by referee #1. An e-folding depth of 5 cm has a much better fit with the observations. With the new TRANSITS runs, our conclusions reinforce the importance of accounting for the e-folding depth measurements across Antarctica. Regarding the x-axis on Fig. 7, the new TRANSITS runs with an e-folding depth of 5 cm move the simulated $\delta^{15}N$-NO_3^- values to more negative values. The better fit with the observations means it is much easier to see the interannual variability in the $\delta^{15}N$-NO_3^-. In addition, the seasonal variability is clearly visible in Fig. 4.

Technical comments:

I do my best to point out a lot of simple errors, but it would behoove the authors to take a closer read on the next version of the manuscript.

Line 10: d15N-NO3- should be (d15N-NO3-)

Done.

Line 20: photochemical processes cannot drive the archiving of nitrate; it drives the loss of nitrate or recycling of nitrate from the snow.

“Photochemical processes” has been replaced with “nitrate recycling”.

Line 34: TOC should be TCO

Done.

Line 38: rephrase this line – it appears as if you are suggesting that NO3- is formed from oxidation of N2

Done.

Line 57: J should be (J)

Done.

Line 64: add a comma after Greenland

Done.

Line 97: this is the first use of PSC, spell it out and explain their purpose here

Done.

Line 169-170: the additional skin layer samples for comparison should be represented in the data figures.

The samples representing spatial variability are already plotted in Fig. S6 and Fig 3. To increase visibility of these samples, we have added an error bar representing the spatial variability to Fig. 3. This is considerably lower than the instrumental variability (error bars are smaller than sample points).

Line 219: a references for the seawater ratio (I assume this means sea salt ratio) should be included.

Keene et al. (1986) reference added for the sea salt ratio.

Line 300: followed should be follows

Done.

Line 303: add the word in after changes

Done.

Line 370: remove and before archived

Done.

Line 398: as a year round does not make sense

Done.

Line 457: inter-decadal should be interannual

Done.

Line 475: Fig 5 should not be cited here

Changed to Fig. 7.

Line 490: remove are

This sentence has been removed following the main comments.

Line 530: up taken should be taken up

This sentence has been removed following the main comments.

Line 536: the idea that “NO3- peaks are substantially modified after burial” undermines so much of the current manuscript that suggests that NO3- is archived once buried. Rephrase.

This sentence has been removed following the main comments.

Line 566: rephrase “form of nitrogen to skin layer”

Done.

Line 612: back to THE skin later with a day, or IS transported away

Done.

Line 624-625: see comment above about better explaining the evaportation results; and Shi et al 2019 reflect field conditions, not laboratory conditions.

Section 4.3.1 Evaporation has been removed following the main comments of referees #1 and #2.

Line 643-653: I have serious issues here with the interpretation of previous literature. First and foremost, the assumption that anthropogenic emissions of NOx are positive in d15N and natural emissions are negative in d15N is false and not up to date. Recent work shows that vehicle emissions are, in fact, negative in d15N (Miller et al., 2017, Vehicle NOx emission plume isotopic signatures: Spatial variability across the eastern United States, J. Geophys. Res. Atmos., 122, doi:10.1002/2016JD025877)/ At least three works show that fertilized soil emissions (which are not considered a natural source in emission inventories) are very negatives in d15N (Yu & Elliott, 2017, Novel method for nitrogen isotopic analysis of soil-emitted nitric oxide. Environmental Science & Technology, 51(11), 6268–6278, https://doi.org/10.1021/acs.est.7b00592; Miller et al., 2018, Isotopic composition of in situ soil NOx emissions in manure fertilized cropland, Geophysical Research Letters, 45(21), 12058-12066, https://doi.org/10.1029/2018GL079619.; Li & Wang, 2008, Nitrogen isotopic signature of soil-released nitric oxide (NO) after fertilizer application. Atmospheric Environment, 42(19), 4747–4754. https://doi.org/10.1016/j.atmosenv.2008.01.042.). Geng et al. make the exact same false interpretation that anthropogenic sources are positive and therefore are ruled out in interpretation of a Summit, Greenland core – do not cite this is evidence when it is simply an unwarranted assumption. Finally, please be more precise in the language here – emission sources emit NO (except diesel engines, which can also emit NO2) or you can call it NOx; they do not “have positive d15N-NO3-“ values since they do not emit nitrate, it is secondarily formed and subject to partitioning in the atmosphere, which Geng et al. invoke as a major mechanism to explain Greenland ice results, and this is wholly ignored in the current work.

We thank the reviewer for providing additional references concerning the negative isotopic signature of anthropogenic emissions of NO_x. We have edited this section to include the recent work on vehicle NO_x emissions and fertilised soil emissions and provided the references suggested by the reviewer. We have removed the Geng et al. reference which discards anthropogenic nitrate as a potential source to Greenland snow. When referring to the isotopic signature of emission sources, we have replaced $\delta^{15}N\text{-}NO_3^-$ with $\delta^{15}N\text{-}NO_x$. In light of the negative source signature of NO_x emissions, our interpretation that anthropogenic sources do not contribute to the atmospheric $\delta^{15}N\text{-}NO_3^-$ at DML remains unchanged based on i) the well-established literature in which photolysis is the major driver of atmospheric $\delta^{15}N\text{-}NO_3^-$ values over low accumulation sites in East Antarctica (e.g. Frey et al., 2009;Erbland et al., 2015;Erbland et al., 2013;Shi et al., 2015;Shi et al., 2018), and ii) modelling study by Lee et al. (2014) that shows fertilised soil NO_x emissions to Antarctica are minor. We modified the text as follows (lines 637-642):

Modified text: "The $\delta^{15}N\text{-}NO_x$ source signature of the main natural NO_x sources (biomass burning, lightning, soil emissions; $\delta^{15}N\text{-}NO_x$ <0 ‰) is lower than anthropogenic NO_x sources, which generally have positive $\delta^{15}N\text{-}NO_x$ values (-13< $\delta^{15}N\text{-}NO_x$ < 13 ‰; e.g. (Hastings et al., 2013;Kendall et al., 2007;Hoering, 1957) except in the case of vehicle and fertilised soil NO_x emissions which have negative $\delta^{15}N\text{-}NO_x$ values (-60< $\delta^{15}N\text{-}NO_3^-$ <12 ‰; Miller et al. (2017);Yu and Elliott (2017);Miller et al. (2018);Li and Wang (2008). However, a NO_3^- source contribution from fertilised soil NO_x emissions to Antarctica is thought to be minor (Lee et al., 2014)."

Line 690-695: a range of -19 per mil to +12 per mil does not at all "nicely match" with the expected -59 per mil to -16 per mil.

Replaced "nicely match" with "falls within the range".

Line 698: add an before annual

Done.

Section 4.3.3 – seems odd to switch to section i, ii, iii, etc here when earlier subsections are numbered in series (i.e. 4.3.3.1, 4.3.3.2, etc).

Replaced i, ii, iii with 1, 2, 3.

Line 780: Concluding that photolysis is an important driver is not an interesting result given the vast evidence for this throughout the EAIS. The other conclusions are still interesting but this should not be the primary focus. Furthermore, the fact that there is less photolysis than expected is really very interesting.

This section has been removed following the main comments of referee #1.

Line 850-851: Interestingly, Geng et al. 2015 ignores surface snow work at Summit, Greenland to invoke that post-depositional processing can explain everything (Fibiger et al. (2016), Analysis of nitrate in the snow and atmosphere at Summit, Greenland: Chemistry and transport, J. Geophys. Res. Atmos., 121, 5010– 5030, doi:10.1002/2015JD024187; Fibiger et al. (2013), The preservation of atmospheric nitrate in snow at Summit, Greenland, Geophys. Res. Lett., 40, 3484–3489, doi:10.1002/grl.50659.). Here, you are showing that is critical to use surface work to best determine how to interpret ice cores. I suggest you reconsider including comparison with Geng's work here.

Done.

Line 855: depending ON the timing

Done.

Line 902: due TO photolysis-driven

Done.

Line 905: This should reference Zatko et al. not Geng et al.

Done.

Line 913: I strongly disagree with the statement that "TRANSITS doe such a good job of simulating NO-3 recycling in Antarctica" unless you do the e-folding fit first and then explore sensitivities. (I do agree that it is an excellent recommendation to use TRANSITS to assess sites that would be useful for interpreting nitrate isotopic records!)

Please see our response to the e-folding depth comment above. Based on the improved fit of the new sensitivity tests using the e-folding depth of 5 cm, we have kept this statement in the manuscript.

Line 919: unpicking is a strange word here – distinguishing?

Conclusions were rewritten following the suggestion of referee #1. "Unpicking" is no longer used.

Line 922: resulting IN an enrichment

Done.

Line 929: this conclusion would make more sense if the e-folding depth model experiments were done first.

Done.

Line 945: THE ground

Done.

Figure 3: how is the data averaged here?

The RACMO precipitation data is published as daily values. See the data publication for further information https://data.bas.ac.uk/full-record.php?id=GB/NERC/BAS/PDC/01137. The wind data from the AWS is hourly. We have added this to the caption.

Figure 4: x-axis on right side is misspelled

Done.

Figure 5: what is scenario 1 vs 2, this is never explained

This is now explained in text (lines 429-443; see comment above) and in the caption of Fig. 5.

Table 2: Archived should be >30 cm not <30 cm, correct?

Yes, this has been corrected.

References

Berhanu, T. A., Meusinger, C., Erbland, J., Jost, R., Bhattacharya, S., Johnson, M. S., and Savarino, J.: Laboratory study of nitrate photolysis in Antarctic snow. II. Isotopic effects and wavelength dependence, The Journal of chemical physics, 140, 244306, 2014.

Chu, L., and Anastasio, C.: Quantum yields of hydroxyl radical and nitrogen dioxide from the photolysis of nitrate on ice, The Journal of Physical Chemistry A, 107, 9594-9602, 2003.

Davis, D. D., Seelig, J., Huey, G., Crawford, J., Chen, G., Wang, Y., Buhr, M., Helmig, D., Neff, W., and Blake, D.: A reassessment of Antarctic plateau reactive nitrogen based on ANTCI 2003 airborne and ground based measurements, Atmospheric Environment, 42, 2831-2848, 2008.

Erbland, J., Vicars, W., Savarino, J., Morin, S., Frey, M., Frosini, D., Vince, E., and Martins, J.: Air–snow transfer of nitrate on the East Antarctic Plateau–Part 1: Isotopic evidence for a photolytically driven dynamic equilibrium in summer, Atmospheric Chemistry and Physics, 13, 6403-6419, 2013.

Erbland, J., Savarino, J., Morin, S., France, J., Frey, M., and King, M.: Air–snow transfer of nitrate on the East Antarctic Plateau–Part 2: An isotopic model for the interpretation of deep ice-core records, Atmospheric Chemistry and Physics, 15, 12079-12113, 2015.

Frey, M., Roscoe, H., Kukui, A., Savarino, J., France, J., King, M., Legrand, M., and Preunkert, S.: Atmospheric nitrogen oxides (NO and NO 2) at Dome C, East Antarctica, during the OPALE campaign, Atmospheric Chemistry and Physics, 15, 7859-7875, 2015.

Frey, M. M., Savarino, J., Morin, S., Erbland, J., and Martins, J.: Photolysis imprint in the nitrate stable isotope signal in snow and atmosphere of East Antarctica and implications for reactive nitrogen cycling, Atmospheric Chemistry and Physics, 9, 8681-8696, 2009.

Frey, M. M., Brough, N., France, J. L., Anderson, P. S., Traulle, O., King, M. D., Jones, A. E., Wolff, E. W., and Savarino, J.: The diurnal variability of atmospheric nitrogen oxides (NO and NO₂) above the Antarctic Plateau driven by atmospheric stability and snow emissions, Atmos. Chem. Phys., 13, 3045-3062, 10.5194/acp-13-3045-2013, 2013.

Hastings, M. G., Casciotti, K. L., and Elliott, E. M.: Stable isotopes as tracers of anthropogenic nitrogen sources, deposition, and impacts, Elements, 9, 339-344, 2013.

Hoering, T.: The isotopic composition of the ammonia and the nitrate ion in rain, Geochimica et Cosmochimica Acta, 12, 97-102, 1957.

Keene, W. C., Pszenny, A. A., Galloway, J. N., and Hawley, M. E.: Sea-salt corrections and interpretation of constituent ratios in marine precipitation, Journal of Geophysical Research: Atmospheres, 91, 6647-6658, 1986.

Kendall, C., Elliott, E. M., and Wankel, S. D.: Tracing anthropogenic inputs of nitrogen to ecosystems, Stable isotopes in ecology and environmental science, 2, 375-449, 2007.

Lee, H.-M., Henze, D. K., Alexander, B., and Murray, L. T.: Investigating the sensitivity of surface-level nitrate seasonality in Antarctica to primary sources using a global model, Atmospheric Environment, 89, 757-767, 2014.

Li, D., and Wang, X.: Nitrogen isotopic signature of soil-released nitric oxide (NO) after fertilizer application, Atmospheric Environment, 42, 4747-4754, https://doi.org/10.1016/j.atmosenv.2008.01.042, 2008.

Meusinger, C., Berhanu, T. A., Erbland, J., Savarino, J., and Johnson, M. S.: Laboratory study of nitrate photolysis in Antarctic snow. I. Observed quantum yield, domain of photolysis, and secondary chemistry, The Journal of chemical physics, 140, 244305, 2014.

Miller, D. J., Wojtal, P. K., Clark, S. C., and Hastings, M. G.: Vehicle NOx emission plume isotopic signatures: Spatial variability across the eastern United States, Journal of Geophysical Research: Atmospheres, 122, 4698-4717, 2017.

Miller, D. J., Chai, J., Guo, F., Dell, C. J., Karsten, H., and Hastings, M. G.: Isotopic Composition of In Situ Soil NOx Emissions in Manure-Fertilized Cropland, Geophysical Research Letters, 45, 12,058-012,066, 2018.

Morin, S., Savarino, J., Bekki, S., Gong, S., and Bottenheim, J.: Signature of Arctic surface ozone depletion events in the isotope anomaly (Δ 17 O) of atmospheric nitrate, 2007.

Pasteris, D., McConnell, J. R., Edwards, R., Isaksson, E., and Albert, M. R.: Acidity decline in Antarctic ice cores during the Little Ice Age linked to changes in atmospheric nitrate and sea salt concentrations, Journal of Geophysical Research: Atmospheres, 119, 5640-5652, 2014.

Shi, G., Buffen, A., Hastings, M., Li, C., Ma, H., Li, Y., Sun, B., An, C., and Jiang, S.: Investigation of post-depositional processing of nitrate in East Antarctic snow: isotopic constraints on photolytic loss, re-oxidation, and source inputs, Atmospheric Chemistry and Physics, 15, 9435-9453, 2015.

Shi, G., Buffen, A., Ma, H., Hu, Z., Sun, B., Li, C., Yu, J., Ma, T., An, C., and Jiang, S.: Distinguishing summertime atmospheric production of nitrate across the East Antarctic Ice Sheet, Geochimica et Cosmochimica Acta, 231, 1-14, 2018.

Shi, G., Chai, J., Zhu, Z., Hu, Z., Chen, Z., Yu, J., Ma, T., Ma, H., An, C., and Jiang, S.: Isotope fractionation of nitrate during volatilization in snow: a field investigation in Antarctica, Geophysical Research Letters, 46, 3287-3297, 2019.

Weller, R., and Wagenbach, D.: Year-round chemical aerosol records in continental Antarctica obtained by automatic samplings, Tellus B: Chemical and Physical Meteorology, 59, 755-765, 2007.

Yu, Z., and Elliott, E. M.: Novel method for nitrogen isotopic analysis of soil-emitted nitric oxide, Environmental science & technology, 51, 6268-6278, 2017.

Zatko, M., Geng, L., Alexander, B., Sofen, E., and Klein, K.: The impact of snow nitrate photolysis on boundary layer chemistry and the recycling and redistribution of reactive nitrogen across Antarctica and Greenland in a global chemical transport model, Atmos. Chem. Phys, 16, 2819-2842, 2016.

Deposition, recycling and archival of nitrate stable isotopes between the air-snow interface: comparison between Dronning Maud Land and Dome C, Antarctica

V. Holly L. Winton[1], Alison Ming[1], Nicolas Caillon[2], Lisa Hauge[1], Anna E. Jones[1], Joel Savarino[2], Xin Yang[1], Markus M. Frey[1]

[1]British Antarctic Survey, Cambridge, CB3 0ET, UK
[2]University of Grenoble Alpes, CNRS, IRD, Grenoble INP, IGE, F-38000 Grenoble, France

Correspondence to: V. Holly L. Winton (~~viewin@bas.ac.uk~~holly.winton@vuw.ac.nz)

Abstract

The nitrogen stable isotopic composition in nitrate (δ^{15}N-NO_3^-) measured in polar ice cores has the potential to provide constraints on past ultraviolet (UV) radiation and thereby total column ozone (TCO) due to the sensitivity of nitrate (NO_3^-) photolysis to UV radiation. However, understanding the transfer of reactive nitrogen at the air-snow interface in Polar Regions is paramount for the interpretation of ice core records of δ^{15}N-NO_3^- and NO_3^- mass concentrations. As NO_3^- undergoes a number of post-depositional processes before it is archived in ice cores, site-specific observations of δ^{15}N-NO_3^- and air-snow transfer modelling are necessary ~~in order~~ to understand and quantify the complex photochemical processes at play. As part of the Isotopic Constraints on Past Ozone Layer Thickness in Polar Ice (ISOL-ICE) project, we report new measurements of NO_3^- mass concentration and δ^{15}N-NO_3^- in the atmosphere, skin layer (operationally defined as the top 5 mm of the snow pack), and snow pit depth profiles at Kohnen Station, Dronning Maud Land (DML), Antarctica. We compare the results to previous studies and new data, presented here, from Dome C, East Antarctic Plateau. Additionally, we apply the conceptual one-dimensional model of TRansfer of Atmospheric Nitrate Stable Isotopes To the Snow (TRANSITS) to assess the impact of ~~photochemical processes~~NO_3^- recycling on ~~that drive the archival of~~ δ^{15}N-NO_3^- and NO_3^- mass concentrations archived in ~~the~~ snow and firn~~pack~~. We find clear evidence of NO_3^- photolysis at DML, and confirmation of previous theoretical, field and laboratory studies that UV-photolysis is driving ~~our hypothesis that UV-photolysis is driving~~ NO_3^- recycling and redistribution at DML. Firstly, strong denitrification of the snow pack is observed through the δ^{15}N-NO_3^- signature which evolves from the enriched snow pack (-3 to 100 ‰), to the skin layer (-20 to 3 ‰), to the depleted atmosphere (-50 to -20 ‰) corresponding to mass loss of NO_3^- from the snow pack. Secondly, constrained by field measurements of snow accumulation rate, light attenuation (e-folding depth) and atmospheric NO_3^- mass concentrations, the TRANSITS model is able to reproduce ~~our~~ observed δ^{15}N-NO_3^- ~~observations in~~ depth profiles. We find that NO_3^- is recycled ~~three~~ two times before it is archived ~~(i.e., below the photic zone)~~ in the snow pack below 15 cm and within 0.75 years (i.e., below the photic zone). Mean annual a~~A~~rchived δ^{15}N-NO_3^- and NO_3^- mass concentration values are 50 ‰ and 60 ng g^{-1}, respectively, at the DML site. We report an

Formatted: Not Superscript/ Subscript

Formatted: Not Superscript/ Subscript

Formatted: Not Superscript/ Subscript

e-folding depth of 2 - 5 cm for the DML site which is considerably lower than Dome C. ~~NO_3^- photolysis is weaker at DML than at Dome C, due primarily to the higher DML snow accumulation rate; this results in a more depleted $\delta^{15}N$-NO_3^- signature at DML than at Dome C.~~A reduced photolytic loss of NO_3^- at DML results in less enrichment of $\delta^{15}N$-NO_3^- than at Dome C mainly due to the smaller e-folding depth but also due to the higher accumulation rate based on TRANSITS modelled sensitivities. Even at a relatively low snow accumulation rate of 6 cm yr^{-1} (water equivalent; w.e.), the accumulation rate at DML is great enough to preserve the seasonal cycle of NO_3^- mass concentration and $\delta^{15}N$-NO_3^-, in contrast to Dome C where the depth profiles are smoothed due to l~~stronger photochemistry~~onger exposure of surface snow layers to incoming UV radiation before burial. TRANSITS sensitivity analysis of $\delta^{15}N$-NO_3^- at DML highlights that the dominant factors controlling the archived $\delta^{15}N$-NO_3^- signature are the e-folding depth and snow accumulation rate~~ and e-folding depth~~, with a smaller role from changes in the snowfall timing and TC~~O~~O~~C~~. Mean TRANSITS model sensitivities of archived $\delta^{15}N$-NO_3^- at the DML site are 100 ‰ for an e-folding depth change of 8 cm; 110 ‰ for an annual snow accumulation rate change of 8.5 cm yr^{-1} (w.e.); 10 ‰ for a change in the dominant snow deposition season between winter and summer, and 10 ‰ for a TCO change of 100 DU. Here we set the framework for the interpretation of a 1000-year ice core record of $\delta^{15}N$-NO_3^- from DML. Ice core $\delta^{15}N$-NO_3^- records at DML will be less sensitive to changes in UV than at Dome C, however the higher snow accumulation rate and more accurate dating at DML allows for higher resolution $\delta^{15}N$-NO_3^- records.

Formatted: Not Superscript/ Subscript

Formatted: Not Superscript/ Subscript

~~1 Introduction~~

~~Nitrate (NO_3^-) is a naturally occurring ion formed by the oxidation of nitrogen, and plays a major role in the global nitrogen cycle. It is one of the most abundant ions in Antarctic snow and is commonly measured in ice cores (e.g. Wolff, 1995). Nitrate in polar ice provides constraints on past solar activity (Traversi et al., 2012), NO_3^- sources and the oxidative capacity of the atmosphere (Geng et al., 2017;Mulvaney and Wolff, 1993;Hastings et al., 2009;Hastings et al., 2004;McCabe et al., 2007;Savarino et al., 2007;Morin et al., 2008). However, NO_3^- is a non-conservative ion in snow, and due to post-depositional processes (e.g. Mulvaney et al., 1998;Zatko et al., 2016), the interpretation of NO_3^- concentration records from ice core records is challenging (Erbland et al., 2015). The recent development of the analysis of nitrogen isotopic composition of NO_3^- ($\delta^{15}N$-NO_3^-) in snow, ice and aerosol provides a powerful means to understand the sources and processes involved in NO_3^- post-depositional processes, i.e., NO_3^- recycling at the interface between air and snow.~~

Formatted: Subscript

~~Primary sources of reactive nitrogen species to the Antarctic lower atmosphere and snow pack include the sedimentation of polar stratospheric clouds (PSC) in late winter (Savarino et al., 2007) and to a minor extent advection of oceanic methyl nitrate (CH_3NO_3) and peroxyacyl nitrates (PAN) ~~(Jacobi et al., 2000;Jones et al., 1999;Beyersdorf et al., 2010;Lee et al., 2014)~~. In the stratosphere, NO_3^- is produced through the stratospheric oxidation of nitrous oxide (N_2O) from extra-terrestrial fluxes of energetic particles and solar radiation, whereas in the troposphere lightning and biomass burning provide background tropospheric reactive nitrogen species to the snow pack (Savarino et al., 2007;Wolff, 1995;Wagenbach et al., 1998). A local~~

~~secondary source of reactive nitrogen (nitrous acid (HONO), nitrogen oxides (NO_x)) originates from post-depositional processes driven by sunlight leading to re-emission from the snow pack and subsequent deposition (Savarino et al., 2007;Frey et al., 2009).~~

~~Local nitrogen dioxide (NO_2) emissions in Polar Regions are produced from NO_3^- photolysis in the snow pack under sunlit conditions (Jones et al., 2001;Honrath et al., 1999;Oncley et al., 2004). Nitrate photolysis occurs at wavelengths (λ) = 290-345 nm with a maximum at 320 nm. Once NO_x is produced by NO_3^- photolysis, it is expected to have a lifetime in the polar troposphere of <1 day before it is oxidised to nitric acid (HNO_3) at Dome C and South Pole (Davis et al., 2004b), and can then be redeposited to the skin layer (e.g. Mulvaney et al., 1998).~~

~~Photolysis rate J depends on the adsorption cross section of NO_3^-, the quantum yield and actinic flux within the snow pack. Photochemical production of NO_2 is dependent on the NO_3^- concentration in the snow pack, the snow pack properties, and the intensity of solar radiation within the snow pack. The latter is sensitive to solar zenith angle and snow optical properties i.e. scattering and adsorption coefficients, which depends on snow density and morphology, and the light absorbing impurity content (France et al., 2011;Erbland et al., 2015;Zatko et al., 2013). Recently, Zatko et al. (2016) found that the range of modelled NO_x fluxes from the snow pack to the overlaying air are similar in both Polar Regions due to the opposing effects of higher concentrations of both photolabile NO_3^- and light absorbing impurities (e.g. dust and black carbon) in Antarctica and Greenland respectively. At Concordia Station on Dome C in East Antarctica, the light penetration depth (e-folding depth) is ~10 cm for wind pack layers and ~20 cm for hoar layers (France et al., 2011). Based on the propagation of light into the snow pack, the snow pack can be divided into three layers. The first layer is known as the skin layer (a few mm thick) where direct solar radiation is converted into diffuse radiation. The second layer is called the active photic zone (below the skin layer layer), where solar radiation is effectively diffuse and the intensity of the radiation decays exponentially (Warren, 1982). The third layer is called the archived zone (below the active photic zone), where no photochemistry occurs.~~

~~Previous research has focused predominantly on the high elevation polar plateau (Dome C). Here, the exponential decay of NO_3^- mass concentrations in the snow pack and thus post-depositional processing of NO_3^- were attributed to either evaporation or ultra-violet (UV) photolysis (Röthlisberger et al., 2000;Röthlisberger et al., 2002). The open debate of which post-depositional process controlled NO_3^- mass concentrations in the snow pack led to the use of a new isotopic tool, the stable isotopic composition of nitrate ($\delta^{15}N$-NO_3^-) Blunier et al. (2005). More recently, theoretical (Frey et al., 2009), laboratory (Meusinger et al., 2014;Erbland et al., 2013;Erbland et al., 2015;Shi et al., 2019;Berhanu et al., 2014), and field (Erbland et al., 2013;Frey et al., 2009;Shi et al., 2015) evidence show that NO_3^- mass loss from the surface snow to the overlying atmosphere and its associated isotopic fractionation is driven by photolysis. The physical release or evaporation of NO_3^- is negligible (Erbland et al., 2013;Shi et al., 2019). between phases during evaporation-condensation processes,~~

Formatted: Font:

~~At Dome C, the large redistribution and net mass loss of NO_3^- below the skin layer and the simultaneous isotopic fractionation of $\delta^{15}N$-NO_3^- in the snow pack indicate that post-depositional processes significantly modify the original NO_3^- concentration and $\delta^{15}N$-NO_3^- composition (Frey et al., 2009). Skin layer observations of $\delta^{15}N$-NO_3^- in the surface snow at Dome C show strong enrichment compared to the atmospheric $\delta^{15}N$-NO_3^- signature. Furthermore, snow pit profiles show an exponential~~

~~decrease of NO_3^- concentration and an enrichment in the $\delta^{15}N$-NO_3^- composition with depth (Erbland et al., 2013). Once NO_x is produced by NO_3^- photolysis, it is expected to have a lifetime in the polar troposphere of <1 day before it is oxidised to nitric acid (HNO_3) at Dome C and South Pole (Davis et al., 2004b), and can then be redeposited to the skin layer (e.g. Mulvaney et al., 1998).~~

~~This research at Dome C laid the foundation for Erbland et al. (2015) to derive a conceptual model of UV-photolysis induced post-depositional processes of NO_3^- at the air-snow interface.TRANSITS is a conceptual multi-layer 1D model which aims to represent NO_3^- recycling at the air-snow interface including processes relevant for NO_3^- snow photochemistry (UV-photolysis of NO_3^-, emission of NO_x, local oxidation, deposition of HNO_3) and explicitly calculates NO_3^- mass concentrations and $\delta^{15}N$-NO_3^- in snow. "Nitrate recycling" is the combination of NO_x production from NO_3^- photolysis in snow, the subsequent atmospheric processing and oxidation of NO_x to form atmospheric HNO_3, the deposition (dry and/or wet) of a fraction of the HNO_3, and the export of another fraction. In NO_3^- recycling, the skin layer is an active component of the atmosphere. This recycling can occur multiple times before NO_3^- is eventually archived below the active photic zone in ice cores (Davis et al., 2008;Erbland et al., 2015;Zatko et al., 2016;Sofen et al., 2014). We refer to atmospheric NO_3^- as the combination (i.e., total) of HNO_3 (gas phase) and particulate NO_3^-.We refer to atmospheric NO_3^- as the combination (i.e., total) of HNO_3 (gas phase) and particulate NO_3^-.The desorption of HNO_3 from the snow crystal reduces the NO_3^- concentration in the snow in coastal Antarctica (Mulvaney et al., 1998). The evaporation of HNO_3 is a two-step process, which involves the recombination of NO_3^- $+ H^+ \longrightarrow HNO_3$ followed by a phase change to HNO_3 (gas-phase). First, theoretical estimates indicated that evaporation of HNO_3 should preferentially remove ^{15}N from the snow and release to the atmosphere leading to depletion in $\delta^{15}N$-NO_3^- in the residual snow pack (Frey et al., 2009). Furthermore, recent laboratory experiments showed that evaporation imposes a negligible fractionation of $\delta^{15}N$-NO_3^-~~ (!!! INVALID CITATION !!! (Erbland et al., 2013;Shi et al., 2019))~~. However, we find that the snow pack is enriched in $\delta^{15}N$-NO_3^- relative to the atmosphere at DML (Figs. 3 and 6) and at Dome C (section 4.3.2). This fractionation observed in field studies cannot therefore be explained by evaporation, and must be attributed to different processes. It therefore follows that evaporation must be only a minor process in the redistribution of NO_3^- between atmosphere and the snow pack above the Antarctic plateau.~~

~~Nitrate evaporation from the snow pack has a $^{15}\varepsilon_{app}$ of ~0 as determined by two independent studies~~ (!!! INVALID CITATION !!! (Erbland et al., 2013;Shi et al., 2019))~~. This indicates that during NO_3^- evaporation, the air above the snow is not replenished and thus there is only a small NO_3^- mass loss. The isotopic fractionation of NO_3^- evaporation is negligible across most of Antarctica at cold temperatures of <-24 °C (Shi et al., 2019) which is the case for DML. However, evaporation of NO_3^- at warmer temperatures (-4 °C) depletes the heavy isotopes of NO_3^- remaining in the snow, and decreases the $\delta^{15}N$-NO_3^- and the remaining snow by a few ‰ contrary to isotope effects of photolysis. In comparison, fractionation constants associated with laboratory studies and field observations of NO_3^- photolysis are large: $^{15}\varepsilon_{app} = -34$ ‰ (Berhanu et al., 2014;Meusinger et al., 2014) and $-54 < {^{15}\varepsilon_{app}} < -60$ ‰ (Frey et al., 2009;Erbland et al., 2013), respectively. The negative fractionation constant obtained from photolysis implies that the remaining NO_3^- in the skin layer snow is enriched in $\delta^{15}N$-NO_3^-. In turn, the atmosphere is left with the source of NO_x that is highly depleted in $\delta^{15}N$-NO_3^-. This enrichment (depletion) is exactly what we~~

Formatted: Highlight

Formatted: Highlight

Formatted: Highlight

Formatted: Highlight

Formatted: Highlight

Formatted: Highlight

Formatted: Highlight

Formatted: Highlight

Formatted: Highlight

~~observe in the snow pack (atmosphere) at DML (Figs. 4 and 6). The marked difference in values from the evaporation experiments and those observed in snow at Dome C allows us to separate out the isotopic signature of evaporation and photolysis processes.~~

~~Year round measurements of NO_3^- mass concentrations and $\delta^{15}N$-NO_3^- in the skin layer and atmosphere at Dome C have provided insights into the annual NO_3^- cycle in Antarctica (Fig. 1) Erbland et al. (2013). In the early winter, the stratosphere undergoes denitrification via formation of PSC. As PSC sediment slowly, there is a delay between the maximum stratospheric NO_3^- concentration and the maximum NO_3^- concentration deposited in the skin layer in late winter (Mulvaney and Wolff, 1993;Savarino et al., 2007). In spring, surface UV increases and initiates photolysis-driven post-depositional processes, which redistribute NO_3^- between the snow pack and overlying air throughout the sunlit summer season. This results in the $\delta^{15}N$-NO_3^- isotopic enrichment of the NO_3^- skin layer reservoir, and maximum atmospheric NO_3^- mass concentrations in October-November. In summer, NO_3^- resembles a strongly asymmetric distribution within the atmosphere-snow column with the bulk residing in the skin layer and only a small fraction in the atmospheric column above.~~

~~Over longer time scales, UV-driven post-depositional processing of NO_3^- is also driven by changes in the degree of post-depositional loss of NO_3^- with greater NO_3^- loss during the glacial period relative to the Holocene. The observed glacial-interglacial difference in post-depositional processing of NO_3^- is dominated by variations in snow accumulation rate (Geng et al., 2015).~~

~~Nitrate is not preserved in the snow pack at sites with very low snow accumulation rates (i.e., Dome C: 2.5-3 cm yr^{-1}) because snow layers remain close to the surface and in contact with the overlaying atmosphere for a relatively long time enhancing the effect of post-depositional processes. At sites with low snow accumulation rates, the source signature of $\delta^{15}N$-NO_3^- is erased by post-depositional process. Therefore, photolysis induced NO_3^- loss and $\delta^{15}N$-NO_3^- fractionation is dependent on snow accumulation. Three distinct transects from coastal Antarctica to the East Antarctic Plateau show that NO_3^- fractionation is strongest with decreasing snow accumulation (Shi et al., 2018;Erbland et al., 2013;Noro et al., 2018). Skin layer NO_3^- mass concentrations are significantly higher at low snow accumulation sites, for example ~160 ng g^{-1} (winter) to 1400 ng g^{-1} (summer) at Dome C compared to 50 ng g^{-1} (winter) to 300 ng g^{-1} (summer) at Dumont d'Urville (DDU) on the Antarctic coast. (Shi et al., 2015;Erbland et al., 2013)Furthermore, the strong inverse linear relationship between NO_3^- concentration and accumulation rate was revealed in a composite of seven ice cores across Dronning Maud Land (DML) Pasteris et al. (2014).Over longer time scales, UV-driven post-depositional processing of NO_3^- is also driven by changes in the degree of post-depositional loss of NO_3^- with greater NO_3^- loss during the glacial period relative to the Holocene. The observed glacial-interglacial difference in post-depositional processing of NO_3^- is dominated by variations in snow accumulation rate (Geng et al., 2015).~~

~~Yet, NO_3^- photolysis leaves its own process-specific imprint in the snow pack (Shi et al., 2019;Erbland et al., 2015;Erbland et al., 2013), which opens up the possibility to use $\delta^{15}N$-NO_3^- to infer past surface UV variability (Frey et al., 2009). However,~~

~~NO_3^- photolysis rates in snow depend on a number of site-specific factors as does the degree of photolytic isotopic fractionation of NO_3^- eventually preserved in ice cores (Erbland et al., 2013;Berhanu et al., 2014). These factors need to be quantitatively understood at a given ice core site to enable quantitative interpretation of ice core records. Here, we carry out a comprehensive study of the air-snow transfer of NO_3^- at Kohnen Station in DML, East Antarctica through δ^{15}N-NO_3^- measurements in the atmosphere, skin layer and snow pits, and compare the observations to Dome C. Due to the previous research outlined above, we assume that the photolysis is the dominant driver of NO_3^- post-depositional processes, and later assess the validity of this this assumption (section 4.3). We apply the Transfer of Atmospheric Nitrate Stable Isotopes To the Snow (TRANSITS) model (Erbland et al., 2015) to i) understand how NO_3^- mass concentrations and δ^{15}N-NO_3^- are archived in deeper snow and ice layers, and ii) investigate the sensitivity of changes in the past snow accumulation rate, snowfall timing, e-folding depth, and TCO on the δ^{15}N-NO_3^- signature. In order to interpret this novel UV proxy, it is paramount to understand the air-snow transfer processes specific to an ice core site, and how δ^{15}N-NO_3^- is archived in the deeper snow and ice layers (Geng et al., 2015;Morin et al., 2009;Erbland et al., 2015). Within the framework of the Isotopic Constraints on Past Ozone Layer Thickness in Polar Ice (ISOL-ICE) project, this study provides a basis for the interpretation of δ^{15}N-NO_3^- from a 1000-year ice core recovered in 2016/17 at Kohnen Station.~~

Formatted: Not Superscript/ Subscript

Formatted: Subscript

1 Introduction

Nitrate (NO_3^-) is a naturally occurring ion, and plays a major role in the global nitrogen cycle. It is one of the most abundant ions in Antarctic snow and is commonly measured in ice cores (e.g. Wolff, 1995). Nitrate in polar ice provides constraints on past solar activity (Traversi et al., 2012), NO_3^- sources and the oxidative capacity of the atmosphere (Geng et al., 2017;Mulvaney and Wolff, 1993;Hastings et al., 2009;Hastings et al., 2004;McCabe et al., 2007;Savarino et al., 2007;Morin et al., 2008). However, NO_3^- is a non-conservative ion in snow, and due to post-depositional processes (e.g. Mulvaney et al., 1998;Zatko et al., 2016), the interpretation of NO_3^- mass concentration records from ice core records is challenging (Erbland et al., 2015). The recent development of the analysis of the nitrogen isotopic composition of NO_3^- (δ^{15}N-NO_3^-) in snow, ice and aerosol provides a powerful means to understand the sources and processes involved in NO_3^- post-depositional processes, i.e., NO_3^- recycling at the interface between air and snow.

Primary sources of reactive nitrogen species to the Antarctic lower atmosphere and snow pack include the sedimentation of polar stratospheric clouds (PSC) in late winter (Savarino et al., 2007) and, to a minor extent, advection of oceanic methyl nitrate (CH_3NO_3) and peroxyacyl nitrates (PAN) (Jacobi et al., 2000;Jones et al., 1999;Beyersdorf et al., 2010), in addition to tropospheric transport of inorganic NO_3^- from lightning, biomass burning and soil emissions (Lee et al., 2014). In the stratosphere, NO_3^- is produced through the stratospheric oxidation of nitrous oxide (N_2O) from extra-terrestrial fluxes of energetic particles and solar radiation (Savarino et al., 2007;Wolff, 1995;Wagenbach et al., 1998). A local secondary source of reactive nitrogen (nitrous acid (HONO), nitrogen oxides (NO_x)) originates from post-depositional processes driven by sunlight leading to re-emission from the snow pack and subsequent deposition (Savarino et al., 2007;Frey et al., 2009).

Local nitrogen dioxide (NO_2) emissions in Polar Regions are produced from NO_3^- photolysis in the snow pack under sunlit conditions (Jones et al., 2001;Honrath et al., 1999;Oncley et al., 2004). Once NO_x is produced by NO_3^- photolysis, it is expected to have a lifetime in the polar troposphere of <1 day before it is oxidised to nitric acid (HNO_3) at Dome C and South Pole (Davis et al., 2004b), and can then be redeposited to the skin layer (e.g. Mulvaney et al., 1998). Nitrate photolysis occurs at wavelengths (λ) = 290 - 345 nm with a maximum at 320 nm. Photolysis rate (J) depends on the adsorption cross section of NO_3^-, the quantum yield, and actinic flux within the snow pack. Photochemical production of NO_2 is dependent on the NO_3^- mass concentration in the snow pack, the snow pack properties, and the intensity of solar radiation within the snow pack. The latter is sensitive to solar zenith angle and snow optical properties, i.e., scattering and adsorption coefficients, which depends on snow density and morphology, and the light absorbing impurity content (e.g. dust and black carbon) (France et al., 2011;Erbland et al., 2015;Zatko et al., 2013). Model results from Zatko et al. (2016) suggest that the range of modelled NO_x fluxes from the snow pack to the overlaying air are similar in both Polar Regions due to the opposing effects of higher concentrations of both photolabile NO_3^- and light absorbing impurities in Antarctica and Greenland, respectively. At Concordia Station on Dome C in East Antarctica, the light penetration depth (e-folding depth) is ~10 cm for wind pack layers and ~20 cm for hoar layers (France et al., 2011). Based on the propagation of light into the snow pack, the snow pack can be divided into three layers. The first layer is known as the skin layer (5 mm thick) where direct solar radiation is converted into diffuse radiation. The second layer is called the active photic zone (below the skin layer layer), where solar radiation is effectively diffuse and the intensity of the radiation decays exponentially (Warren, 1982). The third layer is called the archived zone (below the active photic zone), where no photochemistry occurs.

Previous research has focused predominantly at Dome C on the high elevation polar plateau. Here, the exponential decay of NO_3^- mass concentrations in the snow pack, and thus post-depositional processing of NO_3^-, were attributed to either evaporation or ultraviolet (UV)-photolysis (Röthlisberger et al., 2000;Röthlisberger et al., 2002). The open debate of which post-depositional process controlled NO_3^- mass concentrations in the snow pack led to the use of a new isotopic tool, the nitrogen isotopic composition of NO_3^- ($\delta^{15}N\text{-}NO_3^-$; Blunier et al. (2005). More recently, theoretical (Frey et al., 2009), laboratory (Meusinger et al., 2014;Erbland et al., 2013;Erbland et al., 2015;Shi et al., 2019;Berhanu et al., 2014), and field (Erbland et al., 2013;Frey et al., 2009;Shi et al., 2015) evidence show that NO_3^- mass loss from the surface snow to the overlying atmosphere and its associated isotopic fractionation is driven by photolysis. Fractionation constants, which assume a Rayleigh single loss and irreversible process of NO_3^- removal from the snow between phases during evaporation-condensation processes, have been calculated to separate the isotopic signature of evaporation and photolysis processes. As this approach may oversimplify the processes occurring at the air-snow interface, Erbland et al. (2013) referred to the quantity as an "apparent" fractionation constant ($^{15}\varepsilon_{app}$). Thus, the apparent fractionation constant represents the integrated isotopic effect of the processes involving NO_3^- in the surface of the snow pack and in the lower atmosphere. Nitrate evaporation from the snow pack has a $^{15}\varepsilon_{app}$ of ~0 as determined by two independent studies (Erbland et al., 2013;Shi et al., 2019). This indicates that during NO_3^- evaporation, the air above the snow is not replenished and thus there is only a small NO_3^- mass loss. In comparison, fractionation constants associated with laboratory studies and field observations of NO_3^- photolysis are large: $^{15}\varepsilon_{app}$ = -34 ‰

Formatted: Not Superscript/ Subscript

(Berhanu et al., 2014;Meusinger et al., 2014) and -54< $^{15}\varepsilon_{app}$ <-60 ‰ (Frey et al., 2009;Erbland et al., 2013), respectively. The negative fractionation constant obtained from photolysis implies that the remaining NO_3^- in the skin layer snow is enriched in $\delta^{15}N$-NO_3^-. In turn, the atmosphere is left with the source of NO_x that is highly depleted in $\delta^{15}N$-NO_3^-. It follows that evaporation of NO_3^- is negligible on high-elevation Antarctic sites (Erbland et al., 2013;Shi et al., 2019).

At Dome C, the large redistribution and net mass loss of NO_3^- below the skin layer and the simultaneous isotopic fractionation of $\delta^{15}N$-NO_3^- in the snow pack indicates that post-depositional processes significantly modify the original NO_3^- mass concentration and $\delta^{15}N$-NO_3^- composition (Frey et al., 2009). Skin layer observations of $\delta^{15}N$-NO_3^- in the surface snow at Dome C show strong enrichment compared to the atmospheric $\delta^{15}N$-NO_3^- signature. Furthermore, snow pit profiles display an exponential decrease of NO_3^- mass concentration and an enrichment in the $\delta^{15}N$-NO_3^- composition with depth (Erbland et al., 2013).

This research at Dome C laid the foundation for Erbland et al. (2015) to derive a conceptual model of UV-photolysis induced post-depositional processes of NO_3^- at the air-snow interface. Transfer of Atmospheric Nitrate Stable Isotopes To the Snow (TRANSITS) is a conceptual multi-layer 1D model which aims to represent NO_3^- recycling at the air-snow interface including processes relevant for NO_3^- snow photochemistry (UV-photolysis of NO_3^-, emission of NO_x, local re-oxidation, deposition of HNO_3) and explicitly calculates NO_3^- mass concentrations and $\delta^{15}N$-NO_3^- in snow. The term “NO_3^- recycling” refers to the following processes. Nitrate on the surface of a snow crystal can be lost from the snow pack (Dubowski et al., 2001), either by UV-photolysis or evaporation. UV-photolysis produces NO, NO_2 and HONO while only HNO_3 can evaporate. Both of these processes produce reactive nitrogen that can be released from snow crystal into the interstitial air and rapidly transported out of the snow pack to the overlaying air via wind pumping (Zatko et al., 2013;Jones et al., 2000;Honrath et al., 1999;Jones et al., 2001). Here, NO_2 is either oxidised to HNO_3, which undergoes wet or dry deposition back to the skin layer within a day, or is transported away from the site (Davis et al., 2004a). If HNO_3 is re-deposited to the skin layer, it is available for NO_3^- photolysis and/or evaporation again. Any locally produced NO_2 and NO_3^- that is transported away from the site of emission represents a loss of NO_3^- from the snow pack. Nitrate recycling can occur multiple times before NO_3^- is eventually archived below the active photic zone in ice cores (Davis et al., 2008;Erbland et al., 2015;Zatko et al., 2016;Sofen et al., 2014).

Year round measurements of NO_3^- mass concentrations and $\delta^{15}N$-NO_3^- in the skin layer and atmosphere at Dome C have provided insights into the annual NO_3^- cycle in Antarctica (Fig. 1; Erbland et al. (2013). In the early winter, the stratosphere undergoes denitrification via formation of PSC. As PSC sediment slowly, there is a delay between the maximum stratospheric NO_3^- mass concentration and the maximum NO_3^- mass concentration deposited in the skin layer in late winter (Mulvaney and Wolff, 1993;Savarino et al., 2007). In spring, surface UV increases and initiates photolysis-driven post-depositional processes, which redistribute NO_3^- between the snow pack and overlying air throughout the sunlit summer season. This results in the $\delta^{15}N$-NO_3^- isotopic enrichment of the NO_3^- skin layer reservoir, and maximum atmospheric NO_3^- mass concentrations in October-November. In summer, NO_3^- resembles a strongly asymmetric distribution within the atmosphere-snow column with the bulk residing in the skin layer and only a small fraction in the atmospheric column above.

Nitrate is not preserved in the snow pack at sites with very low snow accumulation rates (i.e., Dome C: 2.5 - 3 cm yr^{-1}) because snow layers remain close to the surface and in contact with the overlaying atmosphere for a relatively long time enhancing the effect of post-depositional processes. At sites with low snow accumulation rates, the source signature of δ^{15}N-NO_3^- is erased by post-depositional process. Therefore, photolysis induced NO_3^- loss and δ^{15}N-NO_3^- fractionation is dependent on snow accumulation. Three distinct transects from coastal Antarctica to the East Antarctic Plateau show that NO_3^- fractionation is strongest with decreasing snow accumulation (Shi et al., 2018;Erbland et al., 2013;Noro et al., 2018). Skin layer NO_3^- mass concentrations are significantly higher at low snow accumulation sites, for example ~160 ng g^{-1} (winter) to 1400 ng g^{-1} (summer) at Dome C compared to 50 ng g^{-1} (winter) to 300 ng g^{-1} (summer) at Dumont d'Urville (DDU) on the Antarctic coast. In contrast to low snow accumulation sites, NO_3^- loss is less pronounced on the coast and seasonal cycles of NO_3^- mass concentration and δ^{15}N-NO_3^- are preserved in the snowpack (Shi et al., 2015;Erbland et al., 2013). Erbland et al. (2013) suggest that NO_3^- loss at the coast reflects both photolysis and evaporation processes, while Shi et al. (2015) proposes that NO_3^- loss at the coast cannot be fully explained by local post-deposition processes and that seasonal cycles in the snowpack reflect stratospheric and troposphere NO_3^- sources during the cold and warm seasons respectively. Furthermore, the strong inverse linear relationship between ice core NO_3^- mass concentration and accumulation rate was revealed in a composite of seven ice cores across Dronning Maud Land (DML; Pasteris et al. (2014). Over longer time scales, UV-driven post-depositional processing of NO_3^- is also driven by changes in the degree of post-depositional loss of NO_3^- with greater NO_3^- loss during the glacial period relative to the Holocene. The observed glacial-interglacial difference in post-depositional processing of NO_3^- is dominated by variations in snow accumulation rate (Geng et al., 2015).

Yet, NO_3^- photolysis leaves its own process-specific imprint in the snow pack (Shi et al., 2019;Erbland et al., 2015;Erbland et al., 2013), which opens up the possibility to use δ^{15}N-NO_3^- to infer past surface-UV variability (Frey et al., 2009). However, NO_3^- photolysis rates in snow depend on a number of site-specific factors as does the degree of photolytic isotopic fractionation of NO_3^- eventually preserved in ice cores (Erbland et al., 2013;Berhanu et al., 2014). These factors need to be quantitatively understood at a given ice core site to enable quantitative interpretation of ice core records. Here, we carry out a comprehensive study of the air-snow transfer of NO_3^- at Kohnen Station in DML, East Antarctica through δ^{15}N-NO_3^- measurements in the atmosphere, skin layer and snow pits, and compare the observations to Dome C. Due to the previous research outlined above, we assume that the photolysis is the dominant driver of NO_3^- post-depositional processes, and later assess the validity of this this assumption (section 4.3). We apply the TRANSITS model (Erbland et al., 2015) to i) understand how NO_3^- mass concentrations and δ^{15}N-NO_3^- values are archived in deeper snow and ice layers, and ii) investigate the sensitivity of changes in the past snow accumulation rate, snowfall timing, e-folding depth of the snow photic zone, and total column ozone (TCO) on the δ^{15}N-NO_3^- signature. In order to interpret this novel UV proxy, it is paramount to understand the air-snow transfer processes specific to an ice core site, and how δ^{15}N-NO_3^- is archived in the deeper snow and ice layers (Geng et al., 2015;Morin et al., 2009;Erbland et al., 2015). Within the framework of the Isotopic Constraints on Past Ozone Layer Thickness in Polar Ice (ISOL-ICE) project, this study provides a basis for the interpretation of δ^{15}N-NO_3^- from a 1000-year ice core recovered in 2016/17 at Kohnen Station.

2 Methods

The ISOL-ICE project aims to understand natural causes of past TCO variability by i) investigating the~~an~~ air-snow exchange processes~~study~~ of NO_3^-, to enable the interpretation of ice core records of NO_3^- and $\delta^{15}N\text{-}NO_3^-$, ii) reconstructing a 1000-year record of UV using a new ice core proxy based on $\delta^{15}N\text{-}NO_3^-$ (Ming et al., submitted; Winton et al., 2019a), and iii) numerical modelling of the natural causes of TCO variability. In the air snow-transfer study presented here, we report new atmospheric, skin layer and snow pit NO_3^- mass concentration and $\delta^{15}N\text{-}NO_3^-$ observations from DML, and compare them to new and published (Erbland et al., 2015;Erbland et al., 2013;Frey et al., 2009) observations from Dome C. Published data from Dome C comprises year round atmospheric and skin layer measurements from 2009-2010 (Erbland et al., 2013), and multiple snow pit profiles (Erbland et al., 2013;Frey et al., 2009). New data from Dome C encompasses an ~~We present a new~~ extended time series at Dome C of ~~year round~~year-round atmospheric and skin layer NO_3^- mass ~~and~~concentration, and $\delta^{15}N\text{-}NO_3^-$ from 2011 - 2015.

Formatted: Not Superscript/ Subscript

Formatted: Not Superscript/ Subscript

Formatted: Not Superscript/ Subscript

2.1 Study sites

The ISOL-ICE campaign was carried out at the summer only, continental Kohnen Station where the deep European Project for Ice Coring in Antarctica (EPICA) Dronning Maud Land (EDML; 75°00' S, 0°04' E; 2982 m a.s.l.; https://www.awi.de/en/expedition/stations/kohnen-station.html) ice core was recovered in 2001 - 2006 to a depth of ~2800 m (Wilhelms et al., 2017). As part of the ISOL-ICE campaign, a new ice core (ISOL-ICE; Winton et al. (2019a)~~)~~ was drilled 1 km from the EDML borehole (Figs. 2a-b). In addition, the ISOL-ICE air-snow transfer study site was located ~200 m from the EDML ice core site (Fig. 2c). Here we compare two ice core drilling sites in Antarctica: Kohnen Station (referred to as DML henceforth) and ~~EPICA~~ Dome C (75°05'59" S, 123°19'56" E; ~~)~~ (Fig. 2). Both sites are similar in terms of the latitude and therefore in terms of radiative forcing at the top of the atmosphere (Table 1). Satellite images of TCO over Antarctica show that the lowest annual TCO values are centred over the South Pole region encompassing DML and usually Dome C although the spatial variability is significant from year to year (https://ozonewatch.gsfc.nasa.gov/). The sites are different in terms of their location with respect to moisture source, elevation and precipitation regime. The DML site is situated ~550 km from the ice shelf edge, is subject to cyclonic activity and receives ~80 % of its precipitation from frontal clouds (Reijmer and Oerlemans, 2002). ~~While~~ Dome C is more remote (~1100 km from the coast) and diamond dust is the dominant form of precipitation. The annual snow accumulation rate also differs between the sites; while both sites have exceptionally low accumulation compared to the coast, DML (annual mean: 6 cm yr^{-1} (water equivalent (~~;~~w.e.)~~)~~; Hofstede et al. (2004);Sommer et al. (2000)~~)~~ receives more than double that of Dome C (annual mean: 2.5 cm yr^{-1} (w.e.)~~);~~~~)~~ Le Meur et al. (2018). ~~Throughout the study we refer to our sampling site as "DML".~~

2.2 Snow and aerosol sampling

Daily skin layer samples, ~~(which we~~ operationally defined as the top 5 mm of the snow pack following Erbland et al. (2013),~~)~~ were collected from the DML site (Fig. 2c) in January 2017 during the ISOL-ICE ice core drilling and ~~atmospheric monitoring~~air-snow transfer campaign. To prevent contamination from the nearby Kohnen Station, snow samples were collected from the "flux site" within the station's designated clean air sector (defined as 45° from both ends of the station building) located ~1 km from the station (Fig. 2c). The skin layer samples were ~~was~~ collected in polyethylene bags (Whirl-pak®) using a stainless steel trowel. A total of 45 skin layer samples were collected daily between 31 December 2016 and 29 January 2017 from a designated sampling site ~~each day~~ during the campaign (75°00.184' S, 000°04.527' E; Fig. 2c). To determine the spatial variability of NO_3^- in the skin layer at the flux site, an additional five skin layer samples were collected in a ~2500 m^2 area of the flux site (75°00.161' S - 000°04.441' E, 75°00.175' S - 000°04.518' E; Fig. 2c).

Adjacent to the skin layer samples, snow was sampled from a 1.6 m snow pit at the flux site (snow pit B; Fig. 2c) and a 2 m snow pit at the "ice core" site (snow pit A; Fig. 2b). Two parallel profiles were sampled~~, i)~~ for i) major ion mass concentrations (including NO_3^-) collected in pre-washed 50 mL Corning® centrifuge tubes at 3 cm resolution by inserting the tube directly into the snow face, and ii) ~~for~~ stable NO_3^- isotope analysis collected in Whirl-pak® bags at 2 cm resolution using a custom-made ~~stainless steel~~stainless-steel tool. Exposure blanks (following the same method as the samples by opening the tube/ Whirl-pak® bag at the field site but not filling the sample container with snow) were also collected for both types of samples. Snow density and temperature were measured every 3 cm, and a visual log of snow pit stratigraphy was recorded.

Daily aerosol filters were collected using high-volume aerosol samplers custom-built at the Institute of Environmental Geosciences (IGE), University of Grenoble-Alpes, France described previously (Frey et al., 2009; Erbland et al., 2013). The high-volume aerosol sampler collected atmospheric aerosol on glass fibre filters (Whatman GF/A filter sheets; 20.3 × 25.4 cm) at an average flow rate of 1.2 $m^3\ min^{-1}$ at standard temperature and pressure (STP; temperature: 273.15 K; pressure: 1 bar) to determine the ~~c~~mass concentration and isotopic composition of atmospheric NO_3^-. It is assumed that the atmospheric NO_3^- collected on glass fibre filters represents the sum of atmospheric particulate NO_3^- and HNO_3 (gas phase). The bulk of HNO_3 present in the gas phase is most likely adsorbed to aerosols on the filter, as described previously (Frey et al., 2009). Following the terminology of Erbland et al. (2013), we refer to "atmospheric NO_3^-" as the combination (i.e., total) of HNO_3 (gas phase) and particulate NO_3^- and is represented by the NO_3^- mass concentrations measured on aerosol filters.

The high-volume aerosol sampler was located 1 m above the snow surface at the flux site at the DML site (Fig. 2c), where a total of 35 aerosol filters were sampled daily between 3 and 27 January 2017. In addition, we coordinated an intensive 4-hour sampling campaign in phase with Dome C, East Antarctica (Fig. 2) between 21 and 23 January 2017. At Dome C, a high-volume aerosol sampler wa~~i~~s located on the roof of the atmospheric shelter (6 m above the snow surface), where a total of 12 samples were collected. At DML, loading and changing of aerosol collection substrates was carried out in a designated clean area. Aerosol laden filters were transferred into individual double zip-lock plastic bags immediately after collection and stored frozen until analysis at the British Antarctic Survey (BAS; major ions) and IGE (NO_3^- isotopic composition). For the atmospheric NO_3^- work, three types of filter blanks were carried out; i) laboratory filter blanks (n = 3; Whatman GF/A filters that underwent the laboratory procedures without going into the field), ii) procedural filter blanks (DML: n = 4; Dome C: n = 1; filters that had been treated as for normal samples but which were not otherwise used; once a week, during daily filter change-over, a procedural blank filter was mounted in the aerosol collector for 5 min without the collector pump in operation – this type of filter provides an indication of the operational blank associated with the sampling procedure), and iii) 24 h exposure filter blanks sampled at the beginning and end of the field campaign (DML: n = 2; Dome C: n = 1; filters treated like a procedural blank but left in the collector for 24 h ~~without switching the collector on~~). All samples were kept frozen below -20 ºC during storage and transport prior to analysis.

In addition, skin layer and aerosol samples w~~have been~~ere sampled continuously at Dome C over the period 2009-2015 following Erbland et al. (2013);Frey et al. (2009). The sampling resolution for skin layer wa~~i~~s every 2-4 days, and weekly for aerosol samples. Data from 2009-2010 have previously been published by Erbland et al. (2013), and we report the 2011 - 2015 data here (Fig. 1).

2.3 Major ion mass concentrations in snow and aerosol

~~Aerosol~~ Atmospheric NO_3^- and other major ions were extracted in 40 mL of ultra-pure water (resistivity of 18.2 MΩ; Milli-Q water) by centrifugation using Millipore Centricon® Plus-70 Filter Units (10 kD filters) in a class-100 clean room at ~~the~~ BAS. Major ion mass concentrations in DML snow samples were determined in an aliquot of melted snow from skin layer and snow pit samples, and aerosol extracts by suppressed ion chromatography (IC) using a Dionex™ ICS-4000 Integrated Capillary HPIC™ System ion chromatograph. A suite of anions, including NO_3^-, chloride (Cl^-), methanesulfonic acid (MSA) and sulphate (SO_4^{2-}), were determined using an AS11-HC column and a CES 500 suppressor. Cations, including sodium (Na^+), were determined using a CS12A column and a CES 500 suppressor. During the course of the sample sequence, instrumental blank solutions and certified reference materials (CRM; ERM-CA616 groundwater standard and ERM-CA408 simulated rainwater standard; Sigma-Aldrich) were measured regularly for quality control and yielded an accuracy of 97 % for NO_3^-. Nitrate mass concentrations in Dome C samples were determined by colorimetry at IGE following the procedure described in Frey et al. (2009). Blank concentrations for exposure blank, procedural blank and laboratory blank and detection limits are reported in Table S1. The non-sea-salt sulphate (nss-SO_4^{2-}) fraction of SO_4^{2-} was obtained by subtracting the contribution of sea-salt-derived SO_4^{2-} from the measured SO_4^{2-} mass concentrations (nss-SO_4^{2-} = SO_4^{2-} - 0.252 × Na^+, where Na^+ and SO_4^{2-} are the measured concentrations in snow pit samples and 0.252 is the SO_4^{2-}/ Na^+ ratio in bulk seawater (Keene et al., 1986).

2.4 Nitrate isotopic composition in snow and aerosol

Samples were shipped frozen to IGE where the NO_3^- isotope analysis was performed. The denitrifier method was used to determine the stable NO_3^- isotopic composition in samples at IGE following Morin et al. (2008). Briefly, samples were pre-concentrated due to the low NO_3^- mass concentrations found in the atmosphere and snow over Antarctica. To obtain 100 nmol of NO_3^- required for NO_3^- isotope analysis, the meltwater of snow samples and aerosol extracts ~~were~~ were sorbed onto 0.3 mL of anion exchange resin (AG1-X8 chloride form; Bio-Rad) and eluted with 5 x 2 mL of 1 M NaCl (high purity grade 99.0 %; American Chemical Society (ACS grade); AppliChem Panreac) following Silva et al. (2000). Recovery tests yielded 100 % recovery of NO_3^- (Frey et al., 2009;Erbland et al., 2013). Once pre-concentrated, NO_3^-, wa~~i~~s converted to N_2O gas by denitrifying bacteria, *Pseudomonas aureofaciens*. The N_2O wa~~i~~s split into O_2 and N_2 on a gold furnace heated to 900 °C followed by gas chromatographic separation and injection into the isotope ratio mass spectrometer (IRMS) for duel O and N analysis using a Thermo Finnigan™ MAT 253 IRMS equipped with a GasBench II™ and coupled to an in-house-built NO_3^- interface (Morin et al., 2009).

Formatted: Not Superscript/ Subscript

Certified reference materials (IAEA USGS-32, USGS-34 and USGS-35; Böhlke et al., 1993; Böhlke et al., 2003) were prepared (matrix match 1 M NaCl in identical water isotopic composition as samples; ACS grade) and subject to the same analytical procedures as snow and aerosol samples. The nitrogen isotopic ratio was referenced against N_2-Air (Mariotti, 1983). We report $^{15}N/^{14}N$ of NO_3^- ($\delta^{15}N$-NO_3^-) as δ-values following Eq. (1).

$$\delta^{15}N\text{-}NO_3^- = (^{15}N/^{14}N_{sample} / ^{15}N/^{14}N_{standard} - 1) \quad (1)$$

For each batch of 60 samples, the overall accuracy of the method wa~~i~~s estimated as the reduced standard deviation of the residuals from the linear regression between the measured reference materials (n = 16) and their expected values. For the snow (n = 118) and aerosol samples (n = 35), the average uncertainty values obtained for $\delta^{15}N$ was 0.5 ‰ for both datasets.

2.5 Light attenuation through the snow pack (e-folding depth)

Measurements of light attenuation through the snow pack were made at the two snow pit sites during the ISOL-ICE campaign following a similar approach of previous studies (France and King, 2012;France et al., 2011). Vertical profiles of down-welling irradiance in the top 0.4 m of the snow pack were measured using a high-resolution spectrometer (HR4000; Ocean Optics) covering a spectral range of 280 to 710 nm. To do this, a fiber optic probe attached to the spectrometer and equipped with a cosine corrector with spectralon diffusing material (CC-3-UV-S; Ocean Optics) was inserted into the snow to make measurements at approximately 0.03 m depth intervals. The fiber optic probe was either inserted horizontally into pre-cored holes, at least 0.5 m in length to prevent stray light, into the side wall of a previously dug snow pit or pushed gradually into the undisturbed snow pack starting at the surface at a 45º angle, which was maintained by a metal frame. Most measurements with integration time ranging between 30 and 200 ms were carried out at noon to minimise changing sky conditions, and each vertical snow profile was completed within 0.5 hr. The spectrometer was calibrated against a known reference spectrum from a Mercury Argon calibration source (HG-1; Ocean Optics), dark spectra were recorded in the field by capping the fibre optic probe and spectral irradiance was then recorded at depth relative to that measured right above the snow surface.

The e-folding depth was then calculated according to the Beer-Bouguer Lambert law. Stratigraphy of the snow pack recorded at each site showed presence of several thin (10 mm) wind crust layers over the top 0.4 m of snow pack. However, calculating e-folding depths for each layer in between wind crusts yielded inconclusive results. Therefore, reported e-folding depths (Fig. S1, Table S2) are based on complete profiles integrating potential effects from wind crust layers. ~~Resulting e-folding depths relevant for the photolysis of NO_3^- (Table S2) show significant standard deviations, and also considerable variability (0.9-4.0~~

~~cm) between profiles, which reflect both systematic experimental errors as well as spatial variability of snow optical properties. They are lower than at Dome C but similar to previous model estimates for South Pole (France et al., 2011;Wolff et al., 2002). The origin of the reduced e-folding depth relative to Dome C is not known but is likely due to greater HUmic-LIke Substances (HULIS) content or different snow morphology (Libois et al., 2013;Zatko et al., 2013).~~ We use e-folding depths observed in this study at DML and those reported previously at Dome C as guidance for our model sensitivity study to quantify the impact of the variability of e-folding depth on archived $\delta^{15}N-NO_3^-$ in snow.

2.6 Nitrate photolysis rate coefficient

Hemispheric or 2π spectral actinic flux from 270 to 700 nm was measured at 2.1 m above the snow surface using an actinic flux spectroradiometer (Meteorologieconsult GmbH; Hofzumahaus et al. (2004). 2π NO_3^- photolysis rate coefficients $J(NO_3^-)$ were then computed using the NO_3^- absorption cross section and quantum yield on ice estimated for -30 ºC from Chu and Anastasio (2003). The mean 2π $J-NO_3^-$ value at DML during January 2017 was 1.02×10^{-8} s^{-1}, and 0.98×10^{-8} s^{-1} during the 1 to 14 January 2017 period. The observed 2π $J(NO_3^-)$ at DML was a factor of three lower than Dome C (2.97×10^{-8} s^{-1}; 1 to 14 January 2012) which was previously measured using the same instrument make and model, and at the same latitude (Kukui et al., 2013). Only ~5 % of the apparent inter-site difference can be attributed to TCO being ~25 DU larger at DML (306 DU) than at Dome C (287 DU) during the comparison period. The remainder was possibly due to greater cloudiness at DML and differences in calibration. In this study, the observed 2π $J(NO_3^-)$ is used to estimate the snow emission flux of NO_2.

2.7 Air-snow transfer modelling

In order to evaluate the driving parameters of isotope air-snow transfer at DML we used the TRANSITS model (Erbland et al., 2015) to simulate snow depth profiles of NO_3^- mass concentration and $\delta^{15}N-NO_3^-$ and compare them to our observations. ~~TRANSITS is a conceptual multi-layer 1D model which aims to represent NO_3^- recycling at the air-snow interface including processes relevant for NO_3^- snow photochemistry (UV-photolysis of NO_3^-, emission of NO_x, local oxidation, deposition of HNO_3) and explicitly calculates NO_3^- mass concentrations and $\delta^{15}N-NO_3^-$ in snow.~~ Due to the reproducible depth profile of observed $\delta^{15}N-NO_3^-$ within 1 km (section 3.3), we assume the $\delta^{15}N-NO_3^-$ composition is spatially uniform at DML and thus a 1D model is appropriate for ~~our~~ the site. The atmospheric boundary layer in the model is represented by a single box above the snow pack. The 1 m snow pack is divided into 1000 layers of 1 mm thickness. Below the photic zone of the snow pack, the NO_3^- mass concentrations and $\delta^{15}N-NO_3^-$ values are assumed to be constant and thus archived during the model run. The model is run for 25 years (with a timestep of one week), which is sufficient to reach steady state. The input data is provided in Table S3.

Photolysis rate coefficients of NO_3^- ($J(NO_3^-)$) above and within the snowpack are used by the TRANSITS model runs as input for this study, and are modelled off-line using the tropospheric ultraviolet and visible (TUV)-snow radiative transfer model (Lee-Taylor and Madronich, 2002). The following assumptions were made: i) a clear aerosol-free sky, ii) extra-terrestrial irradiance from Chance and Kurucz (2010), and iii) a constant Earth-Sun distance as that on 27 December 2010 (Erbland et al., 2015). The TUV-snow radiative transfer model was constrained by optical properties of the Dome C snow pack (France et al., 2011), notably an e-folding depth of i) 10 cm in the top 0.3 m, and ii) 20 cm below 0.3 m (Erbland et al., 2015), to compute J($^{14/15}NO_3^-$) profiles as a function of solar zenith angle (SZA) and TCO (Erbland et al., 2015) (Fig. S2; dashed lines).

The set up used in this paper is similar to Erbland et al. (2015) except for the following modifications. We use the TCO from the NIWA Bodeker combined dataset version 3.3, at the location of the snow pit site, averaged from 2000 to 2016 (http://www.bodekerscientific.com/data/total-column-ozone). The year-round atmospheric NO_3^- mass concentrations are~~is~~ taken from Weller and Wagenbach (2007), and the meteorology data is taken from Utrecht University A~~a~~utomatic ~~weather~~ Weather Station (AWS) at DML05/Kohnen (AWS9; https://www.projects.science.uu.nl/iceclimate/aws/files_oper/oper_20632). The snow accumulation rate is set to 6 cm yr^{-1} (w.e.~~)~~; Sommer et al. (2000), and we refer to this simulation as our "base case" scenario. We carried out a sensitivity analysis to evaluate the impact of variable accumulation rate, timing of snowfall, and e-folding depth on the snow profile of NO_3^- ~~a~~mass concentrations and $\delta^{15}N\text{-}NO_3^-$. Our first set of sensitivity tests account for the new e-folding depth measurements at the DML site; the e-folding depth was varied within the range of observations from this study and previously at Dome C. The second set of sensitivity tests use an e-folding depth of 5 cm and ~~The sensitivity tests~~ were as followes~~d~~: the snow accumulation rate was varied between the bounds seen in the last 1000-years at DML; the snow accumulation rate was varied from year to year according to observations from our snow pit profile which ranged between 6.0 and 7.1 cm yr^{-1} (w.e.);~~-~~ and the timing of the snow accumulation was varied throughout the year~~; and the e-folding depth was varied within the range of observations from this study and previously at Dome C~~. We compare the second set of sensitivity tests to the 5 cm e-folding depth scenario and refer to this as our "5 cm EFD (e-folding depth) case" (section 4.5). To evaluate the sensitivity of archived $\delta^{15}N\text{-}NO_3^-$ to e-folding depth, changes in the J($^{14/15}NO_3^-$) profiles for Dome C (Erbland et al., 2015) were recalculated and used as TRANSITS input by scaling the surface value of J($^{14/15}NO_3^-$) with a new e-folding depth (2, 5, 10, 20 cm). An example is shown in Fig. S2a for SZA = 70º, TCO = 300 DU and an e-folding depth of 5 cm. The top 2 mm are retained from the Dome C ~~base~~ case in Erbland et al. (2015) to account for non-linearities in snow radiative transfer in snow, which are strongest in the non-diffuse zone right below the snow surface (Fig. S2b). It is noted that TUV-snow model estimates of down-welling or 2π J(NO_3^-) above the snow surface at the latitude of Dome C or DML (75º S) compare well to observations at Dome C in January 2012, whereas they are a factor three higher than measurements at DML in January 2017 (Table S4 and section 2.6). This should not affect the results of the sensitivity study, which aims to explore relative changes of archived $\delta^{15}N\text{-}NO_3^-$ due to a prescribed change in e-folding depth.

TRANSITS calculates the average number of recyclings undergone by the archived NO_3^-, i.e., below the zone of active photochemistry. In TRANSITS, the average number of recyclings undergone by NO_3^- in a given box (snow layer or atmosphere) is represented by a tracer (or counter) called CYCL. The CYCL value for primary NO_3^- is set to 0, and CYCL variables in the boxes are incremented by 1 each time NO_2 molecules cross the air-snow interface. The average number of

Formatted: Font color: Auto

Formatted: Not Superscript/ Subscript

Formatted: English (United Kingdom)

Formatted: Subscript

recyclings is calculated as a mass weighted average of the CYCL values of the 52 snow layers (representing one week of snowfall) which are archived below 1 m over the course of 1 year, in order to average out any seasonal variability. Erbland et al. (2015) notes that the number of recyclings represents an average value for the archived NO_3^-, i.e., considering individual ions in the archived NO_3^-, the number of recyclings could be variable as some ions may have travelled through the entire snowpack zone of active photochemistry without being recycled, while some underwent many recyclings.

Formatted: English (United Kingdom)

3 Results

3.1 Snow pit dating

Dating of the snow pits was based on the measured concentrations of Na^+, MSA, and nss-SO_4^{2-} following previous aerosol and ice core studies at DML (Göktas et al., 2002;Weller et al., 2018). Here, Na^+ mass concentrations have a sharp, well-defined peak in the austral spring/late winter, while MSA and nss-SO_4^{2-}, primarily derived from the biogenic production of dimethylsulfide (DMS), record maximum concentrations in the austral autumn. Non-sea salt SO_4^{2-} (nss-SO_4^{2-}) often displays a second peak corresponding to late austral spring/summer sometimes linked to MSA. Spring seasons were defined as 1 September and positioned at the Na^+ peak, while autumn seasons were defined as 1 April and positioned where a MSA and nss-SO_4^{2-} peak aligned (Fig. S3). Annual layer counting of Na^+ layers shows that snow pit A spans 8 years from autumn 2009 to summer 2017 and snow pit B spans 9 years from summer 2008 to summer 2017 with an age uncertainty of ± 1 year at the base of the snow pit. The mean snow accumulation rate for the snow pits is estimated to be 6.3 ± 1.4 cm yr^{-1} (w.e.), consistent with published accumulation rates of 6.0 - 7.1 cm yr^{-1} (w.e.) from snow pits and ice cores from DML (Sommer et al., 2000;Hofstede et al., 2004;Oerter et al., 2000).

3.2 Nitrate mass concentrations

Atmospheric NO_3^- mass concentrations ($C_{aerosol}$) were estimated from high-volume aerosol filters by the ratio of total NO_3^- mass loading to the total volume of air pumped through the filter at STP conditions following Eq. (2), and assuming a uniform loading of the aerosol filter.

$$C_{aerosol} = NO_3^- \text{ mass loading / air volume (STP)} \qquad (2)$$

Aerosol mass concentrations range from 0.5 to 19 ng m^{-3} and show a downward trend throughout January 2017 (R^2=0.55; p= <0.001; Fig. 3). In contrast, NO_3^- mass concentrations in the skin layer increase during the month from 136 to 290 ng g^{-1}. Nitrate mass concentrations in both snow pits, which range from 23 to 142 ng g^{-1}, are substantially lower than those in the skin layer. Compared to Dome C, average annual atmospheric, skin layer and snow pit mass concentrations are lower at DML (Table 2), in agreement with higher NO_3^- mass concentrations found at lower snow accumulation sites (Erbland et al., 2013). The NO_3^- mass concentration profile in the upper 50 cm of the snow pack at Dome C shows an exponential decrease with depth and becomes relatively constant at 35 ng g^{-1} at 20 cm compared to 160 - 1400 ng g^{-1} in the skin layer (Figs. 1 and 4; (Erbland et al., 2013;Frey et al., 2009). While the highest NO_3^- mass concentrations in the snow pack at DML are also found in the skin layer, the mass concentration profile exhibits a different pattern. The sharp decrease in NO_3^- mass concentration occurs in the top ~5 mm at which point the snow pit records inter-annual variability in the NO_3^- mass concentration. Nitrate mass concentrations at DML exhibit a maximum in summer and ~~winter~~ minimum in winter. Although the Dome C depth profiles of NO_3^- mass concentration do not record seasonal variability, year-round measurements of skin layer and atmospheric NO_3^- mass concentrations exhibit sharp maximum during sunlit conditions in spring and summer and low mass concentrations in winter. This annual cycle is consistent both i) spatially across Antarctica (McCabe et al., 2007;Wolff et al., 2008;Erbland et al., 2013;Frey et al., 2009), and ii) temporally over last 7 years (Fig. 1) (Erbland et al., 2015;Erbland et al., 2013;Frey et al., 2009).

While the precision of the IC measurement of NO_3^- is better than 2 %, the spatial variability at DML of NO_3^- in the skin layer exceeds this. During the sampling campaign, five skin layer samples were taken from an area of ~2500 m^2 at the flux site (snow surface had sastrugi up to 10 cm) to understand how representative the snow pit mass concentrations are of the greater study area. We found that the spatial variability of NO_3^- mass concentrations and $\delta^{15}N\text{-}NO_3^-$ at DML was 10 % and 17 % respectively (Fig. 3c-d). At Dome C, the spatial variability of NO_3^- mass concentrations wa~~i~~s between 15 and 20 %. We note that this variability includes the natural spatial variability and the operator sampling technique.

3.3 Isotopic composition of nitrate

Atmospheric $\delta^{15}N\text{-}NO_3^-$ ranges from -49 to -20 ‰ at DML and -9 to 8 ‰ at Dome C during the January campaign, and is depleted with respect to the skin layer, which ranges from -22 to 3 ‰ at DML (Fig. 3). Similar to the NO_3^- mass concentrations, the $\delta^{15}N\text{-}NO_3^-$ in the depth profile at DML exhibits large variability between seasons (-3 to 99 ‰) with more enriched values in spring and summer with respect to winter (Fig. 4). The $\delta^{15}N\text{-}NO_3^-$ values in both snow pits at DML show extremely good reproducibility with depth indicating there is little spatial variability within 1 km at the site (Fig. 4). The $\delta^{15}N\text{-}NO_3^-$ in snow pits at Dome C does not preserve a seasonal cycle. However, in parallel with the exponential decay of NO_3^- mass concentrations with depth at Dome C, there is a strong increase in the $\delta^{15}N\text{-}NO_3^-$ with depth. At Dome C, $\delta^{15}N\text{-}NO_3^-$ increases up to 250 ‰ in the top 50 cm, this increase is weaker at DML (up to ~~8~~100 ‰ in the top 30~~10~~ cm at which point seasonal cycles are evident). At Dome C, although no annual cycle is preserved in the snow pack, the year-round measurements of atmospheric $\delta^{15}N\text{-}NO_3^-$ show a~~in the~~ ~~atmosphere~~ decrease during sunlit conditions in spring and summer (Fig. 1). While the $\delta^{15}N\text{-}NO_3^-$ in the skin layer has a spring minimum that increases to a maximum at the end of summer (Fig. 1). Skin layer $\delta^{15}N\text{-}NO_3^-$ is about 25 ‰ higher than atmospheric $\delta^{15}N\text{-}NO_3^-$. Nitrate mass concentration and $\delta^{15}N\text{-}NO_3^-$ composition data for aerosol, skin layer and snow pit samples are available in Winton et al. (2019b).

Formatted: Not Superscript/ Subscript

3.4 Archived nitrate mass concentration and isotopic composition

We calculate archived values of NO_3^- mass concentration and $\delta^{15}N\text{-}NO_3^-$ which represent the archived mass fraction and isotopic composition reached below the photic zone. Archived values were calculated by averaging the NO_3^- mass concentration and $\delta^{15}N\text{-}NO_3^-$ values below the photic zone, i.e., ~~30~~ 15 cm (section ~~4.4~~4.4). The archived NO_3^- mass

Formatted: Not Superscript/ Subscript

concentration and δ^{15}N-NO_3^- values for snow pit A were 60 ng g^{-1} and 50 ‰,~~ the~~ and the archived NO_3^- mass concentration for snow pit B was 50 ng g^{-1}. Note that no δ^{15}N-NO_3^- values were measured below 30 cm in snow pit B. Observed~~These measured~~ δ^{15}N-NO_3~~$^-$~~ values are half of those expected for a site with a snow accumulation rate of 6 cm yr^{-1} (w.e.) in the spatial survey from Erbland et al. (2013) (Table 2).

3.5 Nitrate mass flux estimates

The total deposition flux (F) of NO_3^- is partitioned into wet and dry deposition fluxes (F_{wet} and F_{dry} respectively; Eq. (3)~~)~~, and can be estimated using the measured mass concentration of NO_3^- in the snow pack (C_{snow}) and the local snow accumulation rate (A; Eq. (4)~~)~~. Estimates of the dry deposition rate (F_{dry}) of NO_3^- were calculated using Eq. (5) using the atmospheric mass concentrations of NO_3^- ($C_{aerosol}$) and a dry deposition velocity ($V_{dry\ deposition}$) of 0.8 cm s^{-1}, and are reported in Table S5. This deposition velocity is based on the dry deposition of HNO_3 at South Pole (Huey et al., 2004) which has a similar snow accumulation rate (6.4 cm yr^{-1} (w.e.); Mosley-Thompson et al. (1999)~~)~~ to DML. Other estimates of dry deposition velocities include 0.05 - 0.5 cm s^{-1} for HNO_3 over snow (Hauglustaine et al., 1994;Seinfeld and Pandis, 1998), 1.0 cm s^{-1} for NO_3^- over the open ocean (Duce et al., 1991), and an apparent deposition velocity of 0.15 cm s^{-1} for summer HNO_3 at Dome C (Erbland et al., 2013). The estimated apparent NO_3^- deposition velocity at Dome C is low because of the strong recycling of NO_3^- on the polar plateau in summer, i.e., reactive nitrogen is re-emitted from the skin layer to the atmosphere. Although gas phase HNO_3 and particulate NO_3^- have different dry deposition rates~~Thus~~, the dry deposition velocity at DML is likely to lie between 0.15 and 0.8 cm s^{-1}. We assume that a constant deposition velocity throughout the campaign is appropriate for DML.

Formatted: Subscript

$$F = F_{wet} + F_{dry} \qquad (3)$$

$$C_{snow} = F / A \qquad (4)$$

$$F_{dry} = C_{aerosol} V_{dry\ deposition} \qquad (5)$$

Note that Eq. (4) does not take into account post-depositional processes of non-conservative ions, such as NO_3^-. We follow the approach of Erbland et al. (2013) who use an archived NO_3^- mass flux (F_a) to represent the downward NO_3^- mass flux which escapes the photic zone towards deeper snow layers. Using simple mass balance, we can then estimate the mass flux of NO_3^- ($F_{re\text{-}emit}$), which is re-emitted from the snow pack to the overlaying atmosphere (Eq. (6)).

$$F_{re\text{-}emit} = F - F_a \qquad (6)$$

Taking this~~a~~ simple mass balance approach, a schematic of NO_3^- mass fluxes for two scenarios are illustrated in Fig. 5~~a~~. Scenario 1 is an average annual budget for DML (Fig. 5a). As the atmospheric campaign did not cover an entire annual cycle, we use estimates of atmospheric NO_3^- mass fluxes at DML reported by Pasteris et al. (2014) and Weller and Wagenbach (2007) of 43 and 45 pg m^{-2} s^{-1}, respectively, as ~~a~~ year round dry deposition fluxes. Due to the linear relationship of ice core NO_3^- mass concentrations with the inverse accumulation, the authors assume that the magnitude of the dry deposition flux is homogenous over the DML region. Mean annual mass concentrations of NO_3^- in our snow pits suggest a total NO_3^- deposition mass flux of 110 pg m^{-2} s^{-1} and therefore a wet deposition mass flux of 65 pg m^{-2} s^{-1}.

However, at relatively low snow accumulation sites where photolysis drives the fractionation of NO_3^- from the surface snow to atmosphere (Frey et al., 2009), it is necessary to take into account the skin layer in the NO_3^- mass flux budget as this air-snow interface is where air-snow transfer of NO_3^- takes place. In scenario 2, w~~W~~e ~~us~~utilise~~e~~ the available NO_3^- mass concentrations measured in aerosol, skin layer, and snow pits from the ISOL-ICE campaign to estimate the mass flux budget for January 2017 (Fig. 5b). The dry deposition mass flux of atmospheric NO_3^- during January 2017 at DML averages 64 ± 38 pg m^{-2} s^{-1} (Table S5). The NO_3^- mass flux to the skin layer is 360 pg m^{-2} s^{-1}, however only 110 pg m^{-2} s^{-1} of NO_3^- is archived. Considering the active skin layer, only 30 % of deposited NO_3^- is archived in the snow pack while 250 pg m^{-2} s^{-1} is re-emitted to the overlaying atmosphere.

3.~~6~~ 6 Fractionation constants

Fractionation constants were calculated following the approach of Erbland et al. (2013). ~~which assumes a Rayleigh single loss and irreversible process of NO_3^- removal from the snow. As this approach may oversimplify the processes occurring at the air-snow interface, Erbland et al. (2013) referred to the quantity as an "apparent" fractionation constant. Thus, the apparent fractionation constant represents the integrated isotopic effect of the processes involving NO_3^- in the surface of the snow pack and in the lower atmosphere.~~ The apparent fractionation constant is denoted as $^{15}\varepsilon_{app}$ and calculated using Eq. (7).

$$\ln(\delta^{15}N f + 1) = {}^{15}\varepsilon \times \ln f + \ln(\delta^{15}N_0 + 1) \qquad (7)$$

where $\delta^{15}N f$ and $\delta^{15}N_0$ are the δ-values in the initial and remaining NO_3^-, and f is the remaining NO_3^- mass concentration. The ε values are related to the commonly used fractionation factor α by $\varepsilon = \alpha - 1$. The $^{15}\varepsilon_{app}$ derived for snow pits in the photic zone is 12 ‰.

3.7 Light attenuation through the snow pack (e-folding depth)

e-folding depths relevant for the photolysis of NO_3^- are reported in Table S2 and show significant standard deviations, and also considerable variability (0.9 - 4.0 cm) between profiles, which reflect both systematic experimental errors as well as spatial variability of snow optical properties. They are shallower than at Dome C but similar to previous model estimates for South Pole (France et al., 2011;Wolff et al., 2002). The origin of the reduced e-folding depth relative to Dome C is not known but is likely due to greater HUmic-LIke Substances (HULIS) content or different snow morphology (section 4.3.2) (Libois et al., 2013;Zatko et al., 2013;Brucker et al., 2010).

3.8 Snow emission of NO_2

Formatted: Heading 2

The potential snow emission flux of NO_2 (F_{NO2}) from NO_3^- photolysis in snow was estimated using Eq. (8).

$$F_{NO2} = \int_{z=0\,m}^{z=1\,m} [NO_3^-]_z \; J(NO_3^-) dz \qquad \text{Eq. (8)}$$

where $J_z(NO_3^-)$ is the photolysis rate coefficient of reaction $NO_3^- + h\nu \rightarrow NO_2 + O^-$ at depth, z, in the snowpack, and is derived by scaling surface measurements (section 2.6) with e-folding depth (2 - 10 cm), and $[NO_3^-]_z$ is the amount of NO_3^- per unit volume of snow at depth, z, in the snowpack. The calculated F_{NO2} is a potential emission flux assuming that all NO_3^- within the snow grain is photo-available, no cage effects are present and NO_2 is vented immediately after release from the snow grain to the air above the snowpack without undergoing any secondary reactions. For the 1 to 14 January 2017 period, model estimates of F_{NO2} scaled approximately linearly with e-folding depth were 0.4, 1.0 and 1.9 x 10^{11} molecule m^{-2} s^{-1} for e-folding depths of 2, 5 and 10 cm, respectively. Spatial variability of NO_3^- in the top 30 cm of surface snow at DML based on snow pits A and B is on the order of 13 % inducing similar variability in the model estimates of F_{NO2}. Estimates of F_{NO2} at Dome C, based on the same model during 1 to 14 January 2012, were larger with 1.2 - 7.3 x 10^{11} molecule m^{-2} s^{-1} (Frey et al., 2013), mostly due to larger $J(NO_3^-)$ values observed above the surface (section 2.6) as well as a larger e-folding depth (10 cm near the surface). It should be borne in mind that the above simple model estimates (Eq. (8)) may significantly underestimate the real emission flux. Previous comparisons of F_{NO2} computed with Eq. (8) and F_{NOx} measured at Dome C showed that observations can exceed model predictions by up to a factor 50 (Frey et al., 2015;Frey et al., 2013). While NO_3^- mass concentrations in snow, the surface actinic flux and the e-folding depth were measured at the DML field site, the quantum yield of NO_3^- photolysis in surface snow (ΦNO_3^-) was not, but introduces significant uncertainty in the model estimates. Previous lab measurements on natural snow samples collected at Dome C showed ΦNO_3^- to vary between 0.003 and 0.05 (Meusinger et al., 2014). As described above (section 2.6) JNO_3^- used in Eq. (8) was calculated with ΦNO_3^- at -30 ºC (= 2 x 10^{-3}) after Chu and Anastasio (2003), which is near the lower end of the observed range. Thus, up to half of the mismatch between Eq. (8) and Dome C observations can be explained by adjusting ΦNO_3^-. Another factor contributing to larger fluxes and not included in Eq. (8) is forced ventilation.

In the more sophisticated TRANSITS model, Erbland et al. (2015) found that the photolytic quantum yield was one of the major controls on archived flux and primary input flux at Dome C. Erbland et al. (2015) initially used a quantum yield of 2.1 x 10^{-3} at 246 K (France et al., 2011) but it underestimated NO_3^- recycling and overestimated primary NO_3^- trapped in snow. Adjusting the quantum yield to 0.026, within the range observed in the lab ~~-~~(Meusinger et al., 2014), gave more realistic archived $\delta^{15}N$-NO_3^- values. However, at Dome C TRANSITS simulated F_{NO2} fluxes were about a factor of 9 - 18 higher than observed F_{NOx}. Erbland et al. (2015) suggested that the discrepancy could result from the simplifications made in the TRANSITS model regarding the fate of NO_3^- photolysis products.

3.9~~7~~ Simulated nitrate mass concentrations and isotopic ratios from TRANSITS modelling

Simulated TRANSITS results for the base case and 5 cm EFD case scenarios at the air-~~-~~snow interface are illustrated in Fig. 6 along with TCO data (Fig. 6a). In the atmosphere, the TRANSITS model is forced with the smoothed profile of year-round atmospheric NO_3^- measurements from the DML site (Weller and Wagenbach, 2007) w~~which has~~here the highest mass concentrations are in spring and summer with a maximum of 80 ng m^{-3} in November and a ~~winter~~ minimum of 2 ng m^{-3} in winter (Fig. 6b). Overall, the simulated values in the base case scenario are higher than the 5 cm EFD case in summer and autumn, and converge to similar values in winter. T~~Although we only have measurements of δ^{15}N-NO$_3^-$ in January, t~~he simulated atmospheric δ^{15}N-NO$_3^-$ values in the base case for January, ~~-~~are greater than the measurements available from this study~~.~~, while the δ^{15}N-NO$_3^-$ values in the 5 cm EFD case fall within the range of observations. T~~T~~he annual cycle of simulated atmospheric δ^{15}N-NO$_3^-$ for the 5 cm EFD case shows a ~~40~~ 50 ‰ dip in spring to -4~~3~~2 ‰ from winter values which coincides with the simulated atmospheric NO$_3^-$ mass concentration increase in spring (Fig. 6c). The highest simulated atmospheric δ^{15}N-NO$_3^-$ values (7 ‰) occur in winter, for both scenarios. In the skin layer, the simulated NO$_3^-$ mass concentrations are an order of magnitude greater than our observations in January and we outline possible reasons for this discrepancy in the discussion (section 4.1). The simulated annual cycle of NO$_3^-$ mass concentrations in the skin layer steadily rise in spring and reach a peak in January when they begin to decline to the lowest mass concentration in winter (Fig. 6d). Simulated skin layer δ^{15}N-NO$_3^-$ values in January for the base case are ~10 ‰ higher than our highest observations for that month but the average January value in the 5 cm EFD case (-7 ‰) falls in the range of observed values (-10 ‰) (Fig. 6e). For the 5 cm EFD case, t~~T~~hey begin to decrease by ~~24~~ 30 ‰ ~~-~~ in spring at the same time as atmospheric δ^{15}N-NO$_3^-$ values decrease. In October and November, the skin layer δ^{15}N-NO$_3^-$ values begin to rise up to -11~~14~~ ‰ in February in the 5 cm EFD case ~~in February~~.

The seasonality of simulated NO$_3^-$ mass concentrations and δ^{15}N-NO$_3^-$ values in the atmosphere and skin layer at DML is~~is~~ consistent with Dome C (Fig. 1). Similar to Dome C, simulated NO$_3^-$ mass concentrations in the skin layer start to rise two months earlier than atmospheric NO$_3^-$ mass concentrations and the summer maximum is later. While the seasonality of δ^{15}N-NO$_3^-$ in the skin layer and atmosphere co-vary, simulated skin layer δ^{15}N-NO$_3^-$ values are enriched relative to atmospheric values ~~on average by 80 ‰~~.

The simulated NO$_3^-$ mass concentrations and δ^{15}N-NO$_3^-$ values in the ~~snow pit~~depth profiles are illustrated in Fig. 7. The e-folding depth sensitivity tests show that a deeper e-folding depth i) increases the δ^{15}N-NO$_3^-$ enrichment in the photic zone, and ii) increases in the mean annual archived δ^{15}N-NO$_3^-$ value (Fig. 7a). Out of the e-folding depths explored in the sensitivity analysis, an e-folding depth in the range of that observed at DML, i.e., 2 - 5 cm, has the closest mean annual δ^{15}N-NO$_3^-$ value to the observations (Fig. 7a). -B~~B~~oth the ~~simulated~~ depth profile of simulated NO$_3^-$ mass concentration and δ^{15}N-NO$_3^-$ in the base case ~~for an accumulation rate of 6 cm yr^{-1} (w.e.)~~ show seasonal variability in the first year with a range of ~~of~~ 380 ng g^{-1} and 20 ‰, which decreases with depth to a range of 95 ng g^{-1} and 10 ‰ in the fourth year. In comparison, in the 5 cm EFD case, the seasonality of δ^{15}N-NO$_3^-$ and NO$_3^-$ mass concentrations in the first year ranges from 290 ng g^{-1} and 40 ‰ to 75 ng g^{-1} and 20 ‰ in the fourth year (Fig. 7a). For the base case scenario, t~~T~~he simulated archived (i.e., annual average of the first year below 1 m) NO$_3^-$ mass concentration, δ^{15}N-NO$_3^-$, and NO$_3^-$ mass flux values are 120 ng g^{-1}, 130 ‰, and 210 pg m^{-2} yr^{-1}, respectively. The simulated annual average $^{15}\varepsilon_{app}$ is -19 ‰ for the top 30 cm (i.e., active photic zone with an e-folding depth of 10 cm). In comparison, in the 5 cm EFD case, the simulated archived NO$_3^-$ mass concentration, δ^{15}N-NO$_3^-$, and NO$_3^-$ mass flux values are 280 ng g^{-1}, 50 ‰, and 480 pg m^{-2} yr^{-1}, respectively. The simulated annual average $^{15}\varepsilon_{app}$ is -11 ‰ for the top 30 cm. The 5 cm EFD case falls within the range of observations for δ^{15}N-NO$_3^-$ (Figs. 7a) but is significantly higher than the observed NO$_3^-$ mass concentrations (Fig. 7c). Also plotted in Figs. 7b-c are the simulated NO$_3^-$, mass concentration and δ^{15}N-

Formatted: Not Highlight
Formatted: Not Highlight
Formatted: Not Highlight
Formatted: Not Highlight
Formatted: Not Highlight
Formatted: Not Highlight
Formatted: Not Highlight
Formatted: Pattern: Clear (Yellow)
Formatted: Not Highlight
Formatted: Pattern: Clear
Formatted: Not Highlight
Formatted: Not Highlight
Formatted: Not Highlight
Formatted: Pattern: Clear
Formatted: Not Highlight
Formatted: Not Highlight
Formatted: Not Highlight
Formatted: Not Highlight
Formatted: Not Highlight
Formatted: Not Highlight
Formatted: Pattern: Clear
Formatted: Not Highlight
Formatted: Not Highlight
Formatted: Not Superscript/ Subscript

NO_3^- depth profiles for accumulation rates of 2.5 cm yr^{-1} (w.e.) and ~~100~~ 11 cm yr^{-1} (w.e.)~~,~~ for the 5 cm EFD case. As the accumulation rate increases, the annual layers of $\delta^{15}N\text{-}NO_3^-$ become thicker, the seasonal amplitude increases, the mean annual $\delta^{15}N\text{-}NO_3^-$ value decreases, and there is less $\delta^{15}N\text{-}NO_3^-$ enrichment in the photic ~~values in the top~~ ~~10 cm decrease~~zone (Fig. 7b). At very low snow accumulation rates, the seasonal cycle is smoothed, as in the case of Dome C (Fig. 7b). A similar pattern is observed for the simulated NO_3^- mass concentrations with depth: seasonal cycles of NO_3^- mass concentrations are more pronounced at higher snow accumulation rates, while inter-annual variability is smoothed at very low accumulation rates such as Dome C (Fig. 7c). The relationship between the snow accumulation rate and $\delta^{15}N\text{-}NO_3^-$ is non-linear (Figs b-c).

Formatted: Not Highlight

Formatted: Not Highlight

Formatted: Highlight

Formatted: Pattern: Clear

Formatted: Pattern: Clear

Formatted: Pattern: Clear

Overall the TRANSITS modelling shows that the i) simulated values in the base case scenario are higher than the 5 cm EFD case, and ii) TRANSITS modelling simulations using the observed e-folding depth of 5 cm are good fit with observations. Differences between the simulated $\delta^{15}N\text{-}NO_3^-$ depth profiles for the two cases and observed $\delta^{15}N\text{-}NO_3^-$ could be due to uncertainties in a number of factors, for example: i) a shallower e-folding depth than modelled (section 4.5.1), ii) lower JNO_3^- values (NO_3^- photolysis rate), which are related to a lower e-folding depth, and would lead to less enrichment of $\delta^{15}N\text{-}NO_3^-$ in the snow pack (section 4.3.2), iii) higher atmospheric NO_3^- input, however $\delta^{15}N\text{-}NO_3^-$ values are not sensitive to variable atmospheric NO_3^- mass concentrations (Erbland et al., 2015), and/or iv) variable snow accumulation which would shift the oscillations to the correct depth and lower the mean $\delta^{15}N\text{-}NO_3^-$ values below the photic zone (section 4.5.2). These differences are further addressed in section 4.5.

~~The simulated archived (i.e., annual average of the first year below 1 m) NO_3^- mass concentration, $\delta^{15}N\text{-}NO_3^-$, and NO_3^- mass flux values are 120 ng g^{-1}, 130 ‰, and 210 pg m^{-2} yr^{-1}, respectively. The simulated annual average $^{15}\varepsilon_{app}$ is -19 ‰ for the top 30 cm (i.e., active photic zone with an e-folding depth of 10 cm).~~

4 Discussion

4.1 Validation of results

Our January 2017 ~~NO_3^-~~ measurements at DML agree well with values reported in the literature, and largely with ~~largely with~~ the simulated 5 cm EFD case ~~results~~ from the TRANSITS model ~~with the exception of~~except for the skin layer NO_3^- mass concentrations. ~~While we made the first measurements of atmospheric, skin layer and snow pit $\delta^{15}N\text{-}NO_3^-$, and skin layer NO_3^- mass concentrations at DML, there are published measurements of NO_3^- mass concentrations in snow pits and~~ In particular, o~~o~~ur NO_3^- ~~concentrations~~ observations in snow pits agree well with published measurements of NO_3^- mass concentrations in snow pits at DML~~those~~ (Weller et al., 2004). While our January 2017 observations of atmospheric NO_3^- mass concentrations are 20 - 30 ng g^{-1} lower than those observed in ~~. Our atmospheric mass NO_3^- concentrations in January 2017 are lower than those observed in~~ 2003 by Weller and Wagenbach (2007), ~~–~~which could be due to inter-~~decadal~~ annual variability of atmospheric NO_3^- mass concentrations ~~(~~which varied by 30 ng g^{-1} over summer between 2003 and 2005~~)~~. ~~or reflect the different filter substrates used (Teflon/nylon versus glass fibre).~~

Formatted: Superscript

Formatted: Not Superscript/ Subscript

Formatted: Not Superscript/ Subscript

~~Overall,~~For the skin layer, the simulated NO$_3^-$ mass concentrations ~~results~~ from TRANSITS are greater than our January observations ~~, particularly the skin layer NO$_3^-$ mass concentrations~~ (Fig. 6d). The discrepancy between the significantly higher simulated NO$_3^-$ mass concentrations than observations in the skin layer was also found at Dome C. Erbland et al. (2015) suggested that this discrepancy could be related to either a sampling artefact, snow erosion or a modelled time response to changes in past primary inputs. We provide an alternative explanation for the extremely high simulated NO$_3^-$ mass concentrations in the skin layer using daily measurements of NO$_3^-$ mass concentration in diamond dust and hoar frost collected ~~daily~~ from Polyvinyl chloride (PVC) sheets at Dome C in summer 2007/08, i.e. new deposition. New deposition of diamond dust had NO$_3^-$ mass concentrations up to 2000 ng g^{-1}, which is four times greater than that observed in natural snow from the skin layer at the same time (Fig. S4). Similarly, new deposition of hoar frost had NO$_3^-$ mass concentrations up to 900 ng g^{-1}, which is three times greater than the skin layer snow. The formation of surface hoar frost occurs by co-condensation, i.e. the simultaneous condensation of water vapour and NO$_3^-$ at the air-snow interface. Recent modelling suggests that co-condensation is the most important process explaining NO$_3^-$ incorporation in snow undergoing temperature gradient metamorphism at Dome C (Bock et al., 2016). Diamond dust can also scavenge high concentrations of HNO$_3$ at Dome C (Chan et al., 2018). Furthermore, the top layer of the snow pack is only 1 mm thick in the TRANSITS model, whereas our observations of the skin layer are 5 mm thick. Due to the photochemical loss of NO$_3^-$ mass concentrations with depth, the highest NO$_3^-$ mass concentrations are expected in the top 1 mm layer which is the layer best in equilibrium with the atmosphere. Here, extremely high mass concentrations of NO$_3^-$ from new deposition from diamond dust and hoar frost are also found. In summary, ~~,In summary,~~ it is likely that we do not measure such high NO$_3^-$ mass concentrations in hoar frost and diamond dust ~~values~~ in the skin layer because of sampling artefacts or blowing snow, which can dilute or remove the diamond dust and hoar frost~~, which is where we would expect the highest concentrations due to the exponential decay of NO$_3^-$ with depth (Fig. S4)~~. ~~If indeed the higher simulated values in the skin layer can be explained by hoar frost and diamond dust, then we can have greater confidence in the depth profile of NO$_3^-$ concentration.~~ It is interesting to note that the~~se~~ higher simulated values in the skin layer do not impact the simulated depth profiles (Fig. ~~5~~7). ~~In summary, it is likely that we do not measure such high hoar frost and diamond dust values in the skin layer because of sampling artefacts or blowing snow, which can dilute or remove the diamond dust and hoar frost.~~

~~**While not yet observed elsewhere on the Antarctic continent, over the short intensive sampling period at DML we observe significant variability in NO$_3^-$ mass concentrations and δ^{15}N-NO$_3^-$ values that resembles a diurnal cycle. Over 4 hours, the skin layer NO$_3^-$ mass concentrations varied by 46 ng g^{-1}, the skin layer δ^{15}N-NO$_3^-$ by 21 ‰, and the atmospheric δ^{15}N-NO$_3^-$ by 18 ‰. Other coastal studies have attributed daily variability to individual storm events**~~

Formatted: Heading 2

~~**(Mulvaney et al., 1998;Weller et al., 1999). We note that the sampling duration is too short to confirm any diurnal patterns but it would be interesting to investigate this further in future work.**~~

4.2 Nitrate deposition

~~**Here we discuss the various processes in which NO_3^- can be deposited to the skin layer at DML. As we have just one month of atmospheric and skin layer data, our ability to look at the deposition on seasonal scales is limited, however we provide new insights into the austral summer deposition processes.**~~

~~**While it is common to measure nitrogen species in snow and aerosol samples as the NO_3^- ion using ion chromatography, nitrogen species can be deposited in various forms either by wet or dry deposition to the skin layer. We note that organic NO_3^- plays are little role in determining snow concentrations (Jones et al., 2007;Wolff et al., 2008), and as such we focus our discussion on inorganic NO_3^-. The various nitrogen species include, i) a neutral salt (NO_3^- co-deposition with sea salt or mineral dust; Wolff et al. (2008)), ii) NO_3^- in air (HNO_3 in gas-phase plus particulate NO_3^-). Following the terminology of Erbland et al. (2013), this is referred to as "atmospheric NO_3^-" and is represented by the NO_3^- mass concentrations measured on our aerosol filters. Atmospheric NO_3^- can either be deposited as dry deposition by adsorption to the snow surface as HNO_3 has a strong affinity for ice surfaces (Abbatt, 2003;Huthwelker et al., 2006) or scavenged by precipitation as wet deposition, and iii) co-condensation of HNO_3 and water vapour onto snow crystals (Thibert and Domine, 1998).**~~

~~**Depending on the deposition pathway, NO_3^- can either be predominantly incorporated into the bulk snow crystal or be adsorbed onto the surface of the snow crystal. Deposition pathways include co-condensation (formation of surface hoar frost), riming (deposition of supercooled fog droplets), and adsorption of HNO_3 onto the snow crystal surface (dry deposition) (Röthlisberger et al., 2002). Both co-condensation (Bock et al., 2016) and dry deposition of HNO_3, at very cold temperatures, can elevate NO_3^- mass concentrations in the skin layer. Furthermore, trace nitrogen impurities present in the interstitial air in the porous snow pack may be incorporated in snow crystals. While scavenging of NO_3^- by snow (wet deposition) occurs sporadically throughout the year, dry deposition of particulate NO_3^- or surface adsorption may take place continuously throughout the year. We see both of these deposition processes taking place during January 2017.**~~

4.2.1 Wet and dry deposition

Here we discuss the various processes in which NO_3^- can be deposited to the skin layer at DML. Firstly, we first look at atmospheric NO_3^- deposition in relation to the source region of the air mass. The mean annual wind direction at the site is 65° (Figs. 3 and S5). There is an excursion from this predominant wind direction between 19 - 22 January, where the wind direction switches to the southwest, i.e., atmosphere transport from the plateau. We do not see elevated NO_3^- mass concentrations during this period nor do we see a marked difference in isotopic signature that is similar to Dome C at this time (Fig. 4). This, in line with air mass back trajectories (not shown) suggests that transport of NO_3^- re-emitted from inland sites of the Antarctic, carrying a distinctively enriched $\delta^{15}N\text{-}NO_3^-$ signature, did not influence DML during our campaign. We can also rule out any downwind contamination from the station.

Secondly, we use ~~Precipitation at DML can occur either through sporadic cyclonic intrusions of marine air masses from the adjacent ocean associated with large amounts of precipitation, or clear sky diamond dust that contributes smaller amounts to the total precipitation (Schlosser et al., 2010). Overall, extreme precipitation events dominate the total precipitation (Turner et~~

~~al., 2019). In austral summer, the transport of marine aerosol to DML is mediated by two synoptic situations, i) low-pressure systems from the eastern South Atlantic associated with high marine aerosol concentrations, and ii) persistent long-range transport that provides background aerosol deposition during clear sky conditions (Weller et al., 2018). Weller et al. (2018) suggest that dry deposition of marine aerosol is dominant over wet deposition at DML. In contrast, Dome C receives predominantly diamond dust, and thus aerosol deposition is different there.~~

~~More specifically, precipitation during our sampling campaign in January 2017 was relatively low compared to previous years. Modelled daily precipitation at the nearest Regional Atmospheric Climate Model (RACMO2; Van Meijgaard et al. (2008)) grid point (75.0014°S, 0.3278°W) is illustrated in Fig. 3a. The largest precipitation event of the month was on 1 January (0.27 mm) resulting from a low-pressure system in the South Atlantic (Fig. S5). For the rest of the month, half of the days had zero precipitation and the other half had very little precipitation (~0.05 mm per day).~~

~~We use~~ m~~the~~ odelled daily precipitation at the nearest Regional Atmospheric Climate Model (RACMO2; Van Meijgaard et al. (2008) grid point (75.0014°S, 0.3278°W; Fig. 3a) ~~RACMO2 daily precipitation data~~ to identify ~~whether~~ the influence of cyclonic intrusions of marine air masses ~~provide~~ to wet deposition of NO_3^- ~~to the site in January~~. We observe that ~~. In the skin layer, we observe that NO_3^- mass concentrations and other sea salt ions co-vary (Fig. S6) suggesting similar deposition pathways of these ions.~~ s~~S~~ome peaks in the skin layer NO_3^- mass concentration are accompanied by fresh snow laden with relatively high sea salt aerosol mass concentrations and atmospheric NO_3^- mass concentrations, for example on 1, 13, and 18 January 2017 (Fig. S6). ~~In the skin layer, we observe that NO_3^- mass concentrations and other sea salt ions co-vary (Fig. S6) suggesting similar deposition pathways of these ions.~~ ~~Such deposition events have also been observed on the Antarctic coast (Wolff et al., 2008). During the formation of precipitation, essentially all HNO_3 is removed from the gas-phase due to its high solubility in liquid clouds (Seinfeld and Pandis, 1998). Therefore, HNO_3 can be scavenged from the atmosphere and deposited as NO_3^- in the skin layer. The uptake of HNO_3 onto the snow and ice crystal surface during and after precipitation can also contribute further to the NO_3^- mass concentrations found in the skin layer. On some~~Whereas on other precipitation days, we observe lower atmospheric NO_3^- mass concentrations and higher skin layer NO_3^- mass concentrations that could be a result of HNO_3 scavenging~~. Mulvaney et al. (1998) observed higher skin layer concentrations in days when there was little snow accumulation and concluded that~~ ~~NO_3^- is directly up taken onto the surface by dry deposition of particulate NO_3^- and surface adsorption of HNO_3 (gas-phase) (e.g. Mulvaney et al., 1998)~~. With only one month of data it is difficult to see the impact of wet deposition on the NO_3^- mass concentration in the skin layer; i.e. whether fresh snowfall dilutes the NO_3^- mass concentration in the skin layer or whether it scavenges HNO_3 (gas-phase) resulting in higher mass concentrations of NO_3^- in the skin layer. ~~Most likely both processes are occurring.~~ ~~We note that due to post-depositional processes (section 3) any short-term signals observed in the skin layer are unlikely to be preserved. Even at the South Pole where the snow accumulation rate is slightly higher (8.5 cm yr^{-1} (w.e.); (Mosley-Thompson et al., 1999) than DML deposition, NO_3^- peaks are substantially modified after burial (Dibb and Whitlow, 1996).~~

Thirdly, we

investigate daily changes in the atmospheric and skin layer NO_3^- mass concentrations and $\delta^{15}N$-NO_3^- over the campaign to see the influence of dry deposition, by adsorption of atmospheric NO_3^- to the snow surface. ~~4.2.2 Dry deposition~~~~NO_3^- is directly up taken onto the surface by dry deposition of particulate NO_3^- and surface adsorption of HNO_3 (gas-phase) (e.g. Mulvaney et al., 1998)~~

~~In order to investigate dry deposition of NO_3^-, we first look at atmospheric NO_3^- in relation to the wind direction and air mass back trajectories. The mean annual wind direction at the site is 65°, and January 2017 is no exception (Figs. 3 and S7). There is an excursion from the predominant wind direction between 19-22 January, where the wind direction switches to the southwest. Although there are no studies indicating fractionation of $\delta^{15}N$-NO_3^- in the atmosphere during atmospheric transport from the plateau to the coast, we do not see elevated NO_3^- mass concentrations during this period nor do we see a marked difference in isotopic signature that is similar to Dome C at this time (Fig. 4). This, in line with air mass back trajectories (not shown) suggests that long-range transport of NO_3^- re-emitted from inland sites of the Antarctic did not reach DML during our campaign. We can also rule out any downwind contamination from the station.~~

~~High concentrations of sea salt and mineral dust can promote the conversion of HNO_3 (gas-phase) to aerosol, as well as trapping NO_3^- (gas-phase) on salty snow surfaces. We see a relationship between sea salt aerosol and atmospheric NO_3^- (R^2= 0.59; p=<0.001) suggesting that even 550 km inland from the coast sea salt could promote the conversion of HNO_3 to atmospheric NO_3^-, although we acknowledge that our filters capture both aerosol NO_3^- and HNO_3, and sea salt concentrations are much higher at Halley and coastal Antarctica where this mechanism sporadically occurs (Wolff et al., 2008).~~

~~Scavenging of atmospheric NO_3^- is largely responsible for the~~on the high mass concentrations observed in the skin layer. Temporal v~~V~~ariation in the mass concentration and isotopic signature of aerosol and surface snow at DML over January 2017 suggests atmospheric NO_3^- is the source of NO_3^- to the skin layer. Throughout the month, the increase in the skin layer mass concentration of summer NO_3^- appears to be closely related to the decrease in the atmospheric NO_3^- mass concentrations (Fig. 3). There is a lag between atmospheric and skin layer NO_3^- i.e. atmospheric NO_3^- mass concentrations precede skin layer NO_3^- mass concentrations by day or two, however a longer time series is required to confirm this. The lag suggests that atmospheric NO_3^- is a source of NO_3^- to the skin layer, in line with Dome C where the underlying snow pack is the dominant source of NO_3^- to the skin layer via ~~-~~ photolytic recycling and re-deposition~~the overlying air in summer~~. Furthermore, as atmospheric NO_3^- is deposited to the snow surface, ^{15}N is preferentially removed first leaving the air isotopically depleted relative to the isotopically enriched snow (Frey et al., 2009). Figs. 3-4 illustrate~~s~~ that the $\delta^{15}N$-NO_3^- in the atmosphere is depleted with respect to the $\delta^{15}N$-NO_3^- in the skin layer snow. In the short time series, there are some periods where the $\delta^{15}N$-NO_3^- in the snow and atmosphere are in phase, for example, 3 - 13 January 2017. During other periods, the $\delta^{15}N$-NO_3^- in the snow and atmosphere switch to being out of phase emphasising NO_3^- isotopic fractionation during those periods. Both HNO_3 and peroxynitric acid (HNO_4) can be adsorbed to the snow surface in tandem (Jones et al., 2014), and although we have no direct measurements of these during the campaign, based on previous studies we suggest that HNO_3 is ~~the~~ dominantly adsorbed ~~most likely form of nitrogen~~ to the skin layer (Jones et al., 2007;Chan et al., 2018).

Formatted: Normal

Formatted: Not Superscript/ Subscript

Formatted: Not Superscript/ Subscript

Formatted: Not Superscript/ Subscript

We conclude that HNO_3^- scavenging, adsorption and cyclonic intrusions of marine air masses deliver NO_3^- to the skin layer at DML in summer. During the campaign, deposition is not influenced by the transport of airmasses from the polar plateau which carry a distinct atmospheric $\delta^{15}N-NO_3^-$ signature. ~~Furthermore, the adsorption of HNO_3 on ice surfaces is temperature dependent with higher uptake at lower temperatures (Abbatt, 1997;Jones et al., 2014). However, there is only a relatively small temperature difference between Dome C and DML (summer mean temperature -30 °C and -25 °C respectively) which is not enough to drive a large difference in HNO_3 uptake (Jones et al., 2014). In addition, the uptake is not dependent on the HNO_3 concentration in the air (Abbatt, 1997). However, the seasonal temperature difference at an individual site (i.e., DML or Dome C) is far greater, which could allow a seasonal dependence on the uptake and loss of NO_3^- in the skin layer, which results in the retention of a greater proportion of NO_3^- in summer (Chan et al., 2018).We note that due to post-depositional processes (section 3) any short-term signals observed in the skin layer are unlikely to be preserved. Even at the South Pole where the snow accumulation rate is slightly higher (8.5 cm yr^{-1} (w.e.); (Mosley-Thompson et al., 1999) than DML deposition, NO_3^- peaks are substantially modified after burial (Dibb and Whitlow, 1996).~~

Formatted: Not Superscript/ Subscript

Formatted: Not Superscript/ Subscript

4.2.2~~3~~ ~~Annual cycle~~Temporal variability of nitrate deposition

The seasonality of simulated skin layer and atmospheric NO_3^- mass concentrations at DML matches observations at other Antarctic sites. ~~We use the simulated annual cycle of NO_3^- from TRANSITS model to describe the seasonal evolution of NO_3^- deposition to DML. While NO_3^- deposited to DML can be sourced from the sedimentation of polar stratospheric clouds in winter and we assume the atmospheric NO_3^- loading is uniform under the polar vortex, in spring and summer NO_3^- net deposition is related to local photochemistry and subsequent post-depositional processing rather than primary NO_3^- sources. At this time, deposition of NO_3^- can be through the transport of re-emitted NO_3^- from the surface snow at low accumulation regions of the polar plateau, or NO_3^- produced *in situ* at DML in spring and summer.~~ Year-round measurements of ~~The annual cycle of~~ atmospheric and/or skin layer NO_3^- mass ~~deposition~~ concentration have previously been ~~made~~ observed at DML (Figs. 5 and 6; Weller and Wagenbach (2007), Halley Station (Mulvaney et al., 1998;Jones et al., 2011), ~~and~~ Neumayer Station~~s~~ (Wagenbach et al., 1998), and ~~the low snow accumulation site at~~ Dome C (Fig. 1). These measurements describe the seasonal evolution of NO_3^- deposition to the skin layer from the atmosphere.~~(Weller and Wagenbach, 2007) indicates how much NO_3^- is deposited to the skin layer from the atmosphere (Figs. 5 and 6). Year-round NO_3^- mass concentrations have been measured in surface snow at the coastal sites of Halley (Mulvaney et al., 1998;Jones et al., 2011) and Neumayer Stations (Wagenbach et al., 1998), and the low snow accumulation site at Dome C (Fig. 1). An agreement with our simulated results , at all Antarctic sites the highest atmospheric NO_3^- mass concentrations are found during summer when the solar radiation is close to its annual maximum and NO_3^- photolysis is strongest. The summer maximum at Dome C results from co-condensation of NO_3^- (Bock et al., 2016). This intense uptake in the skin layer in summer is driven by the strong temperature gradient in the upper few centimetres of the snow pack, highlighting that both physical (deposition; Bock et al. (2016); Chan et al., 2018) and~~

Formatted: Not Superscript/ Subscript

Formatted: Highlight

Formatted: Highlight

Formatted: Highlight

Formatted: Highlight

Formatted: Highlight

~~chemical (NO_3^- re-emission; Erbland et al. (2015)) processes explain the cycling of NO_3^- between the air and snow. The lowest NO_3^- mass concentrations in the skin layer are found in winter.~~

~~Year-round atmospheric NO_3^- data at DML and Dome C shows atmospheric NO_3^- is at a minimum in April to June and reaches a maximum in late November, slightly out of phase with skin layer NO_3^- (Wagenbach et al., 1998;Erbland et al., 2013) (Figs. 1 and 6).(Figs. 1 and 6). The fact that the seasonality of simulated skin layer and atmospheric NO_3^- at DML matches observations at other sites in Antarctica gives confidence in our TRANSITS model results (Fig. 6).~~

We also observe variability on shorter timescales. While not yet observed elsewhere on the Antarctic continent, over the short intensive sampling period at DML we observe significant variability in NO_3^- mass concentrations and $\delta^{15}N-NO_3^-$ values that resembles a diurnal cycle. Over 4 hours, the skin layer NO_3^- mass concentrations varied by 46 ng g^{-1}, the skin layer $\delta^{15}N-NO_3^-$ by 21 ‰, and the atmospheric $\delta^{15}N-NO_3^-$ by 18 ‰. Other coastal studies have attributed daily variability to individual storm events (Mulvaney et al., 1998;Weller et al., 1999). ~~We note that~~ T~~t~~he sampling duration in this study is too short to confirm any diurnal patterns but it would be interesting to investigate this further in future work. We note that due to post-depositional processes (section 4.3) any short-term signals observed in the skin layer are unlikely to be preserved.

4.2.43 Nitrate mass fluxes

Our two NO_3^- mass flux scenarios in Fig. 5 highlight the importance of the skin layer in the air-snow transfer of NO_3^-. Like Dome C, the greatest deposition flux of NO_3^- is to the skin layer. The January dry deposition flux is greater than the annual mean flux estimated by Pasteris et al. (2014) and Weller and Wagenbach (2007) which is to be expected given the higher atmospheric NO_3^- mass concentrations in summer (Fig. 6). The wet deposition flux, calculated for the greater DML region by Pasteris et al. (2014), falls within our two scenarios. Furthermore, the simulated archived NO_3^- mass flux at DML of 210 pg m^{-2} s^{-1} for the base case and 480 pg m^{-2} s^{-1} for the 5 cm EFD case over predict~~s~~ the observed NO_3^- archived mass flux of 110 pg m^{-2} s^{-1} due to the higher simulated archived NO_3^- mass concentrations. Interestingly, the simulated archived mass flux at Dome C (88 pg m^{-2} s^{-1}) is lower than DML, yet the NO_3^- deposition flux to the skin layer in January at Dome C is similar to DML. We continue our discussion focusing on the recycling and redistribution of NO_3^- that occurs in the active skin layer emphasising its importance.

4.3 ~~Recycling and~~ Post-depositional processes

4.3.1 Nitrate redistribution

In corroboration with earlier work on the East Antarctic plateau,

~~Post-depositional loss and redistribution of NO_3^- is the dominant control on snow pack mass concentrations and $\delta^{15}N-NO_3^-$ isotopic signature on the Antarctic Plateau(Erbland et al., 2015). Recycling of NO_3^- at the air-snow interface comprises the following processes. Nitrate on the surface of a snow crystal can be lost from the snow pack (Dubowski et al., 2001), either by~~

Formatted: Highlight

Formatted: Highlight

Formatted: Highlight

Formatted: Highlight

Formatted: Not Highlight

Formatted: Not Highlight

Formatted: Not Highlight

Formatted: Not Highlight

Formatted: Heading 3

~~UV photolysis or evaporation. UV photolysis produces NO, NO_2 and HONO while only HNO_3 can evaporate. Both of these processes produce reactive nitrogen that can be released from snow crystal into the interstitial air and rapidly transported out of the snow pack to the overlaying air via wind pumping (Zatko et al., 2013;Jones et al., 2000;Honrath et al., 1999;Jones et al., 2001). Here, NO_2 is either oxidised to HNO_3, which undergoes wet or dry deposition back to skin layer within a day, or transported away from the site (Davis et al., 2004a). If HNO_3 is re-deposited on the snow skin layer, it is available for NO_3^- photolysis and/or evaporation again. Nitrate can be recycled multiple times between the boundary layer and the skin layer before it is buried in deeper layers of the snow pack. Photolysis and/or evaporation of NO_3^- and subsequent recycling between the air and snow alters the concentration and $\delta^{15}N$-NO_3^- that is ultimately preserved in ice cores. Nitrate recycling therefore redistributes NO_3^- from the active snow pack column to the skin layer via the atmosphere. Any locally produced NO_2 that is transported away from the site of emission represents a loss of NO_3^- from the snow pack.~~

~~4.3.1 Evaporation~~

~~The desorption of HNO_3 from the snow crystal reduces the NO_3^- concentration in the snow in coastal Antarctica (Mulvaney et al., 1998). The evaporation of HNO_3 is a two-step process, which involves the recombination of $NO_3^- + H^+ \longrightarrow HNO_3$ followed by a phase change to HNO_3 (gas-phase). First, theoretical estimates indicated that evaporation of HNO_3 should preferentially remove ^{15}N from the snow and release to the atmosphere leading to depletion in $\delta^{15}N$-NO_3^- in the residual snow pack (Frey et al., 2009). Furthermore, recent laboratory experiments showed that evaporation imposes a negligible fractionation of $\delta^{15}N$-NO_3^- (Erbland et al., 2013;Shi et al., 2019). However, we find that the snow pack is enriched in $\delta^{15}N$-NO_3^- relative to the atmosphere at DML (Figs. 3 and 6) and at Dome C (section 4.3.2). This fractionation observed in field studies cannot therefore be explained by evaporation, and must be attributed to different processes. It therefore follows that evaporation must be only a minor process in the redistribution of NO_3^- between atmosphere and the snow pack above the Antarctic plateau.~~

~~4.3.2 Photolysis~~

~~We focus our discussion on photolysis, which is the dominant process responsible for NO_3^- loss and redistribution and associated $\delta^{15}N$-NO_3^- isotopic fractionation at low accumulation sites in Antarctica (Erbland et al., 2013;France et al., 2011). Nitrate photolysis occurs in the photochemically active zone of the snow pack, known as the snow photic zone. Below this, NO_3^- is buried. Nitrate photolysis in the active snow pack results in the production of NO_2 leading to a reduction in the NO_3^- concentration with depth in the snow pack (Fig. 4). In the photolysis-induced fractionation of NO_3^-, ^{14}N is preferentially removed first resulting in an enrichment of $\delta^{15}N$-NO_3^- in the snow pack. An individual snow layer is enriched when it is near the surface during sunlit conditions, i.e. spring and summer. Therefore, spring snow layers undergo strong $\delta^{15}N$-NO_3^- enrichment as they are exposed to UV near the surface for the longest; late summer and autumn layers experience less $\delta^{15}N$-NO_3^- enrichment as they are exposed for less time before sunlight disappears at the start of polar winter, during which new precipitation buries existing snowfall.~~

Formatted: Highlight

Formatted: Highlight

Formatted: Highlight

Formatted: Highlight

Formatted: Highlight

Formatted: Highlight

Formatted: Highlight

Field Code Changed

Formatted: Highlight

~~We provide five lines of evidence that photolysis is the dominant process for NO$_3^-$ recycling and redistribution at DML.~~ we find clear evidence of NO$_3^-$ redistribution via photolysis at DML, and confirmation of our hypothesis that UV-photolysis is driving NO$_3^-$ recycling at DML. Firstly, the highly enriched δ^{15}N-NO$_3^-$ values of~~of~~ snow at DML ~~and other Antarctic sites~~(-3 to 99 ‰), and the highly depleted atmospheric δ^{15}N-NO$_3^-$ values at DML (-20 to -49 ‰) are among the most extreme observed on earth (Fig. ~~S8~~S7;~~)~~ Savarino et al. (2007), and cannot be explained by any known anthropogenic, marine or other natural sources. The δ^{15}N-NO$_x$ ~~NO$_3^-$~~ source signature of the main natural NO$_x$ sources (biomass burning, lightning, soil emissions ~~is lower~~; δ^{15}N-NO$_x$~~$_3$~~$^-$ <0 ‰) is lower than anthropogenic NO$_x$ sources, which generally have positive δ^{15}N-NO~~$_3^-$~~$_x$ values (-13< δ^{15}N-NO$_x$~~$_3$~~$^-$ < 13 ‰; e.g.~~)~~ Hastings et al. (2013);Kendall et al. (2007);Hoering (1957) except in the case of vehicle and fertilised soil NO$_x$ emissions which have negative δ^{15}N-NO$_x$ values (-60< δ^{15}N-NO$_3^-$ <12 ‰; Miller et al. (2017);Yu and Elliott (2017);Miller et al. (2018);Li and Wang (2008). However, a NO$_3^-$ source contribution from fertilised soil NO$_x$ emissions to Antarctica is thought to be minor (Lee et al., 2014). Such low atmospheric δ^{15}N-NO$_3^-$ values at DML show a marked difference to other mid-latitude tropospheric aerosol (-10< δ^{15}N-NO$_3^-$ <10 ‰; Freyer (1991). We acknowledge that stratospheric NO$_3^-$ contributes to NO$_3^-$ mass concentrations in snow in Antarctica. Although its isotopic signature is uncertain, estimates of stratospheric δ^{15}N-NO$_3^-$ are 19 ± 3 ‰ (Savarino et al., 2007), and fall well outside of atmospheric observations at DML. T~~T~~herefore, δ^{15}N-NO$_3^-$ observations of aerosol, skin layer and snow pit at DML (-49< δ^{15}N-NO$_3^-$ <99 ‰) lie outside ~~of~~ the range of natural and anthropogenic source end members (with the exception of anthropogenic emissions NO$_x$ from vehicle and fertilised soil which can be ignored as a source to Antarctica)~~,~~ and ~~thus~~ cannot be explained by a mixture~~ing~~ of sources (Fig. S7) or attributed ~~. Thus, our measurements at DML are unrelated~~ to seasonal variations in mid-low latitude NO$_x$ sources e.g. increased springtime agricultural emissions~~, which has been observed in the mid-latitudes~~. ~~The contribution of natural sources to the Greenland snow pack δ^{15}N-NO$_3^-$ signature has also been discarded (Geng et al., 2014;Geng et al., 2015). Furthermore, the negative atmospheric δ^{15}N-NO$_3^-$ values at DML (-20 to -49 ‰) are extremely low. Such low atmospheric δ^{15}N-NO$_3^-$ values have only been observed in Antarctica, and show marked difference to other mid-latitude tropospheric aerosol (-10< δ^{15}N-NO$_3^-$ <10 ‰;~~ Freyer (1991);Li and Wang (2008);Miller et al. (2018);Yu and Elliott (2017)~~. We acknowledge that stratospheric NO$_3^-$ contributes to NO$_3^-$ mass concentrations in snow in Antarctica. Although its isotopic signature is uncertain, estimates of stratospheric δ^{15}N-NO$_3^-$ are 19 ± 3 ‰ (Savarino et al., 2007), and fall well outside of atmospheric observations at DML.~~ The unique snow and aerosol δ^{15}N-NO$_3^-$ signature ~~of low accumulation Antarctic snow and aerosol~~ is thus related to post-depositional processes specific to low accumulation sites in Antarctica.

Secondly, denitrification of the snow pack is seen through the δ^{15}N-NO$_3^-$ signature which evolves from the enriched snow pack (-3 to 99 ‰), to the skin layer (-22 to 3 ‰), to the depleted atmosphere (-49 to -20 ‰) corresponding to mass loss from the snow pack (Figs. 4 and S7). Denitrification causes the δ^{15}N-NO$_3^-$ of the residual snow pack NO$_3^-$ to increase exponentially as NO$_3^-$ mass concentrations decrease.

Thirdly, sensitivity analysis with TRANSITS, where photolysis is the driving process, is able to explain the observed snow pit δ^{15}N-NO$_3^-$ variability when the e-folding depth is taken into account (section 4.5).

Formatted: Not Highlight

~~Th~~Fourthly, enrichment of $\delta^{15}N\text{-}NO_3^-$ is observed in the top 30 cm of the snowpack at DML indicating NO_3^- photolytic redistribution at DML in the photic zone of the snow pack (Fig. 7).~~i~~

~~Nitrate isotope enrichment takes place in the top 25 cm, which is consistent with an e-folding depth of 10 cm used in the base case scenario.~~ In the photic zone~~Here~~, the $\delta^{15}N\text{-}NO_3^-$ observations closely match the simulated $\delta^{15}N\text{-}NO_3^-$ values from TRANSITS~~ and show enrichment to this depth indicating NO_3^- photolytic redistribution at DML in the active photic zone of the snow pack (Fig. 7)~~. ~~Below the photic zone, $\delta^{15}N\text{-}NO_3^-$ values oscillate around a mean of ~125 ‰. The mean values of the $\delta^{15}N\text{-}NO_3^-$ observations are lower than the simulated values, which could be related to uncertainties in a number of factors, for example: i) a shallower e-folding depth than modelled. During our field measurements, we derived a lower e-folding depth of 2-5 cm (Fig. S1) at DML which could explain the lower enrichment in $\delta^{15}N\text{-}NO_3^-$ (section 4.5.2), ii) lower JNO_3^- values (NO_3^- photolysis rate), which are related to a lower e-folding depth, and would lead to less enrichment of $\delta^{15}N\text{-}NO_3^-$ in the snow pack, iii) higher atmospheric NO_3^- input, however $\delta^{15}N\text{-}NO_3^-$ values are not sensitive to variable atmospheric NO_3^- mass concentrations (Erbland et al., 2015), and/or iv) variable accumulation which would shift the oscillations to the correct depth and lower the mean $\delta^{15}N\text{-}NO_3^-$ values below the photic zone (section 4.5.1). The difference between the simulated and snow pit values shows that DML site is less sensitive to photolysis than we expected from TRANSITS modelling of $\delta^{15}N\text{-}NO_3^-$ along an accumulation gradient (Erbland et al., 2015).~~

~~Additionally, although not the focus of the study, denitrification causes the $\delta^{18}O\text{-}NO_3^-$ values to increase in the residual NO_3^- snow pack.~~

Thirdly, ~~the application of TRANSITS to DML observations show that our observed atmospheric, skin layer and snow depth profiles of $\delta^{15}N\text{-}NO_3^-$ are similar to the simulated values where photolysis is the driving process (Figs. 6-7).~~ ~~Sensitivity analysis with TRANSITS is able to explain the observed snow pit $\delta^{15}N\text{-}NO_3^-$ variability (section 4.5).~~ ~~the application of TRANSITS to DML observations show that our observed atmospheric, skin layer and snow depth profiles of $\delta^{15}N\text{-}NO_3^-$ are similar to the simulated values where photolysis is the driving process (Figs. 6-7).~~ ~~Nitrate isotope enrichment takes place in the top 25 cm, which is consistent with an e-folding depth of 10 cm. Here, the $\delta^{15}N\text{-}NO_3^-$ observations closely match the simulated $\delta^{15}N\text{-}NO_3^-$ values and show enrichment to this depth indicating NO_3^- photolytic redistribution at DML in the active photic zone of the snow pack (Fig. 7). Below the photic zone, $\delta^{15}N\text{-}NO_3^-$ values oscillate around a mean of ~125 ‰. The mean values of the $\delta^{15}N\text{-}NO_3^-$ observations are lower than the simulated values, which could be related to uncertainties in a number of factors, for example: i) a shallower e-folding depth than modelled. During our field measurements, we derived a lower e-folding depth of 2-5 cm (Fig. S1) at DML which could explain the lower enrichment in $\delta^{15}N\text{-}NO_3^-$ (section 4.5.2), ii) lower JNO_3^- values (NO_3^- photolysis rate), which are related to a lower e-folding depth, and would lead to less enrichment of $\delta^{15}N\text{-}NO_3^-$ in the snow pack, iii) higher atmospheric NO_3^- input, however $\delta^{15}N\text{-}NO_3^-$ values are not sensitive to variable atmospheric NO_3^- mass concentrations (Erbland et al., 2015), and/or iv) variable accumulation which would shift the oscillations to the correct depth and lower the mean $\delta^{15}N\text{-}NO_3^-$ values below the photic zone (section 4.5.1~~

Lastly,~~ we ~~ calculated fractionation constants~~ s ~~($^{15}\varepsilon_{app}$) using our simulated results from the TRANSITS model base case f~~Nitrate evaporation from the snow pack has a $^{15}\varepsilon_{app}$ of ~0 as determined by two independent studies (Erbland et al., 2013;Shi~~

Formatted: Highlight

Formatted: Highlight

Formatted: Highlight

Formatted: Highlight

Formatted: Highlight

Formatted: Font: 10 pt, Font color: Auto

Field Code Changed

~~et al., 2019). This indicates that during NO_3^- evaporation, the air above the snow is not replenished and thus there is only a small NO_3^- mass loss. The isotopic fractionation of NO_3^- evaporation is negligible across most of Antarctica at cold temperatures of <-24 °C (Shi et al., 2019) which is the case for DML. However, evaporation of NO_3^- at warmer temperatures (-4 °C) depletes the heavy isotopes of NO_3^- remaining in the snow, and decreases the $\delta^{15}N\text{-}NO_3^-$ and the remaining snow by a few ‰ contrary to isotope effects of photolysis. In comparison, fractionation constants associated with laboratory studies and field observations of NO_3^- photolysis are large: $^{15}\varepsilon_{app}$ = -34 ‰ (Berhanu et al., 2014;Meusinger et al., 2014) and -54 < $^{15}\varepsilon_{app}$ < -60 ‰ (Frey et al., 2009;Erbland et al., 2013), respectively. The negative fractionation constant obtained from photolysis implies that the remaining NO_3^- in the skin layer snow is enriched in $\delta^{15}N\text{-}NO_3^-$. In turn, the atmosphere is left with the source of NO_x that is highly depleted in $\delta^{15}N\text{-}NO_3^-$. This enrichment (depletion) is exactly what we observe in the snow pack (atmosphere) at DML (Figs. 4 and 6). The marked difference in values from the evaporation experiments and those observed in snow at Dome C allows us to separate out the isotopic signature of evaporation and photolysis processes~~~~at DML of 12 ‰ and -19 ‰ using the active photic zone section of the snow pack (top 30 cm), and using our simulated results from the TRANSITS model respectively. The later nicely matches the~~all in the range of expected $^{15}\varepsilon_{app}$ values ($-59 < {}^{15}\varepsilon_{app} < -16$ ‰) within the "transition zone" characterised by snow accumulation rates typical of sites located between the Antarctic plateau and coast ~~of (~~5 - 20 cm yr^{-1} (w.e.);~~)~~ ~~modelled by~~ Erbland et al. (2015). While the $^{15}\varepsilon_{app}$ for the 5 cm EFD case is lower than predicted for a site with the same snow accumulation rate highlighting the sensitivity of e-folding depth on NO_3^- redistribution. ~~, and implies a weaker photolytic loss of NO_3^- than Dome C ($^{15}\varepsilon_{app}$ < -59 ‰) (Erbland et al., 2013). The discrepancy between our observed and simulated $^{15}\varepsilon_{app}$ is due to the higher snow accumulation rate, which preserves seasonality, and with a noisy signal, there is no pure separation of the loss processes assuming Rayleigh isotopic fractionation. The single-process Raleigh model does not work well at sites with annual signal in $\delta^{15}N\text{-}NO_3^-$.~~ Erbland et al. (2013) noted that uncertainties in the $^{15}\varepsilon_{app}$ for snow pits in the transition zone were greater than coastal and plateau zones indicating that the assumed single loss Rayleigh model is not appropriate for transition zones. The discrepancy between our observed (12 ‰) and simulated (-19 and -11 ‰ for the base case and 5 cm EFD case respectively) $^{15}\varepsilon_{app}$ is due to the higher snow accumulation rate, which preserves seasonality, and with a noisy signal, there is no pure separation of the loss processes assuming Rayleigh isotopic fractionation.

4.3.2~~3~~ Nitrate recycling

Only ~~two~~ three studies have attempted to quantify the degree of NO_3^- recycling between the air and snow (Davis et al., 2008;Erbland et al., 2015;Zatko et al., 2016). Erbland et al. (2015) used the TRANSITS model to estimate that NO_3^- is recycled 4 times on average before burial beneath the photic zone at Dome C, similar to the findings of Davis et al. (2008) for the same site. Using the approach of Erbland et al. (2015), we find that NO_3^- is recycled 3 times on average before it is archived at DML for the base case, and 2 times on average for the 5 cm EFD case. Thus, a shallower e-folding depth reduces the recycling strength. These findings are ~~A lower recycling factor than Dome C is~~ consistent with spatial patterns of NO_3^- recycling factors across Antarctica reported by Zatko et al. (2016). ~~Erbland et al. (2015)~~As Dome C and DML lie on the same latitude (75° S), incoming UV-radiation (except for cloud cover) should not impact the efficiency of photolysis and thus recycling at the two sites. ~~While photolysis-driven NO_3^- recycling can occur at all polar sites, the most intense enrichment of $\delta^{15}N$-NO_3^- in the depth profile is seen at Dome C and Vostok (Erbland, 2011).~~ Below we provide some explanations for the weakened recycling at DML.

1. Higher snow accumulation rate

The TRANSITS modelling shows the influence of the snow accumulation rate on the depth profile of NO_3^- mass concentration and $\delta^{15}N$-NO_3^-, including the preservation of a seasonal cycle at higher snow accumulation rates (Fig. 7). At low accumulation sites, i.e., Dome C, the annual layer thickness is thinner so that NO_3^- in ~~the skin layer and thinner~~those layers ~~snow layers~~ is exposed to sunlight (and the actinic flux) and photochemical processes for longer ~~allowing~~ resulting ~~more photochemistry and thus a very active snow pack with~~ strong NO_3^- recycling and $\delta^{15}N$-NO_3^- enrichment in the snowpack~~t~~. At DML, which has a higher snow accumulation rate than Dome C, the sn~~skin~~ow layers are ~~is~~ buried more rapidly, leaving less time ~~t~~for~~o~~ ~~adsorb additional~~ HNO_3 to adsorb to the skin layer ~~from the atmosphere~~ and less time for photolysis to redistribute snow pack NO_3^- to the overlying air for re-adsorption to the skin layer. Therefore, photolysis-driven recycling of NO_3^- is largely dependent on the time that NO_3^- remains in the snow photic zone. ~~Following photolysis at DML, the recycling of NO_3^- at the air snow interface alters the depth profile of $\delta^{15}N$-NO_3^- in the top skin layer but below the skin layer $\delta^{15}N$-NO_3^- in snow remains intact as there is less redistribution and a lower loss of NO_3^- than at Dome C.~~

2. Shallower e-folding depth

Based on measurements we derived an e-folding depth for DML ranging between 2 and 5 cm (Fig. S1). ~~This estimate is similar to a modelled value at South Pole (3.7 cm; Wolff et al. (2002) which has a similar accumulation rate, and Alert, Canada (5-6 cm; King and Simpson, 2001).~~ The e-folding depth at Dome C is considerably deeper, ranging between 10 cm to 20 cm depending on the snow properties (France et al., 2011) ~~(France et al., 2011).~~ . The e-folding depth depends on the density and grain size of snow crystals, and the concentration of impurities. In terms of published values, impurity concentrations are generally higher at DML, for example dust and major ion concentrations (Delmonte et al., 2019;Legrand and Delmas, 1988), due to proximity to marine sources. Yet station pollution is greater at Dome C (Helmig et al., 2020), and thus the lower e-folding depth is unrelated to black carbon concentrations. Furthermore, there is considerate variability in snow grain size ~~is~~across Antarctica. The larger e-folding depth in windcrust layers at Dome C is due to larger grain sizes in those layers (France et al., 2011). Snow grain size may be smaller at DML, which will increase scattering (Brucker et al., 2010), but further work is required to confirm if this is the dominate factor influencing the lower e-folding depth at DML. ~~(France et al., 2011)~~Sensitivity studies show that NO_3^- impurities make a small contribution to the e-folding depth compared to scattering by snow grains which dominate (France et al., 2011;Chan et al., 2015;Zatko et al., 2013).(France et al., 2011;Delmonte et al., 2019;Legrand and Delmas, 1988)

3. ~~as an (Frey et al., 2009) edto France et al. (2012)Using concentrations in the range of those observed at Dome C and DML we find that e hasTherefore, the France et al. (2011);Zatko et al. (2013)~~. ~~Wthat The larger e-folding depth at Dome C is due to the larger grain sizes (France et al., 2011;Gay et al., 2002)and low impurity content.The~~

Formatted: Numbered + Level: 1 + Numbering Style: 1, 2, 3, … + Start at: 1 + Alignment: Left + Aligned at: 1.27 cm + Indent at: 1.9 cm

~~impact of impurities in the range of observed polar snow concentrations on e-folding depth is small compared to the contribution from scattering by snow grains (France et al., 2011;Zatko et al., 2013).~~Lower photolysis rate

At DML, NO_3^- photolysis produces a lower snow emission flux of NO_2 ~~produces a lower NO_x flux~~ to the atmosphere ~~and lower $^{15}\varepsilon_{app}$~~ than at Dome C (section 3.8). This is due to i) the shallower e-folding depth compared to Dome C which implies reduced emission flux of NO_x, and ii) the reduced UV exposure time of surface snow due to higher annual snow accumulation compared to Dome C. Furthermore, the large $^{15}\varepsilon_{app}$ associated with NO_3^- photolysis has been determined for snow at Dome C (Berhanu et al., 2014;Frey et al., 2009;Erbland et al., 2013) and DML. At both sites, $\delta^{15}N\text{-}NO_3^-$ is enriched in the remaining skin layer. However, at DML, the $^{15}\varepsilon_{app}$ is lower which implies a weaker photolytic loss of NO_3^- associated with a higher snow accumulation rate. The lower snow emission flux of NO_2 and lower $^{15}\varepsilon_{app}$~~highlighting~~ are evidence of a ~~that the photolysis rate is lower thus the~~reduced recycling strength at DML relative to Dome C.~~is reduced (section 4.3.2~~3~~).~~

~~Furthermore, the large $^{15}\varepsilon_{app}$ associated with NO_3^- photolysis has been determined for snow at Dome C~~ (!!! INVALID CITATION !!! (Berhanu et al., 2014;Frey et al., 2009;Erbland et al., 2013))~~ and DML. At both sites, $\delta^{15}N\text{-}NO_3^-$ is enriched in the remaining skin layer snow. However, at DML, the $^{15}\varepsilon_{app}$ is lower due to less active photochemistry associated with a higher snow accumulation rate. Our results are consistent with Zatko et al. (2016) who suggest that the large fractionation constant associated with photolysis is greatest on the polar plateau where strong winds are most efficient at exporting NO_3^- away from the site.~~

~~i.~~4. Lower nitrate uptake at warmer temperatures

~~Temperature can control skin layer NO_3^- uptake and loss. At colder snow temperatures, there is greater adsorption of HNO_3 to the skin layer (Abbatt, 1997;Jones et al., 2014). Although the difference in the mean annual temperature at Dome C compared to DML (~5 °C) is not large enough to explain the significantly higher skin layer NO_3^- mass concentrations there. Compounding this, NO_3^- loss by evaporation is also dependent on temperature with maximum NO_3^- loss at higher temperatures, i.e., diffusion of NO_3^- in ice is slower at colder temperatures (Thibert and Domine, 1998). A compilation of NO_3^- concentration data from Greenland and Antarctic ice cores showed that at very low accumulation rates lower temperatures lead to higher NO_3^- mass concentrations preserved in the snow (Röthlisberger et al., 2000). Although the snow accumulation rate is closely linked to temperature, photolysis is the dominant NO_3^- loss process at low snow accumulation sites in Antarctica. Therefore, any differences in temperature between DML and Dome C could partly explain the greater uptake of HNO_3 to the skin layer, higher mass concentrations of NO_3^- in the skin layer, and stronger recycling at Dome C compared to DML.~~T~~Furthermore, the~~ adsorption of HNO_3 on ice surfaces is temperature dependent with higher uptake at lower temperatures (Abbatt, 1997;Jones et al., 2014). Nitrate loss by evaporation is also dependent on temperature with maximum NO_3^- loss at higher temperatures (Thibert and Domine, 1998;Röthlisberger et al., 2000). The seasonal temperature difference at an individual site (i.e., DML or Dome C) could allow a seasonal dependence on the uptake and loss of NO_3^- in the skin layer, which results in the retention of a greater proportion of NO_3^- in summer (Chan et al., 2018). However, t~~However, t~~here is only a relatively small temperature difference between Dome C and DML ~~(summer mean temperature -30 °C and -25 °C respectively)~~ (Table 1) which is not

Formatted: Normal, No bullets or numbering

Formatted: Not Superscript/ Subscript

Formatted: List Paragraph, Numbered + Level: 1 + Numbering Style: 1, 2, 3, … + Start at: 1 + Alignment: Left + Aligned at: 1.27 cm + Indent at: 1.9 cm

Formatted: Not Highlight

Formatted: Not Highlight

Formatted: Not Highlight

enough to drive a large difference in HNO_3 uptake (Jones et al., 2014). ~~In addition, the uptake is not dependent on the HNO_3 concentration in the air (Abbatt, 1997). However, the seasonal temperature difference at an individual site (i.e., DML or Dome C) is far greater, which could allow a seasonal dependence on the uptake and loss of NO_3^- in the skin layer, which results in the retention of a greater proportion of NO_3^- in summer (Chan et al., 2018).~~

~~ii.~~1. ~~Lower photolysis rate~~

~~iii.~~1. ~~At DML, NO_3^- photolysis produces a lower NO_x flux to the atmosphere and lower $^{15}\varepsilon_{app}$ highlighting that the photolysis rate is lower thus the recycling strength is reduced (section 4.3.2). Furthermore, the large $^{15}\varepsilon_{app}$ associated with NO_3^- photolysis has been determined for snow at Dome C (Berhanu et al., 2014;Frey et al., 2009;Erbland et al., 2013) and DML. At both sites, δ^{15}N-NO_3^- is enriched in the remaining skin layer snow. However, at DML, the $^{15}\varepsilon_{app}$ is lower due to less active photochemistry associated with a higher snow accumulation rate. Our results are consistent with Zatko et al. (2016) who suggest that the large fractionation constant associated with photolysis is greatest on the polar plateau where strong winds are most efficient at exporting NO_3^- away from the site.~~

~~iv.~~5. Lower export of locally produced nitrate

The degree of NO_3^- recycling is also determined by atmospheric transport patterns across Antarctica. Export of locally produced NO_x on the Antarctic Plateau~~,~~ leads to greater enrichment in the depth profile~~s~~ of δ^{15}N-NO_3^- relative to the coast due to isotopic mass balance (Savarino et al., 2007;Zatko et al., 2016)~~.~~. ~~Zatko et al. (2016) modelled the export of snow sourced NO_x away from the original site of NO_3^- photolysis, and found that the largest loss of NO_3^- occurs in central Antarctica where most NO_3^- is transported away by katabatic winds. At the coast, photolysis driven loss of NO_3^- from the snow is minimal due to high snow accumulation rates. Here, O~~observations of enriched atmospheric δ^{15}N-NO_3^- at the coast ~~show~~ suggest that NO_x has been ~~transported~~ sourced ~~away~~ from *in situ* production on the Antarctic Plateau ~~the location of its production on the Antarctic Plateau to the coast~~ (Savarino et al., 2007;Morin et al., 2009;Shi et al., 2018). If there was less~~The greater export of NO_3^- from Dome C allows efficient removal of recycled NO_3^- from that site, resulting in a lower archived NO_3^- mass flux and enriched δ^{15}N-NO_3^- signature in the surface snow. The enrichment of δ^{15}N-NO_3^- is due to the isotopic mass balance rather than an increase for photolysis intensity.~~ ~~With less~~ export of NO_3^- away from the DML site than Dome C, locally sourced NO_x would be~~is~~ redeposited back to the skin layer at the site ~~of the emission~~ and the depth profile of the δ^{15}N-NO_3^- would~~is~~ not be as dramatically impacted as sites where there is substantial loss of NO_3^-~~Dome C where there is substantial loss of NO_3^-~~.

Formatted: Numbered + Level: 1 + Numbering Style: 1, 2, 3, … + Start at: 1 + Alignment: Left + Aligned at: 1.27 cm + Indent at: 1.9 cm

Field Code Changed

Formatted: Not Highlight

Formatted: Not Highlight

Formatted: Not Highlight

Formatted: Not Highlight

Formatted: Not Highlight

Formatted: Not Highlight

Formatted: Not Highlight

Formatted: Font: Italic

Formatted: Not Highlight

Formatted: Not Highlight

Formatted: Not Superscript/ Subscript

Formatted: Not Highlight

Formatted: Not Highlight

~~4.3.3 Snow emission of NO_2~~

~~We estimate the potential snow emission flux of NO_2 (F_{NO2}) from NO_3^- photolysis in snow using Eq. (8).~~

Formatted: Heading 3

$$\cancel{F_{NO2} = \int_{z=0\,m}^{z=1\,m} [NO_3^-]_z \, J(NO_3^-) dz} \qquad \text{Eq. (8)}$$

~~where $J_z(NO_3^-)$ is the photolysis rate coefficient of reaction $NO_3^- + hv \rightarrow NO_2 + O^-$ at depth, z, in the snowpack, and is derived by scaling surface measurements (section 2.6) with e-folding depth (= 2-10 cm), and $[NO_3^-]_z$ is the amount of NO_3^- per unit volume of snow at depth, z, in the snowpack. The calculated F_{NO2} is a potential emission flux assuming that all NO_3^- within the snow grain is photo-available, no cage effects are present and NO_2 is vented immediately after release from the snow grain to the air above the snowpack without undergoing any secondary reactions. For the 1 to 14 January 2017 period, model estimates of F_{NO2} scaled approximately linearly with e-folding depth were 0.4, 1.0 and 1.9 x 10^{11} molecule m^{-2} s^{-1} for e-folding depths of 2, 5 and 10 cm, respectively. Spatial variability of NO_3^- in the top 30 cm of surface snow at DML based on snow pit A and B is on the order of 13 % inducing similar variability in the model estimates of F_{NO2}. Estimates of F_{NO2} at Dome C, based on the same model during 1 to 14 January 2012, were larger with 1.2-7.3 x 10^{11} molecule m^{-2} s^{-1} (Frey et al., 2013), mostly due to larger $J(NO_3^-)$ values observed above the surface (section 2.6) as well as a larger e-folding depth (= 10 cm near the surface). It should be noted that the observed F_{NOx} was found to be up to 50 times larger than model estimates, which is attributed to the poorly constrained quantum yield of NO_3^- photolysis in natural snow (Frey et al., 2015;Frey et al., 2013). In summary, the weakened air-snow recycling at DML is due to i) the shallower e-folding depth compared to Dome C which implies reduced emission flux of NO_x, and ii) the reduced UV exposure time of surface snow due to higher annual accumulation compared to Dome C. We estimate that NO_3^- has a mean lifetime in the skin layer of 12 days to 3 years before it is photolysed back to atmosphere.~~

~~Based on field, laboratory and theory, we conclude that NO_3^- photolysis is the dominant post-depositional process on the Antarctic plateau controlling NO_3^- mass concentrations and $\delta^{15}N$-NO_3^- values in the snow and atmosphere. Nitrate photolysis in snow causes $\delta^{15}N$-NO_3^- fractionation of the magnitude needed to explain field and lab observations. The development of TRANSITS allows us to model the archived $\delta^{15}N$-NO_3^- values taking into account all parameters in the air-snow system.~~

Formatted: Highlight

4.4 Preservation and archival

We provide new constraints on the archival values and archival time of NO_3^- at DML. ~~The photolysis-driven recycling of NO_3^- is largely dependent on the time that NO_3^- remains in the snow photic zone. Post-depositional loss of NO_3^- at DML was quantified in a number of firn cores and snow pits by Weller et al. (2004) who found that ~26 % of the NO_3^- originally deposited to the snow pack was lost. The e-folding time for NO_3^- at the site was reported as ~20 years, and NO_3^- was archived after 5 to 6 years of deposition (or 1.1 – 1.4 m depth) which is the time it takes for the NO_3^- mean concentration to become representative of the last 100 years. At this point, the authors considered post-depositional loss of NO_3^- to be negligible, and therefore archived. However, no skin layer measurements were made in the study and given how active the skin layer is NO_3^-~~

~~redistribution and recycling, we use our skin layer measurements to provide new constraints on the archival values and time of NO_3^- at DML.~~

Taking the high observed skin layer NO_3^- mass concentrations into account (average of 230 ng g^{-1} in January for DML), we calculate a post-depositional NO_3^- loss of 60 ng g^{-1} (or 75 %) and enrichment of 170 ‰ from the snow pack at DML following the approach of Weller et al. (2004). Fig. 7 shows a clear signal of $\delta^{15}N$-NO_3^- enrichment in the top 30 cm of the snowpack where the simulated 5 cm EFD case depth profile parallels the observed depth profile indicating NO_3^- photolytic redistribution at DML in the photic zone of the snow pack. Assuming all NO_3^- is archived below the photic zone, i.e., an e-folding depth of 5 cm, archival occurs below a depth of 15 cm, where NO_3^- has a residence time of 0.75 years in the photic zone corresponding to one summer. At this point, the amplitude of the annual cycle of observed $\delta^{15}N$-NO_3^- at DML does not vary. Our observed archived values of 50 ‰ and 60 ng g^{-1} agree well with the mean values of the snow pit below the photic zone, and the archived $\delta^{15}N$-NO_3^- value~~s~~ of the 5 cm EFD case (50 ‰). ~~. The for the 5 cm EFD case areXXXX and for the base case.~~ The seasonal variability of the simulated $\delta^{15}N$-NO_3^- ~~5 cm EFD case~~ depth profile for the 5 cm EFD case is constant between 30-80 ‰ below the photic zone indicating that no further enrichment or NO_3^- redistribution is taking place in the archived section of the snow pack. The DML site has a lower observed archived $\delta^{15}N$-NO_3^- value and is less sensitive to NO_3^- recycling ~~photolysis~~ than expected from TRANSITS modelling of $\delta^{15}N$-NO_3^- along a snow accumulation gradient (Table 2; Erbland et al. (2015), and we suggest this is due to the~~a~~ lower observed e-folding depth than modelled. ~~Differences between the values for the two scenarios andcould be 12What about the higher simulated mass concentrations than observed – why does a lower e-folding depth increase the nitrate conc???~~

Despite the relatively high NO_3^- mass concentrations and enriched $\delta^{15}N$-NO_3^- in the skin layer at DML, clear seasonal cycles remain in the depth profile in contrast to the lower snow accumulation site of Dome C where the depth profile is relatively constant below the photic zone (Fig. 4). At higher snow accumulation rates, the seasonality of atmospheric NO_3^- mass concentrations and $\delta^{15}N$-NO_3^- is preserved due to faster burial. Even at 6 cm yr^{-1} (w.e.), the snow layers remain in the active photic zone for 0.75 years and the weaker recycling factor is low enough to conserve the seasonality. Whereas at Dome C, snow layers remain within the photic zone for longer (about 3 years or 3 summers), due to the deeper e-folding depth and NO_2 emission and redistribution continues until the seasonal cycle becomes smoothed (Fig. 4). At Dome C, archival of NO_3^- occurs below a depth of 30 cm. Compared to Dome C, the archived values at DML have a similar mass concentration (Dome C: 35 ng g^{-1}) but lower $\delta^{15}N$-NO_3^- value (Dome C: 300 ‰), due to the deeper photic zone, stronger redistribution and recycling there.

~~**Our archived values of 50 ‰ and 60 ng g^{-1} agree well with the mean values of the snow pit below the photic zone (30 cm), and are lower than the simulated archived values from TRANSITS (120 ng g^{-1} and 130 ‰) due to the stronger photochemistry in the model. Due to the larger e-folding depth and hence larger photic zone at Dome C, NO_3^- has a longer residence time of 3 years (3 summers) in the photic zone. Here, archival of NO_3^- occurs below a depth of 30 cm. Compared to Dome C, the archived values at DML have a similar concentration (Dome C: 35 ng g^{-1}) but lower $\delta^{15}N$-NO_3^- value (Dome C: 300 ‰), due to the thicker photic zone, stronger redistribution and recycling there.**~~

Formatted: Not Superscript/ Subscript

Formatted: Not Highlight

Formatted: Not Highlight

Formatted: Not Superscript/ Subscript

Formatted: Not Superscript/ Subscript

Formatted: Not Superscript/ Subscript

Formatted: Subscript

4.5 Sensitivity of $\delta^{15}\mathrm{N\text{-}NO_3^-}$ to deposition parameters and implications for interpreting ice core records of $\delta^{15}\mathrm{N\text{-}NO_3^-}$ at DML

As first proposed by Frey et al. (2009) and later confirmed by field and lab studies (Erbland et al., 2015;Berhanu et al., 2014;Shi et al., 2019) it is UV-photolysis of $\mathrm{NO_3^-}$ that dominates post-depositional fractionation of $\delta^{15}\mathrm{N\text{-}NO_3^-}$ in snow and firn. Yet the extent of photolytic fractionation and the $\delta^{15}\mathrm{N\text{-}NO_3^-}$ signature ultimately preserved in firn and ice depends on the UV-spectrum of down-welling irradiance and~~,~~ on the time snow layers are exposed to incoming UV-radiation~~ as well as on the snow optical properties~~. Previous studies showed that $\delta^{15}\mathrm{N\text{-}NO_3^-}$ is sensitive to TCO but also to deposition parameters such as the annual snow accumulation rate (Shi et al., 2018;Noro et al., 2018;Erbland et al., 2013). Thus, if all deposition parameters remained constant or are well-constrained it should be theoretically possible to use $\delta^{15}\mathrm{N\text{-}NO_3^-}$ as an ice core proxy for past surface UV-radiation and stratospheric ozone. Understanding the depositional parameters and their impact on $\delta^{15}\mathrm{N\text{-}NO_3^-}$ is paramount for the interpretation of $\delta^{15}\mathrm{N\text{-}NO_3^-}$ signals preserved in ice cores. As the interpretation of $\delta^{15}\mathrm{N\text{-}NO_3^-}$ is site-specific, we investigate the sensitivity of the $\delta^{15}\mathrm{N\text{-}NO_3^-}$ signature at DML to snow accumulation rate, e-folding depth and TCO. Throughout section 4.5 we compare sensitivity results to a "base case" simulation which was simulated using the ~~As the~~ mean annual snow accumulation rate at DML ~~is~~ of 6 cm (w.e.) yr^{-1} and an e-folding depth of 10 cm~~, we take this simulation as our base case.~~. The base case simulation and snow pit $\delta^{15}\mathrm{N\text{-}NO_3^-}$ depth profiles parallel each other in the top 30 cm of the snow pack, but below the active photic zone, there is an offset between the depth profiles in terms of i) the amplitude of the summer and winter $\delta^{15}\mathrm{N\text{-}NO_3^-}$ values, and ii) the mean $\delta^{15}\mathrm{N\text{-}NO_3^-}$ value (Fig. 7).

4.5.1 Sensitivity of the ice core $\delta^{15}\mathrm{N\text{-}NO_3^-}$ signal to e-folding depth

We measured an e-folding depth at DML between 2 and 5 cm which is lower than that employed in the base case TRANSITS model simulation (10 cm). Furthermore, a range of e-folding depth values, between 3.7 and 20 cm, have been reported for Antarctica (Wolff et al., 2002;France et al., 2011). The positive bias of the TRANSITS base case simulation in archived $\delta^{15}\mathrm{N\text{-}NO_3^-}$ at DML may be due to e-folding depth being smaller than at Dome C as indicated by direct observations. In order to test this assumption, the sensitivity of archived $\delta^{15}\mathrm{N\text{-}NO_3^-}$ to the e-folding depth parameter needs to be quantified, which has not been done before as far as we know. Zatko et al. (2016) modelled the e-folding depth over Antarctica and investigated the impact of snow-sourced $\mathrm{NO_x}$ fluxes but not on $\delta^{15}\mathrm{N\text{-}NO_3^-}$. Fig.7a shows that the e-folding depth has a large influence on the $\delta^{15}\mathrm{N\text{-}NO_3^-}$ depth profile in terms of i) depth of the photic zone and thus depth of the $\delta^{15}\mathrm{N\text{-}NO_3^-}$ enrichment, and ii) the mean archived $\delta^{15}\mathrm{N\text{-}NO_3^-}$ value below the photic zone. A larger e-folding depth increases the $\delta^{15}\mathrm{N\text{-}NO_3^-}$ enrichment in the photic zone and increases the archived mean $\delta^{15}\mathrm{N\text{-}NO_3^-}$ value. For example, an e-folding depth of 10 cm at DML gives $\delta^{15}\mathrm{N\text{-}NO_3^-}$ enrichment down to 30 cm and an archived mean $\delta^{15}\mathrm{N\text{-}NO_3^-}$ value of 125 ‰ in the snow pack compared to an e-folding depth of 20 cm, which enriches the snow pack down to 45 cm and more than doubles the archived mean $\delta^{15}\mathrm{N\text{-}NO_3^-}$ value to 320 ‰. Meanwhile, an e-folding depth of 2 cm gives minimal enrichment and a low archived mean $\delta^{15}\mathrm{N\text{-}NO_3^-}$ value of 25 ‰. In comparison to the base case simulation, which has an e-folding depth of 10 cm, a lower e-folding depth of 5 cm decreases the archived mean $\delta^{15}\mathrm{N\text{-}NO_3^-}$ in the snow pack to ~50 ‰, closely matching our snow pit observations. Hence, a shallower e-

Formatted: Not Superscript/ Subscript

Formatted: Not Highlight

folding depth of 5 cm can explain the more depleted δ^{15}N-NO$_3^-$ snow pit profile, relative to the base case simulation, as NO$_3^-$ photolysis occurs in a shallower depth. Therefore, e-folding depth knowledge is required to understand the sensitivity of archived δ^{15}N-NO$_3^-$ at specific sites. We continue our sensitivity analysis using an e-folding depth of 5 cm and observed accumulation rate and refer to this scenario as our "5 cm EFD case".

4.5.~~1~~ 2 Sensitivity of the ice core δ^{15}N-NO$_3^-$ signal to accumulation rate

The δ^{15}N-NO$_3^-$ signal is also ~~indeed~~ sensitive to the snow accumulation rate at DML. ~~Here, the accumulation rate varied between 2.5 and 11 cm yr^{-1} (w.e.) over the last 1000 years (Sommer et al., 2000).~~ Figs. 7b-c~~e-d~~ show~~s~~ the potential impact of the~~is~~ variability in the snow accumulation rate on the NO$_3^-$ mass concentration and δ^{15}N-NO$_3^-$ signature at DML calculated with the TRANSITS model using an e-folding depth of 5 cm. Even in the 5 cm EFD case, there is still an offset with the snow pit δ^{15}N-NO$_3^-$ depth profile below the active photic zone. ~~Considering that the actual snow accumulation rate varied between 3.5 and 7.1 cm yr^{-1} (w.e.) in our snow pit, our δ^{15}N-NO$_3^-$ measurements fall within the simulated δ^{15}N-NO$_3^-$ depth profile for the accumulation rates over the past 1000 years.~~ ~~Below the active photic zone, there is an offset between the base case and snow pit δ^{15}N-NO$_3^-$ depth profile in terms of i) the amplitude of the summer and winter δ^{15}N-NO$_3^-$ values, and ii) the mean δ^{15}N-NO$_3^-$ value (Fig. 7).~~ To account for the~~is~~ offset, ~~-~~we investigated how the timing of snow deposition altered the δ^{15}N-NO$_3^-$ depth profile. Rather than assuming a constant accumulation rate of 6 cm yr^{-1} (w.e.), as in the 5 cm EFD case~~base case,~~ we find that a variable snow accumulation rate, based on our observations from the snow pit, alters the depth of the summer and winter δ^{15}N-NO$_3^-$ peaks (Fig. ~~7e~~7b~~.~~). Using the actual annual snow accumulation rate~~s~~ improves the model fit in the top 30 cm~~; Fig 7e~~). Furthermore, the timing of the snow accumulation throughout the year has a significant control on the amplitude of the seasonal δ^{15}N-NO$_3^-$ cycle. Snowfall at DML has a bimodal distribution with higher accumulation in austral autumn and early austral summer (Fig. S8~~9~~). In Fig. 7d, we modified the timing of the snow accumulation during the year by depositing 90 % of the annual snowfall in i) the first week of winter, and ii) the first week of summer, which represents the upper bound for snow accumulation in winter and summer respectively. The remaining 10 % of the annual snowfall is distributed evenly across the rest of the weeks of the year. Summer snow accumulation results in a higher δ^{15}N-NO$_3^-$ enrichment compared to winter snow accumulation, as the exposure of summer layers to UV is longer and thus NO$_3^-$ photolysis is stronger. Therefore, the timing and rate of snowfall can explain the misalignment between snow pit observations and 5 cm EFD case, ~~base case~~ simulation, which shifts the depth and amplitude of the δ^{15}N-NO$_3^-$ peaks in the depth profile.

~~Although the mean snow pit δ^{15}N-NO$_3^-$ is ~50 ‰ lower, the snow pit depth profile parallels the base case profile for the top 30 cm. Here, there is a clear enrichment of δ^{15}N-NO$_3^-$ in both the snow pit and base case profiles corresponding to the depth of the photic zone (30 cm), and demonstrating that NO$_3^-$ photolysis is taking place in this section of the snow pack. Below the photic zone, the seasonal variability of the base case δ^{15}N-NO$_3^-$ depth profile is constant between 100-153 ‰ indicating that no further enrichment or NO$_3^-$ redistribution is taking place in the archived section of the snow pack.~~

Formatted: Not Highlight

Formatted: Not Highlight

Formatted: Not Highlight

Formatted: Not Highlight

Formatted: Not Highlight

Formatted: Not Highlight

Formatted: Not Highlight

~~Despite the relatively high NO$_3^-$ mass concentrations and enriched δ^{15}N-NO$_3^-$ in the skin layer at DML, clear seasonal cycles remain in the depth profile in contrast to the lower snow accumulation site of Dome C where the depth profile is relatively constant below the photic zone. Figs. 7a-b indicate that at higher snow accumulation rates, the seasonality of atmospheric NO$_3^-$ and δ^{15}N-NO$_3^-$ is preserved due to faster burial. Even at 6 cm yr^{-1} (w.e.), the snow layers remain in the active photic zone for 0.75 years and the weaker recycling factor is low enough to conserve the seasonality. Whereas at Dome C, snow layers remain within the photic zone for longer (about 3 years), and NO$_3^-$ loss and redistribution continues until the seasonal cycle becomes smoothed (Figs. 7a-b). Thus, NO$_3^-$ recycling is strongest in the lowermost snow accumulation regions.~~

~~Below the active photic zone, there is an offset between the base case and snow pit δ^{15}N-NO$_3^-$ depth profile in terms of i) the amplitude of the summer and winter δ^{15}N-NO$_3^-$ values, and ii) the mean δ^{15}N-NO$_3^-$ value (Fig. 7). To account for this offset we investigated how the timing of snow deposition altered the δ^{15}N-NO$_3^-$ depth profile. Rather than assuming a constant accumulation rate of 6 cm yr^{-1} (w.e.), as in the base case, we find that a variable snow accumulation rate, based on our observations from the snow pit, alters the depth of the summer and winter δ^{15}N-NO$_3^-$ peaks (Fig. 7b.). Using the actual annual accumulation rates improves the model fit (~10 cm depth; Fig 7a). Furthermore, the timing of the snow accumulation throughout the year has a significant control on the amplitude of the seasonal δ^{15}N-NO$_3^-$ cycle. Snowfall at DML has a bimodal distribution with higher accumulation in austral autumn and early austral summer (Fig. S9). In Fig. 7c, we modified the timing of the snow accumulation during the year by depositing 90 % of the annual snowfall in i) the first week of winter, and ii) the first week of summer, which represents the upper bound for snow accumulation in winter and summer respectively. The remaining 10 % of the annual snowfall is distributed evenly across the rest of the weeks of the year. Summer snow accumulation results in a higher δ^{15}N-NO$_3^-$ enrichment compared to winter snow accumulation, as the exposure of summer layers to UV is longer and thus NO$_3^-$ photolysis is stronger. Therefore, the timing and rate of snowfall can explain the misalignment between snow pit observations and base case simulation, which shifts the depth and amplitude of the δ^{15}N-NO$_3^-$ peaks in the depth profile.~~

On centennial to millennial timescales, the snow accumulation rate has varied in regions of Antarctica (e.g. Thomas et al., 2017), which could potentially modify the degree of post-depositional processing and thus impact the archival and temporal variability of δ^{15}N-NO$_3^-$ in ice cores. For example, the snow accumulation rate varied between 2.5 and 11 cm yr^{-1} (w.e.) over the last 1000 years at DML (Sommer et al., 2000). ~~Interestingly, Geng et al. (2015) found that post-depositional loss of NO$_3^-$ in Greenland could fully account for the large difference between the glacial and Holocene δ^{15}N-NO$_3^-$ signature.~~ At DML, higher snow accumulation rates would result in ~~lower~~ lower NO$_3^-$ mass concentrations and more depleted δ^{15}N-NO$_3^-$ values in the skin layer, thus reducing the recycling strength and lowering the sensitivity of the UV proxy recorded in the ice over time, and vice versa. TRANSITS modelling predicts that the upper and lower bounds of δ^{15}N-NO$_3^-$ values in a 1000-year ice core from DML that has an accumulation rate between 2.5 and 11 cm yr^{-1} (w.e.) and e-folding depth of 5 cm to be between ~~70~~ 30 and~~-~~ ~~360~~ 140 ‰. Furthermore, δ^{15}N-NO$_3^-$ values could range between ~~90~~40 and~~-~~ ~~110~~ 50 ‰ depending on the timing of snowfall and extreme precipitation events, which are known to play a dominant role in snowfall variability across Antarctica (Turner et al., 2019). At DML, snow pit observations suggest that the variation of δ^{15}N-NO$_3^-$ between the polar day and polar night is 20

Formatted: Not Highlight

Formatted: Not Highlight

Formatted: Not Highlight

Formatted: Not Highlight

Formatted: Not Highlight

‰. This seasonality is ~~within the range of~~less than δ^{15}N-NO$_3^-$ values expected for changes in snow accumulation rates over time ~~(Fig. 7)~~. Therefore, any ~~seasonal~~ variation in snow accumulation~~ice core δ^{15}N-NO$_3^-$~~ will need to be accounted for in order to observe decadal, centennial and millennial scale trends in δ^{15}N-NO$_3^-$.

~~4.5.2 Sensitivity of the ice core δ^{15}N-NO$_3^-$ signal to e-folding depth~~

~~We measured an e-folding depth at DML (2-5 cm) which is lower than that employed in the TRANSITS model (10 cm). Furthermore, a range of e-folding depth values, between 3.7 and 20 cm, have been reported for AntarcticaThis estimate is similar to a modelled value at South Pole (3.7 cm; (Wolff et al., 2002;France et al., 2011) which has a similar accumulation rate, and Alert, Canada (5-6 cm; King and Simpson, 2001). The positive bias of the TRANSITS simulation in archived δ^{15}N-NO$_3^-$ at DML may be due to e-folding depth being smaller than at Dome C as indicated by direct observations. In order to test this assumption, the sensitivity of archived δ^{15}N-NO$_3^-$ to the parameter e-folding depth needs to be quantified, which has not been done before as far as we know. Zatko et al. (2016) modelled the e-folding depth over Antarctica and investigated the impact of snow-sourced NO$_x$ fluxes but not on δ^{15}N-NO$_3^-$. The e-folding depth has a large influence on the δ^{15}N-NO$_3^-$ depth profile in terms of i) depth of the photic zone and thus depth of the δ^{15}N-NO$_3^-$ enrichment, and ii) the mean archived δ^{15}N-NO$_3^-$ value below the photic zone (Fig. 7d). A larger e-folding depth strengthens the δ^{15}N-NO$_3^-$ enrichment in the photic zone and archived mean δ^{15}N-NO$_3^-$ value. For example, an e-folding depth of 10 cm at DML gives δ^{15}N-NO$_3^-$ enrichment down to 25 cm and an archived mean δ^{15}N-NO$_3^-$ value of 125 ‰ in the snow pack compared to an e-folding depth of 20 cm, which enriches the snow pack to 45 cm and more than doubles the archived mean δ^{15}N-NO$_3^-$ value to 320 ‰. Meanwhile, an e-folding depth of 2 cm gives minimal enrichment and a low archived mean δ^{15}N-NO$_3^-$ value of 25 ‰. In comparison to the base case simulation, which has an e-folding depth of 10 cm, a lower e-folding depth of 5 cm decreases the archived mean δ^{15}N-NO$_3^-$ in the snow pack to ~50 ‰, closely matching our snow pit observations. Hence, a shallower e-folding depth of 5 cm can explain the more depleted δ^{15}N-NO$_3^-$ snow pit profile, relative to the base case simulation, as NO$_3^-$ photolysis occurs in a shallower depth. Therefore, e-folding depth knowledge is required to understand the sensitivity of archived δ^{15}N-NO$_3^-$ at specific sites. A lower e-folding depth and variable snowfall throughout the year can explain the misalignment between the snow pit observations and simulated δ^{15}N-NO$_3^-$ depth profiles.~~

4.5.3 Sensitivity of ice core δ^{15}N-NO$_3^-$ signal to TCO

Fig. 8 shows the ~~strong~~ sensitivity of δ^{15}N-NO$_3^-$ to variations in ~~decreasing~~ TCO. For each week, a constant amount of ozone (e.g. 100 DU) was added or subtracted from these present day values. A decrease in TCO will increase UV radiation reaching the surface at an ice core site. As a result, stronger photolysis enhances NO$_3^-$ loss, redistribution and recycling from the snow pack and ultimately decreases the archived NO$_3^-$ mass concentration. Furthermore, a decrease in TCO enriches the δ^{15}N-NO$_3^-$ signature as the snow is exposed to a greater UV dose. We ~~expect~~ predict that a change of 100 Dobson Units (DU), i.e. the amount that ozone ~~now~~ decreases each spring as a result of stratospheric ozone destruction processes, will result in a ~~22~~ 10 ‰ change in δ^{15}N-NO$_3^-$ at DML. ~~(Erbland et al., 2015)~~The variability in δ^{15}N-NO$_3^-$ induced by TCO is ~~similar~~ less than~~to~~ the

Formatted: Not Highlight

seasonal variability of $\delta^{15}N\text{-}NO_3^-$ recorded in the snow pit (20 ‰), and less than the predicted variability of $\delta^{15}N\text{-}NO_3^-$ due to ~~variability~~ changes in snow accumulation (~~340~~ 110 ‰) or e-folding depth (100 ‰).~~,~~ As the above sensitivities have been evaluated individually, TCO depletion over many years may still be recoverable from ice core $\delta^{15}N\text{-}NO_3^-$ if the other factors are constrained. For example, the e-folding depth at the DML site appears stable over the 8 year snow pit: the modelled $\delta^{15}N\text{-}NO_3^-$ sensitivity of 100 ‰ represents an upper limit for changes in the e-folding depth ranging between 2 and 10 cm and if the e-folding depth had changed recently, in an irregular manor, a regular annual cycle in $\delta^{15}N\text{-}NO_3^-$ wouldn't be evident (Fig. 4). Although additional studies of e-folding depth are required to confirm the variability of e-folding depth. ~~thus the development of a large ozone hole is unlikely to be observed above the natural background $\delta^{15}N\text{-}NO_3^-$ variability in the ice core at this site.~~ The sensitivity of $\delta^{15}N\text{-}NO_3^-$ to TCO is greater at Dome C than DML (Fig. 8) due to the longer duration of surface snow exposure to UV radiation, stronger recycling and greater enrichment of $\delta^{15}N\text{-}NO_3^-$ in the photic zone. The sensitivity of $\delta^{15}N\text{-}NO_3^-$ to NO_3^- recycling at DML is lower than expected from TRANSITS modelling for the same snow accumulation rate by Erbland et al. (2015), namely due to a lower e-folding depth than modelled, and thus ~~is~~ the sensitivity of $\delta^{15}N\text{-}NO_3^-$ as a UV proxy is also lower than expected (Fig. 8).

4.5.4 Implications for interpreting ice core $\delta^{15}N\text{-}NO_3^-$

Site-specific air-snow transfer studies provide an understanding of the mechanisms that archive $\delta^{15}N\text{-}NO_3^-$ in ice cores, thus allowing for the interpretation of longer records of $\delta^{15}N\text{-}NO_3^-$ from the site. Ice core records of archived NO_3^- mass concentrations and $\delta^{15}N\text{-}NO_3^-$ at DML are a result of ~~three~~ two uptake and loss cycles that occur in the top ~~30~~ 15 cm during sunlit conditions. While we do not observe further redistribution of NO_3^- in layers deeper than the photic zone, we cannot rule out any further NO_3^- diffusion within the firn or ice sections of an ice core. This redistribution unlikely results in a loss of NO_3^- but could migrate NO_3^- to different layers, for example in acidic layers around volcanic horizons (Wolff, 1995).

There are a number of factors that will control the variability of the archived $\delta^{15}N\text{-}NO_3^-$ signature in ice cores recovered from DML. The $\delta^{15}N\text{-}NO_3^-$ signature in the snow pack is most sensitive to changes in the snow accumulation rate and e-folding depth, with snowfall timing and TCO ~~also~~ playing a smaller role. The e-folding depth could change over time due to higher or lower dust or black carbon concentrations or a change in the snow grain size in a particular snow layer. The snow accumulation rate and e-folding depth could influence the archived $\delta^{15}N\text{-}NO_3^-$ composition by up to 110 and ~~3~~100 %, respectively, over the last 1000-years. This magnitude is comparable to modelled enrichment in ice ~~-~~core $\delta^{15}N\text{-}NO_3^-$ (0 to 363 ‰) due to photolysis-driven loss of NO_3^- at low accumulation sites in Antarctica by Zatko et al. (2016). While the timing of snowfall and changes in TCO will have a smaller impact of 1~~2~~0 ‰ on archived $\delta^{15}N\text{-}NO_3^-$. Ice core $\delta^{15}N\text{-}NO_3^-$ records at DML will be less sensitive to changes in UV than those at Dome C (Fig. 8), however the higher snow accumulation rate and more accurate dating at DML allows for higher resolution ice core $\delta^{15}N\text{-}NO_3^-$ records. We acknowledge that in addition, other factors such as light absorbing impurities (Zatko et al., 2013), local meteorology, source of emissions and transport of NO_x and NO_3^-, atmospheric oxidant concentrations, and polar NO_3^- formation can influence the rate of recycling and export of snow sourced NO_x. We discussed

Formatted: Not Highlight

Formatted: Not Highlight

Formatted: Not Superscript/ Subscript

Formatted: Not Highlight

Formatted: Not Highlight

above that atmospheric δ^{15}N-NO_3^- values are unlikely to be influenced or sourced from snow exported up wind from the polar plateau due to the local meteorology at DML at least for the duration of the campaign. Yet these factors may have changed over time.

Given a variable snow accumulation rate and ~~smaller~~ shallower e-folding depth, which we provide evidence for at DML, t~~, t~~he TRANSITS model is able to reproduce our snow pit observations, justifying our previous assumption that photolysis is the main driver of NO_3^- post-depositional processes at DML. In fact, TRANSITS does such a good job at simulating NO_3^- recycling in Antarctica that we recommend that this tool is employed before the commencement of future ice core δ^{15}N-NO_3^- studies to understand the sensitivity of the signal to various factors. Taking changes in snow accumulation into account, it may be possible to reconstruct past UV and TCO on longer timescales from the δ^{15}N-NO_3^- signal in DML ice cores provided other factors such as the e-folding depth have remained the same.

5 Conclusions

Nitrogen ~~Our key findings are:~~

stable nitrate i~~I~~sotopes of NO_3^- are a powerful tool for ~~unpicking~~disentangling post-depositional processes affecting ice core signals of NO_3^- at low accumulation sites in Antarctica.~~;~~

At DML, post-depositional loss of NO_3^- is controlled predominantly by NO_3^- photolys~~istic loss~~.~~;~~

P~~P~~hotolysis redistributes NO_3^- between the snow pack and atmosphere resulting in an enrichment of δ^{15}N-NO_3^- in the skin layer.~~;~~

~~TRANSITS, a photolysis driven model, modelling suggests that NO_3^-~~Nitrate is recycled ~~three~~ two times before it is archived in the snow pack below 15 cm and within 0.75 years.~~;~~

Once archived, the seasonal variability of δ^{15}N-NO_3^- values and NO_3^- mass concentrations oscillate between -1 to 80 ‰ and 30 to 80 ng g^{-1}, respectively.~~;~~ The e-folding depth at DML ranges between 2 - 5 cm, which is lower than previous observations at Dome C (10 and 20 cm). As constraints on e-folding depth are critical for calculating photolytic loss of snow pack NO_3^- and for interpreting δ^{15}N-NO_3^- preserved in ice cores, additional studies of e-folding depth across a range of Antarctic sites would help determine key factors influencing this parameter.

TRANSITS, a photolysis driven model, can explain the observed snow depth profiles of δ^{15}N-NO_3^- at DML constrained by an e-folding depth of 5 cm, the observed snow accumulation rate, and variable snowfall timing.

TRANSITS sensitivity analysis showed that the δ^{15}N-NO_3^- signature in the snow pack is most sensitive to changes in the e-folding depth (100 ‰ for an 8 cm change in e-folding depth) and the snow accumulation rate (~~up to 300~~ 100 ‰ for an 8.5 cm yr^{-1} (w.e.) change in annual snow accumulation rate~~%~~) ~~and e-folding depth (up to 300 %)~~, with snowfall timing (1~~~2~~0 ‰ for a change in dominant snowfall season~~%~~) and total column ozone (1~~~2~~0 ‰ for a 100 DU change in TCO~~%~~) ~~also~~ playing a smaller role. The NO_3^- recycling process at DML is weaker than Dome C, largely because of the higher snow accumulation rate and lower e-folding depth. ~~;~~

Formatted: Font:

Formatted: Not Superscript/ Subscript

Formatted: Normal, No bullets or numbering

Formatted: Not Highlight

Formatted: Not Superscript/ Subscript

Formatted: Not Highlight

Formatted: Not Highlight

Formatted: Not Highlight

Formatted: Not Highlight

Formatted: Not Highlight

Formatted: Not Superscript/ Subscript

Formatted: Not Highlight

Formatted: Not Highlight

Formatted: Not Highlight

Formatted: Not Highlight

Formatted: Not Highlight

Formatted: Not Highlight

Formatted: Superscript

Formatted: Not Highlight

Formatted: Not Highlight

Formatted: Not Highlight

TRANSITS has now been tested at two sites in Antarctica, namely DML and Dome C, and we recommend applying this model to new ice core sites to understand the sensitivity of the $\delta^{15}N\text{-}NO_3^-$ signal before embarking on new ice core projects. ~~;~~ By accounting for variability in the snow accumulation rate and assuming a constant e-folding depth, it may be possible to reconstruct past UV-radiation at ice core sites with very a low accumulation rate and low accumulation variability, as low accumulation variability will have little effect on $\delta^{15}N\text{-}NO_3^-$ in comparison to the UV dose reaching the ground.

~~;~~

~~Constraints on e-folding depth are critical for calculating photolytic loss of snow pack NO_3^- and for interpreting $\delta^{15}N\text{-}NO_3^-$ preserved in ice cores;~~

~~Additional studies of e-folding depth across a range of Antarctic sites would help determine key factors influencing this parameter;~~

- ~~The NO_3^- recycling process at DML is weaker than Dome C, largely because of the higher snow accumulation rate and lower e-folding depth;~~
- ~~TRANSITS has now been tested at two sites in Antarctica, namely DML and Dome C, and we recommend applying this model to new ice core sites to understand the sensitivity of the $\delta^{15}N\text{-}NO_3^-$ signal before embarking on new ice core projects;~~
- ~~By accounting for variability in the snow accumulation rate and assuming a constant e-folding depth, it may be possible to reconstruct past UV-radiation at ice core sites with very a low accumulation rate and low accumulation variability, as low accumulation variability will have little effect on $\delta^{15}N\text{-}NO_3^-$ in comparison to the UV dose reaching ground.~~

Formatted: Not Highlight

Formatted: Not Highlight

Formatted: Highlight

Acknowledgments

This project was funded by a National Environment Research Council (NERC) Standard Grant (NE/N011813/1) to M.F. V.H.L.W would like to thank the University of Cambridge Doctoral Training Program (DTP) for funding a NERC Research Experience Project (REP) that contributed to this ~~manuscript~~research. We would like to thank British Antarctic Survey (BAS) and Alfred Wegener Institute (AWI) staff for their field and logistics support at Halley Station and Kohnen Station, respectively. Technical support for nitrate isotope analysis at the Institut des Géosciences de l'Environnement (IGE), Grenoble was provided by Joris Leglise, Ines Ollivier and Ilan Bourgeois. We thank Joseph Erbland for providing the TRANSITS model. Field samples collected at Dome C was possible through the program SUNITEDC/CAPOXI (grant 1011/1177) funded by the Institut Polaire Français IPEV. J.S and N.C thank the ANR (Investissements d'avenir ANR-15-IDEX-02 and EAIIST grant ANR-16-CE01-0011-01) and the INSU program LEFE-CHAT for supporting the stable isotope laboratory. This is publication 1 of PANDA platform on which isotope analysis were performed. PANDA was partially funded by the LabEx OSUG@2020 (ANR10 LABX56). All winter over personal who collected the year-round Dome C samples in extreme conditions, year~~s~~ after year~~s~~, are deeply acknowledged. In addition, we thank Emily Ludlow, Shaun Miller, Catriona Sinclair, Rebecca Tuckwell, and Neil Brough for technical support at BAS. Thanks to James France for discussions around the e-folding depth measurements and interpretation, and to John Turner for discussions of the local meteorology. We acknowledge Utrecht

University who supplied the AWS data for AWS9 at DML05/Kohnen (https://www.projects.science.uu.nl/iceclimate/aws/files_oper/oper_20632), and the precipitation data from the RACMO2 model (https://doi.org/10/c2pv). We would like to thank Bodeker Scientific, funded by the New Zealand Deep South National Science Challenge, for providing the combined NIWA-BS total column ozone database. Wind roses were plotted using the openair package in R. The data set for the DML nitrate isotopic ratios and nitrate mass concentrations in aerosol, skin layer and snow pits is available through the Polar Data Centre https://doi.org/10.5285/1467b446-54eb-45c1-8a31-f4af21e60e60, and supporting data are also included as figures and tables in the supplement.

Author contributions

V.H.L.W, J.S and M.F designed the research. V.H.L.W, M.F and J.S, N.C collected samples at DML and Dome C, respectively. V.H.L.W analysed the major ion data. V.H.L.W, L.H, and N.C analysed the nitrate isotope data. A.M and V.H.L.W designed the TRANSITS experiments. A.M performed the TRANSITS experiments. M.F did e-folding depth and snow emission flux calculations. V.H.L.W prepared the manuscript with contributions from all co-authors.

References

, !!! INVALID CITATION !!! (Berhanu et al., 2014;Frey et al., 2009;Erbland et al., 2013).

, !!! INVALID CITATION !!! (Erbland et al., 2013;Shi et al., 2019).

Abbatt, J. P.: Interaction of HNO3 with water-ice surfaces at temperatures of the free troposphere, Geophysical Research Letters, 24, 1479-1482, 1997.

Abbatt, J. P.: Interactions of atmospheric trace gases with ice surfaces: Adsorption and reaction, Chemical reviews, 103, 4783-4800, 2003.

Berhanu, T. A., Meusinger, C., Erbland, J., Jost, R., Bhattacharya, S., Johnson, M. S., and Savarino, J.: Laboratory study of nitrate photolysis in Antarctic snow. II. Isotopic effects and wavelength dependence, The Journal of chemical physics, 140, 244306, 2014.

Beyersdorf, A. J., Blake, D. R., Swanson, A., Meinardi, S., Rowland, F., and Davis, D.: Abundances and variability of tropospheric volatile organic compounds at the South Pole and other Antarctic locations, Atmospheric Environment, 44, 4565-4574, 2010.

Blunier, T., Floch, G. L., Jacobi, H. W., and Quansah, E.: Isotopic view on nitrate loss in Antarctic surface snow, Geophysical Research Letters, 32, 2005.

Bock, J., Savarino, J., and Picard, G.: Air–snow exchange of nitrate: a modelling approach to investigate physicochemical processes in surface snow at Dome C, Antarctica, Atmospheric Chemistry and Physics, 16, 12531-12550, 2016.

Brucker, L., Picard, G., and Fily, M.: Snow grain-size profiles deduced from microwave snow emissivities in Antarctica, Journal of Glaciology, 56, 514-526, 2010.

Chan, H., King, M., and Frey, M.: The impact of parameterising light penetration into snow on the photochemical production of NOx and OH radicals in snow, Atmos. Chem. Phys, 15, 7913-7927, 2015.

Chan, H. G., Frey, M. M., and King, M. D.: Modelling the physical multiphase interactions of HNO 3 between snow and air on the Antarctic Plateau (Dome C) and coast (Halley), Atmospheric Chemistry and Physics, 18, 1507-1534, 2018.

Chance, K., and Kurucz, R. L.: An improved high-resolution solar reference spectrum for earth's atmosphere measurements in the ultraviolet, visible, and near infrared, Journal of quantitative spectroscopy and radiative transfer, 111, 1289-1295, 2010.

Chu, L., and Anastasio, C.: Quantum yields of hydroxyl radical and nitrogen dioxide from the photolysis of nitrate on ice, The Journal of Physical Chemistry A, 107, 9594-9602, 2003.

Davis, D., Chen, G., Buhr, M., Crawford, J., Lenschow, D., Lefer, B., Shetter, R., Eisele, F., Mauldin, L., and Hogan, A.: South Pole NOx chemistry: an assessment of factors controlling variability and absolute levels, Atmospheric Environment, 38, 5375-5388, 2004a.

Davis, D., Eisele, F., Chen, G., Crawford, J., Huey, G., Tanner, D., Slusher, D., Mauldin, L., Oncley, S., and Lenschow, D.: An overview of ISCAT 2000, Atmospheric Environment, 38, 5363-5373, 2004b.

Davis, D. D., Seelig, J., Huey, G., Crawford, J., Chen, G., Wang, Y., Buhr, M., Helmig, D., Neff, W., and Blake, D.: A reassessment of Antarctic plateau reactive nitrogen based on ANTCI 2003 airborne and ground based measurements, Atmospheric Environment, 42, 2831-2848, 2008.

Delmonte, B., Winton, H., Baroni, M., Baccolo, G., Hansson, M., Andersson, P., Baroni, C., Salvatore, M. C., Lanci, L., and Maggi, V.: Holocene dust in East Antarctica: Provenance and variability in time and space, The Holocene, 0959683619875188, 2019.

Dibb, J. E., and Whitlow, S. I.: Recent climate anomalies and their impact on snow chemistry at South Pole, 1987-1994, Geophysical Research Letters, 23, 1115-1118, 1996.

Dubowski, Y., Colussi, A., and Hoffmann, M.: Nitrogen dioxide release in the 302 nm band photolysis of spray-frozen aqueous nitrate solutions. Atmospheric implications, The Journal of Physical Chemistry A, 105, 4928-4932, 2001.

Duce, R. A., Liss, P. S., Merrill, J. T., Atlas, E. L., Buat-Menard, P., Hicks, B. B., Miller, J. M., Prospero, J. M., Arimoto, R., Church, T. M., Ellis, W., Galloway, J. N., Hansen, L., Jickells, T. D., Knap, A. H., Reinhardt, K. H., Schneider, B., Soudine, A., Tokos, J. J., Tsunogai, S., Wollast, R., and Zhou, M.: The atmospheric input of trace species to the world ocean, Global Biogeochem. Cycles, 5, 193-259, 10.1029/91gb01778, 1991.

Erbland, J.: Isotopic constrains on the interpretation of the nitrate record in the Vostok ice core, University of Grenoble, University of Grenoble, 299 pp., 2011.

Erbland, J., Vicars, W., Savarino, J., Morin, S., Frey, M., Frosini, D., Vince, E., and Martins, J.: Air–snow transfer of nitrate on the East Antarctic Plateau–Part 1: Isotopic evidence for a photolytically driven dynamic equilibrium in summer, Atmospheric Chemistry and Physics, 13, 6403-6419, 2013.

Erbland, J., Savarino, J., Morin, S., France, J., Frey, M., and King, M.: Air–snow transfer of nitrate on the East Antarctic Plateau–Part 2: An isotopic model for the interpretation of deep ice-core records, Atmospheric Chemistry and Physics, 15, 12079-12113, 2015.

France, J., King, M., Frey, M., Erbland, J., Picard, G., Preunkert, S., MacArthur, A., and Savarino, J.: Snow optical properties at Dome C (Concordia), Antarctica; implications for snow emissions and snow chemistry of reactive nitrogen, Atmospheric Chemistry and Physics, 11, 9787-9801, 2011.

France, J., and King, M.: The effect of measurement geometry on recording solar radiation attenuation in snowpack (e-folding depth) using fibre-optic probes, Journal of Glaciology, 58, 417-418, 2012.

France, J., Reay, H., King, M., Voisin, D., Jacobi, H., Domine, F., Beine, H., Anastasio, C., MacArthur, A., and Lee-Taylor, J.: Hydroxyl radical and NOx production rates, black carbon concentrations and light-absorbing impurities in snow from field measurements of light penetration and nadir reflectivity of onshore and offshore coastal Alaskan snow, Journal of Geophysical Research: Atmospheres, 117, 2012.

Frey, M., Roscoe, H., Kukui, A., Savarino, J., France, J., King, M., Legrand, M., and Preunkert, S.: Atmospheric nitrogen oxides (NO and NO_2) at Dome C, East Antarctica, during the OPALE campaign, Atmospheric Chemistry and Physics, 15, 7859-7875, 2015.

Frey, M. M., Savarino, J., Morin, S., Erbland, J., and Martins, J.: Photolysis imprint in the nitrate stable isotope signal in snow and atmosphere of East Antarctica and implications for reactive nitrogen cycling, Atmospheric Chemistry and Physics, 9, 8681-8696, 2009.

Frey, M. M., Brough, N., France, J. L., Anderson, P. S., Traulle, O., King, M. D., Jones, A. E., Wolff, E. W., and Savarino, J.: The diurnal variability of atmospheric nitrogen oxides (NO and NO₂) above the Antarctic Plateau driven by atmospheric stability and snow emissions, Atmos. Chem. Phys., 13, 3045-3062, 10.5194/acp-13-3045-2013, 2013.

Freyer, H.: Seasonal variation of 15N/14N ratios in atmospheric nitrate species, Tellus B, 43, 30-44, 1991.

Gay, M., Fily, M., Genthon, C., Frezzotti, M., Oerter, H., and Winther, J.-G.: Snow grain-size measurements in Antarctica, Journal of Glaciology, 48, 527-535, 2002.

Geng, L., Alexander, B., Cole-Dai, J., Steig, E. J., Savarino, J., Sofen, E. D., and Schauer, A. J.: Nitrogen isotopes in ice core nitrate linked to anthropogenic atmospheric acidity change, Proceedings of the National Academy of Sciences, 111, 5808-5812, 2014.

Geng, L., Zatko, M. C., Alexander, B., Fudge, T., Schauer, A. J., Murray, L. T., and Mickley, L. J.: Effects of postdepositional processing on nitrogen isotopes of nitrate in the Greenland Ice Sheet Project 2 ice core, Geophysical Research Letters, 42, 5346-5354, 2015.

Geng, L., Murray, L. T., Mickley, L. J., Lin, P., Fu, Q., Schauer, A. J., and Alexander, B.: Isotopic evidence of multiple controls on atmospheric oxidants over climate transitions, Nature, 546, 133, 2017.

Göktas, F., Fischer, H., Oerter, H., Weller, R., Sommer, S., and Miller, H.: A glacio-chemical characterization of the new EPICA deep-drilling site on Amundsenisen, Dronning Maud Land, Antarctica, Annals of Glaciology, 35, 347-354, 2002.

Hastings, M., Jarvis, J., and Steig, E.: Anthropogenic impacts on nitrogen isotopes of ice-core nitrate, Science, 324, 1288-1288, 2009.

Hastings, M. G., Steig, E., and Sigman, D.: Seasonal variations in N and O isotopes of nitrate in snow at Summit, Greenland: Implications for the study of nitrate in snow and ice cores, Journal of Geophysical Research: Atmospheres, 109, 2004.

Hastings, M. G., Casciotti, K. L., and Elliott, E. M.: Stable isotopes as tracers of anthropogenic nitrogen sources, deposition, and impacts, Elements, 9, 339-344, 2013.

Hauglustaine, D., Granier, C., Brasseur, G., and Megie, G.: The importance of atmospheric chemistry in the calculation of radiative forcing on the climate system, Journal of Geophysical Research: Atmospheres, 99, 1173-1186, 1994.

Helmig, D., Liptzin, D., Hueber, J., and Savarino, J.: Impact of exhaust emissions on chemical snowpack composition at Concordia Station, Antarctica, The Cryosphere, 14, 199-209, 2020.

Hoering, T.: The isotopic composition of the ammonia and the nitrate ion in rain, Geochimica et Cosmochimica Acta, 12, 97-102, 1957.

Hofstede, C. M., van de Wal Roderik, S., Kaspers, K. A., Van Den Broeke, M. R., Karlöf, L., Winther, J.-G., Isaksson, E., Lappegard, G., Mulvaney, R., and Oerter, H.: Firn accumulation records for the past 1000 years on the basis of dielectric profiling of six cores from Dronning Maud Land, Antarctica, Journal of Glaciology, 50, 279-291, 2004.

Hofzumahaus, A., Lefer, B., Monks, P., Hall, S., Kylling, A., Mayer, B., Shetter, R., Junkermann, W., Bais, A., and Calvert, J.: Photolysis frequency of O_3 to $O(^1D)$: Measurements and modeling during the International Photolysis Frequency Measurement and Modeling Intercomparison (IPMMI), Journal of Geophysical Research: Atmospheres, 109, 2004.

Honrath, R., Peterson, M. C., Guo, S., Dibb, J. E., Shepson, P., and Campbell, B.: Evidence of NOx production within or upon ice particles in the Greenland snowpack, Geophysical Research Letters, 26, 695-698, 1999.

Huey, L. G., Tanner, D., Slusher, D., Dibb, J. E., Arimoto, R., Chen, G., Davis, D., Buhr, M., Nowak, J., and Mauldin Iii, R.: CIMS measurements of HNO_3 and SO_2 at the South Pole during ISCAT 2000, Atmospheric environment, 38, 5411-5421, 2004.

Huthwelker, T., Ammann, M., and Peter, T.: The uptake of acidic gases on ice, Chemical reviews, 106, 1375-1444, 2006.

Jacobi, H.-W., Weller, R., Jones, A., Anderson, P., and Schrems, O.: Peroxyacetyl nitrate (PAN) concentrations in the Antarctic troposphere measured during the photochemical experiment at Neumayer (PEAN'99), Atmospheric Environment, 34, 5235-5247, 2000.

Jones, A., Weller, R., Minikin, A., Wolff, E., Sturges, W., McIntyre, H., Leonard, S., Schrems, O., and Bauguitte, S.: Oxidized nitrogen chemistry and speciation in the Antarctic troposphere, Journal of Geophysical Research: Atmospheres, 104, 21355-21366, 1999.

Jones, A., Weller, R., Wolff, E., and Jacobi, H. W.: Speciation and rate of photochemical NO and NO_2 production in Antarctic snow, Geophysical Research Letters, 27, 345-348, 2000.

Jones, A., Weller, R., Anderson, P., Jacobi, H. W., Wolff, E., Schrems, O., and Miller, H.: Measurements of NOx emissions from the Antarctic snowpack, Geophysical Research Letters, 28, 1499-1502, 2001.

Jones, A., Wolff, E., Ames, D., Bauguitte, S.-B., Clemitshaw, K., Fleming, Z., Mills, G., Saiz-Lopez, A., Salmon, R., and Sturges, W.: The multi-seasonal NO_y budget in coastal Antarctica and its link with surface snow and ice core nitrate: results from the CHABLIS campaign, Atmospheric Chemistry and Physics Discussions, 7, 4127-4163, 2007.

Jones, A., Brough, N., Anderson, P., and Wolff, E. W.: HO_2NO_2 and HNO_3 in the coastal Antarctic winter night: a" lab-in-the-field" experiment, Atmospheric Chemistry and Physics, 14, 11843-11851, 2014.

Jones, A. E., Wolff, E. W., Ames, D., Bauguitte, S.-B., Clemitshaw, K., Fleming, Z., Mills, G., Saiz-Lopez, A., Salmon, R. A., and Sturges, W.: The multi-seasonal NO y budget in coastal Antarctica and its link with surface snow and ice core nitrate: results from the CHABLIS campaign, Atmospheric Chemistry and Physics, 11, 9271-9285, 2011.

Keene, W. C., Pszenny, A. A., Galloway, J. N., and Hawley, M. E.: Sea-salt corrections and interpretation of constituent ratios in marine precipitation, Journal of Geophysical Research: Atmospheres, 91, 6647-6658, 1986.

Kendall, C., Elliott, E. M., and Wankel, S. D.: Tracing anthropogenic inputs of nitrogen to ecosystems, Stable isotopes in ecology and environmental science, 2, 375-449, 2007.

King, M. D., and Simpson, W. R.: Extinction of UV radiation in Arctic snow at Alert, Canada (82 N), Journal of Geophysical Research: Atmospheres, 106, 12499-12507, 2001.

Kukui, A., Loisil, R., Kerbrat, M., Frey, M., Gil Roca, J., Jourdain, B., Ancellet, G., Bekki, S., Legrand, M., and Preunkert, S.: OH and RO2 radicals at Dome C (East Antarctica): first observations and assessment of photochemical budget, EGU General Assembly Conference Abstracts, 2013.

Le Meur, E., Magand, O., Arnaud, L., Fily, M., Frezzotti, M., Cavitte, M., Mulvaney, R., and Urbini, S.: Spatial and temporal distributions of surface mass balance between Concordia and Vostok stations, Antarctica, from combined radar and ice core data: first results and detailed error analysis, The Cryosphere, 2018.

Lee-Taylor, J., and Madronich, S.: Calculation of actinic fluxes with a coupled atmosphere–snow radiative transfer model, Journal of Geophysical Research: Atmospheres, 107, 2002.

Lee, H.-M., Henze, D. K., Alexander, B., and Murray, L. T.: Investigating the sensitivity of surface-level nitrate seasonality in Antarctica to primary sources using a global model, Atmospheric Environment, 89, 757-767, 2014.

Legrand, M. R., and Delmas, R. J.: Soluble impurities in four Antarctic ice cores over the last 30 000 years, Annals of Glaciology, 10, 116-120, 1988.

Li, D., and Wang, X.: Nitrogen isotopic signature of soil-released nitric oxide (NO) after fertilizer application, Atmospheric Environment, 42, 4747-4754, https://doi.org/10.1016/j.atmosenv.2008.01.042, 2008.

Libois, Q., Picard, G., France, J., Arnaud, L., Dumont, M., Carmagnola, C., and King, M.: Influence of grain shape on light penetration in snow, The Cryosphere, 7, 1803-1818, 2013.

Mariotti, A.: Atmospheric nitrogen is a reliable standard for natural 15N abundance measurements, Nature, 303, 685, 1983.

McCabe, J. R., Thiemens, M. H., and Savarino, J.: A record of ozone variability in South Pole Antarctic snow: Role of nitrate oxygen isotopes, Journal of Geophysical Research: Atmospheres, 112, 2007.

Meusinger, C., Berhanu, T. A., Erbland, J., Savarino, J., and Johnson, M. S.: Laboratory study of nitrate photolysis in Antarctic snow. I. Observed quantum yield, domain of photolysis, and secondary chemistry, The Journal of chemical physics, 140, 244305, 2014.

Miller, D. J., Wojtal, P. K., Clark, S. C., and Hastings, M. G.: Vehicle NOx emission plume isotopic signatures: Spatial variability across the eastern United States, Journal of Geophysical Research: Atmospheres, 122, 4698-4717, 2017.

Miller, D. J., Chai, J., Guo, F., Dell, C. J., Karsten, H., and Hastings, M. G.: Isotopic Composition of In Situ Soil NOx Emissions in Manure-Fertilized Cropland, Geophysical Research Letters, 45, 12,058-012,066, 2018.

Morin, S., Savarino, J., Frey, M. M., Yan, N., Bekki, S., Bottenheim, J. W., and Martins, J. M.: Tracing the origin and fate of NOx in the Arctic atmosphere using stable isotopes in nitrate, Science, 322, 730-732, 2008.

Morin, S., Savarino, J., Frey, M. M., Domine, F., Jacobi, H. W., Kaleschke, L., and Martins, J. M.: Comprehensive isotopic composition of atmospheric nitrate in the Atlantic Ocean boundary layer from 65 S to 79 N, Journal of Geophysical Research: Atmospheres, 114, 2009.

Mosley-Thompson, E., Paskievitch, J. F., Gow, A. J., and Thompson, L. G.: Late 20th century increase in South Pole snow accumulation, Journal of Geophysical Research: Atmospheres, 104, 3877-3886, 1999.

Mulvaney, R., and Wolff, E. W.: Evidence for winter/spring denitrification of the stratosphere in the nitrate record of Antarctic firn cores, Journal of Geophysical Research: Atmospheres, 98, 5213-5220, 1993.

Mulvaney, R., Wagenbach, D., and Wolff, E.: Postdepositional change in snowpack nitrate from observation of year-round near-surface snow in coastal Antarctica, Journal of Geophysical Research: Atmospheres, 103, 11021-11031, 1998.

Noro, K., Hattori, S., Uemura, R., Fukui, K., Hirabayashi, M., Kawamura, K., Motoyama, H., Takenaka, N., and Yoshida, N.: Spatial variation of isotopic compositions of snowpack nitrate related to post-depositional processes in eastern Dronning Maud Land, East Antarctica, GEOCHEMICAL JOURNAL, 52, e7-e14, 10.2343/geochemj.2.0519, 2018.

Oerter, H., Wilhelms, F., Jung-Rothenhäusler, F., Göktas, F., Miller, H., Graf, W., and Sommer, S.: Accumulation rates in Dronning Maud Land, Antarctica, as revealed by dielectric-profiling measurements of shallow firn cores, Annals of Glaciology, 30, 27-34, 2000.

Oncley, S., Buhr, M., Lenschow, D., Davis, D., and Semmer, S.: Observations of summertime NO fluxes and boundary-layer height at the South Pole during ISCAT 2000 using scalar similarity, Atmospheric Environment, 38, 5389-5398, 2004.

Pasteris, D., McConnell, J. R., Edwards, R., Isaksson, E., and Albert, M. R.: Acidity decline in Antarctic ice cores during the Little Ice Age linked to changes in atmospheric nitrate and sea salt concentrations, Journal of Geophysical Research: Atmospheres, 119, 5640-5652, 2014.

Reijmer, C., and Oerlemans, J.: Temporal and spatial variability of the surface energy balance in Dronning Maud Land, East Antarctica, Journal of Geophysical Research: Atmospheres, 107, ACL 9-1-ACL 9-12, 2002.

Röthlisberger, R., Hutterli, M. A., Sommer, S., Wolff, E. W., and Mulvaney, R.: Factors controlling nitrate in ice cores: Evidence from the Dome C deep ice core, Journal of Geophysical Research: Atmospheres, 105, 20565-20572, 2000.

Röthlisberger, R., Hutterli, M. A., Wolff, E. W., Mulvaney, R., Fischer, H., Bigler, M., Goto-Azuma, K., Hansson, M. E., Ruth, U., and Siggaard-Andersen, M.-L.: Nitrate in Greenland and Antarctic ice cores: a detailed description of post-depositional processes, Annals of Glaciology, 35, 209-216, 2002.

Savarino, J., Kaiser, J., Morin, S., Sigman, D., and Thiemens, M.: Nitrogen and oxygen isotopic constraints on the origin of atmospheric nitrate in coastal Antarctica, Atmospheric Chemistry and Physics, 7, 1925-1945, 2007.

Schlosser, E., Manning, K., Powers, J., Duda, M., Birnbaum, G., and Fujita, K.: Characteristics of high-precipitation events in Dronning Maud Land, Antarctica, Journal of Geophysical Research: Atmospheres, 115, 2010.

Seinfeld, J. H., and Pandis, S. N.: From air pollution to climate change, Atmospheric Chemistry and Physics, 1326, 1998.

Shi, G., Buffen, A., Hastings, M., Li, C., Ma, H., Li, Y., Sun, B., An, C., and Jiang, S.: Investigation of post-depositional processing of nitrate in East Antarctic snow: isotopic constraints on photolytic loss, re-oxidation, and source inputs, Atmospheric Chemistry and Physics, 15, 9435-9453, 2015.

Shi, G., Buffen, A., Ma, H., Hu, Z., Sun, B., Li, C., Yu, J., Ma, T., An, C., and Jiang, S.: Distinguishing summertime atmospheric production of nitrate across the East Antarctic Ice Sheet, Geochimica et Cosmochimica Acta, 231, 1-14, 2018.

Shi, G., Chai, J., Zhu, Z., Hu, Z., Chen, Z., Yu, J., Ma, T., Ma, H., An, C., and Jiang, S.: Isotope fractionation of nitrate during volatilization in snow: a field investigation in Antarctica, Geophysical Research Letters, 46, 3287-3297, 2019.

Silva, S., Kendall, C., Wilkison, D., Ziegler, A., Chang, C. C., and Avanzino, R.: A new method for collection of nitrate from fresh water and the analysis of nitrogen and oxygen isotope ratios, Journal of Hydrology, 228, 22-36, 2000.

Sofen, E., Alexander, B., Steig, E., Thiemens, M., Kunasek, S., Amos, H., Schauer, A., Hastings, M., Bautista, J., and Jackson, T.: WAIS Divide ice core suggests sustained changes in the atmospheric formation pathways of sulfate and nitrate since the 19th century in the extratropical Southern Hemisphere, Atmospheric Chemistry and Physics, 14, 5749-5769, 2014.

Sommer, S., Appenzeller, C., Röthlisberger, R., Hutterli, M. A., Stauffer, B., Wagenbach, D., Oerter, H., Wilhelms, F., Miller, H., and Mulvaney, R.: Glacio-chemical study spanning the past 2 kyr on three ice cores from Dronning Maud Land, Antarctica: 1. Annually resolved accumulation rates, Journal of Geophysical Research: Atmospheres, 105, 29411-29421, 10.1029/2000jd900449, 2000.

Thibert, E., and Domine, F.: Thermodynamics and kinetics of the solid solution of HNO3 in ice, The Journal of Physical Chemistry B, 102, 4432-4439, 1998.

Thomas, E. R., van Wessem, J. M., Roberts, J., Isaksson, E., Schlosser, E., Fudge, T., Vallelonga, P., Medley, B., Bertler, N., and van de Broeke, M.: Review of regional Antarctic snow accumulation over the past 1000 years, Climate of the Past Discussion, 2017.

Traversi, R., Usoskin, I., Solanki, S., Becagli, S., Frezzotti, M., Severi, M., Stenni, B., and Udisti, R.: Nitrate in polar ice: a new tracer of solar variability, Solar Physics, 280, 237-254, 2012.

Turner, J., Phillips, T., Thamban, M., Rahaman, W., Marshall, G. J., Wille, J. D., Favier, V., Winton, H., Thomas, E., and Wang, Z.: The Dominant Role of Extreme Precipitation Events in Antarctic Snowfall Variability, Geophysical Research Letters, 2019.

Van Meijgaard, E., Van Ulft, L., Van de Berg, W., Bosveld, F., Van den Hurk, B., Lenderink, G., and Siebesma, A.: The KNMI regional atmospheric climate model RACMO version 2.1, Koninklijk Nederlands Meteorologisch Instituut, 43, 2008.

Wagenbach, D., Legrand, M., Fischer, H., Pichlmayer, F., and Wolff, E.: Atmospheric near-surface nitrate at coastal Antarctic sites, Journal of Geophysical Research: Atmospheres, 103, 11007-11020, 1998.

Warren, S. G.: Optical properties of snow, Reviews of Geophysics, 20, 67-89, 1982.

Weller, R., Minikin, A., König-Langlo, G., Schrems, O., Jones, A., Wolff, E., and Anderson, P.: Investigating possible causes of the observed diurnal variability in Antarctic NOy, Geophysical research letters, 26, 2853-2856, 1999.

Weller, R., Traufetter, F., Fischer, H., Oerter, H., Piel, C., and Miller, H.: Postdepositional losses of methane sulfonate, nitrate, and chloride at the European Project for Ice Coring in Antarctica deep-drilling site in Dronning Maud Land, Antarctica, Journal of Geophysical Research: Atmospheres, 109, 2004.

Weller, R., and Wagenbach, D.: Year-round chemical aerosol records in continental Antarctica obtained by automatic samplings, Tellus B: Chemical and Physical Meteorology, 59, 755-765, 2007.

Weller, R., Legrand, M., and Preunkert, S.: Size distribution and ionic composition of marine summer aerosol at the continental Antarctic site Kohnen, Atmospheric Chemistry and Physics, 18, 2413-2430, 2018.

Wilhelms, F., Miller, H., Gerasimoff, M. D., Drücker, C., Frenzel, A., Fritzsche, D., Grobe, H., Hansen, S. B., Hilmarsson, S. Æ., Hoffmann, G., Hörnby, K., Jaeschke, A., Jakobsdóttir, S. S., Juckschat, P., Karsten, A., Karsten, L., Kaufmann, P. R., Karlin, T., Kohlberg, E., Kleffel, G., Lambrecht, A., Lambrecht, A., Lawer, G., Schärmeli, I., Schmitt, J., Sheldon, S. G., Takata, M., Trenke, M., Twarloh, B., Valero-Delgado, F., and Wilhelms-Dick, D.: The EPICA Dronning Maud Land deep drilling operation, Annals of Glaciology, 55, 355-366, 10.3189/2014AoG68A189, 2017.

Winton, V. H. L. W., Caillon, N., Hauge, L., Mulvaney, R., Rix, J., Tuckwell, R., Savarino, J., and Frey, M.: Ice core chemistry, density, conductivity, dust, snow accumulation rate, and stable nitrate isotopic composition of the 120 m ISOL-ICE ice core, Dronning Maud Land, Antarctica (Version 1.0) [Data set], in, UK Polar Data Centre, Natural Environment Research Council, UK Research & Innovation. 10.5285/1467b446-54eb-45c1-8a31-f4af21e60e60, 2019a.

Winton, V. H. L. W., Frey, M., Hauge, L., Caillon, N., and Savarino, J.: Major ion chemistry and stable nitrate isotopic composition of aerosol, skin layer snow and snow pits at Dronning Maud Land, Antarctica (Version 1.0) [Data set], in, UK Polar Data Centre, Natural Environment Research Council, UK Research & Innovation. 10.5285/1467b446-54eb-45c1-8a31-f4af21e60e60, 2019b.

Wolff, E., Jones, A. E., Bauguitte, S.-B., and Salmon, R. A.: The interpretation of spikes and trends in concentration of nitrate in polar ice cores, based on evidence from snow and atmospheric measurements, Atmospheric Chemistry and Physics, 8, 5627-5634, 2008.

Wolff, E. W.: Nitrate in polar ice, in: Ice core studies of global biogeochemical cycles, Springer, 195-224, 1995.

Wolff, E. W., Jones, A. E., Martin, T. J., and Grenfell, T. C.: Modelling photochemical NOx production and nitrate loss in the upper snowpack of Antarctica, Geophysical Research Letters, 29, 5-1-5-4, 2002.

Yu, Z., and Elliott, E. M.: Novel method for nitrogen isotopic analysis of soil-emitted nitric oxide, Environmental science & technology, 51, 6268-6278, 2017.

Zatko, M., Geng, L., Alexander, B., Sofen, E., and Klein, K.: The impact of snow nitrate photolysis on boundary layer chemistry and the recycling and redistribution of reactive nitrogen across Antarctica and Greenland in a global chemical transport model, Atmos. Chem. Phys, 16, 2819-2842, 2016.

Zatko, M. C., Grenfell, T. C., Alexander, B., Doherty, S. J., Thomas, J. L., and Yang, X.: The influence of snow grain size and impurities on the vertical profiles of actinic flux and associated NO x emissions on the Antarctic and Greenland ice sheets, Atmospheric Chemistry and Physics, 13, 3547-3567, 2013.

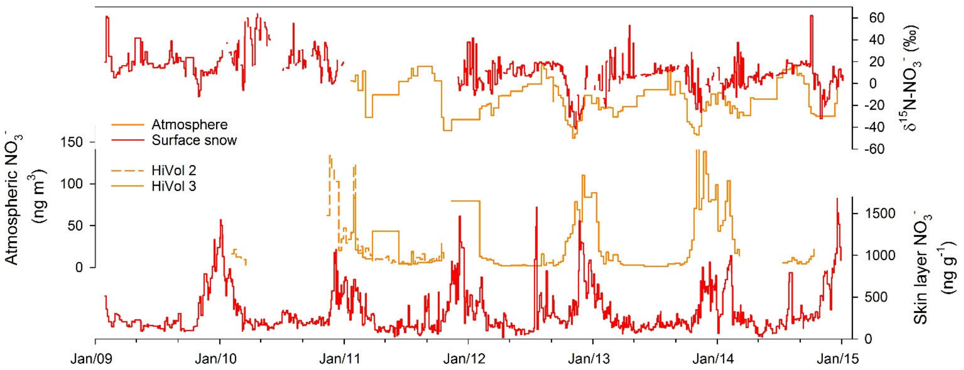

Figure 1: ~~Year round~~Year-round atmospheric and skin layer NO_3^- mass concentration and $\delta^{15}N\text{-}NO_3^-$ at Dome C. Two high-volume aerosol samplers were used at Dome C (HiVol 2 and HiVol 3) over the campaign and showed good reproducibility. Data source: years 2009-2010: Erbland et al. (2013); 2011-2015: this study.

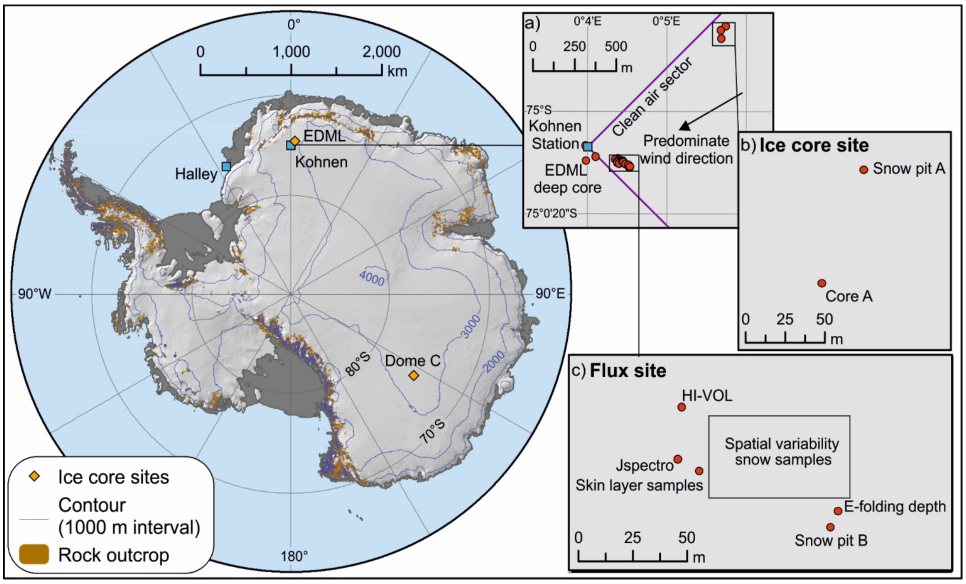

Figure 2: Map of ISOL-ICE ice core drilling and atmospheric campaign, and ice core sites and Antarctica stations mentioned in this study. a) Insert of Kohnen Station in Dronning Maud Land (DML) highlighting the predominate wind direction, deep EDML ice core site and the ISOL-ICE “ice core” (b) and “flux” ~~and~~ (c) ~~“ice cores”~~ sites. ~~;~~ b) ISOL-ICE “ice core site” showing ice core, firn core and snow pit A locations. ~~;~~ ~~and~~ c) ISOL-ICE “flux” site showing location of *in situ* atmospheric instruments, surface snow, snow pit and aerosol sampling locations and e-folding depth measurements.

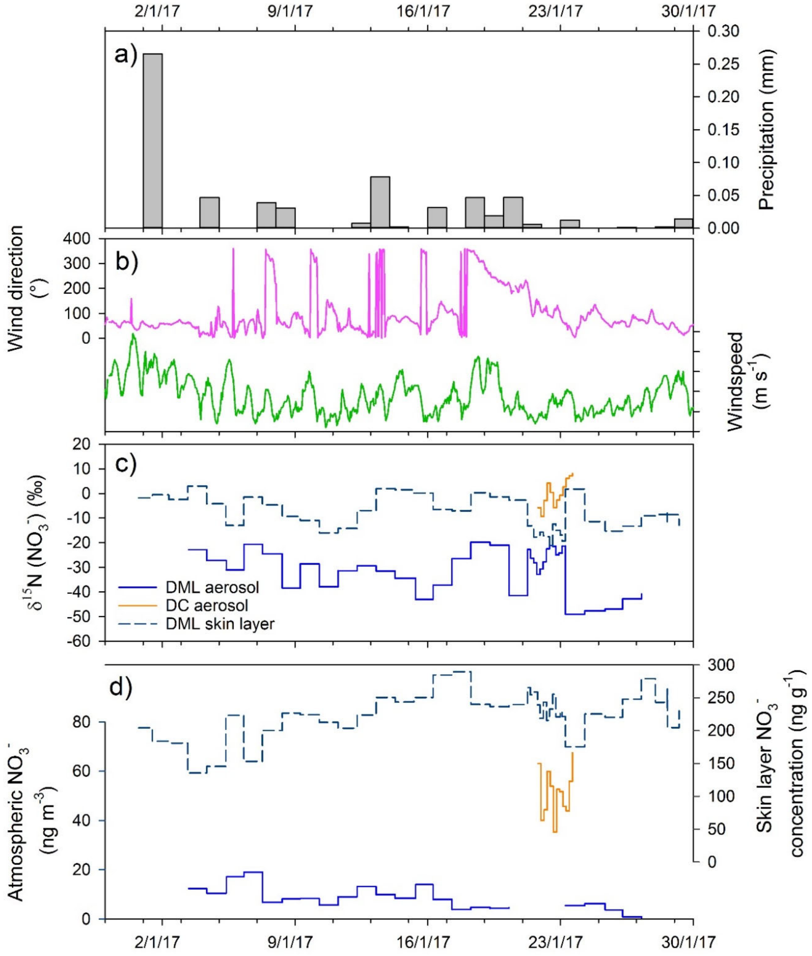
2/1/17
9/1/17
16/1/17
23/1/17
30/1/17
a)
Precipitation (mm)
0.30
0.25
0.20
0.15
0.10
0.05
0.00
b)
Wind direction (°)
400
300
200
100
0
Windspeed (m s^{-1})
c)
δ^{15}N (NO$_3^-$) (‰)
20
10
0
-10
-20
-30
-40
-50
-60
DML aerosol
DC aerosol
DML skin layer
d)
Atmospheric NO$_3^-$ (ng m^{-3})
80
60
40
20
0
Skin layer NO$_3^-$ concentration (ng g^{-1})
300
250
200
150
100
50
0

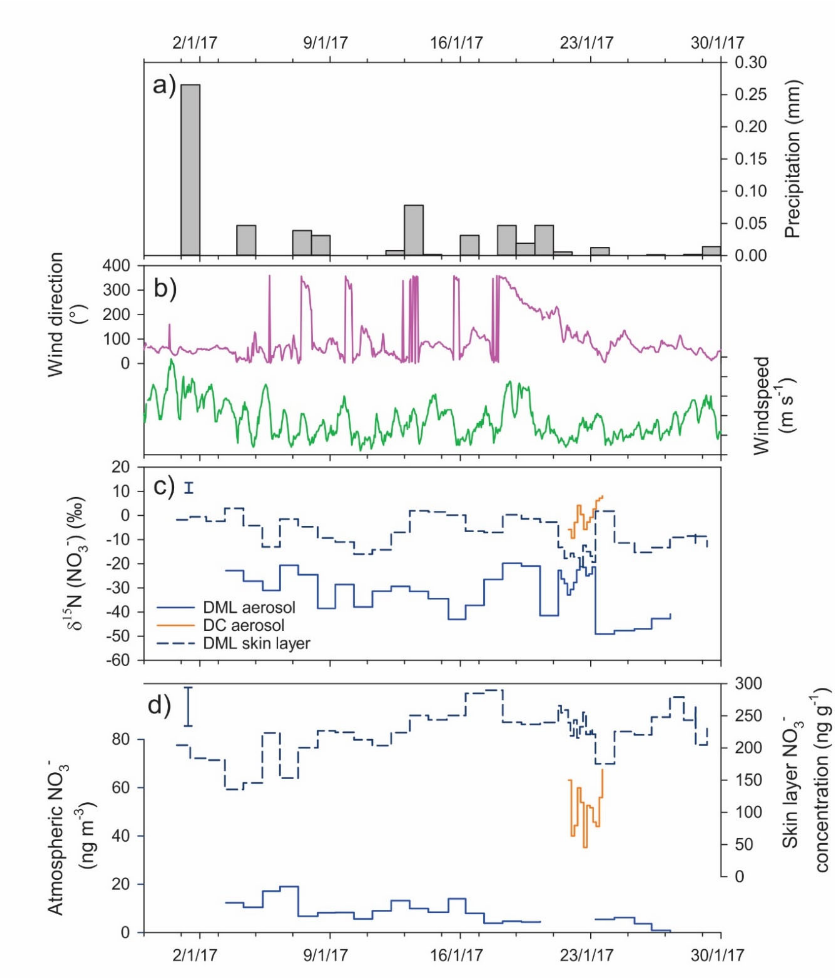

Figure 3: January 2017 time series in~~at~~ Dronning Maud Land (DML) of a) daily precipitation, b) hourly wind direction and wind speed, c) atmospheric and skin layer δ^{15}N-NO$_3^-$, and d) atmospheric and skin layer NO$_3^-$ mass concentration. Error bars in panels c-d indicate the spatial variability of the site determined by multiple skin layer samples collected on 28/01/2017. The spatial variability exceeds the instrumental error which is smaller than the symbol size. Meteorological data source: University of Utrecht (AWS9; DML05/Kohnen; 75°00'S, 00°00' E/W; ~2900 m.a.s.l.). Precipitation data source: RACMO2 (https://doi.org/10/c2pv).

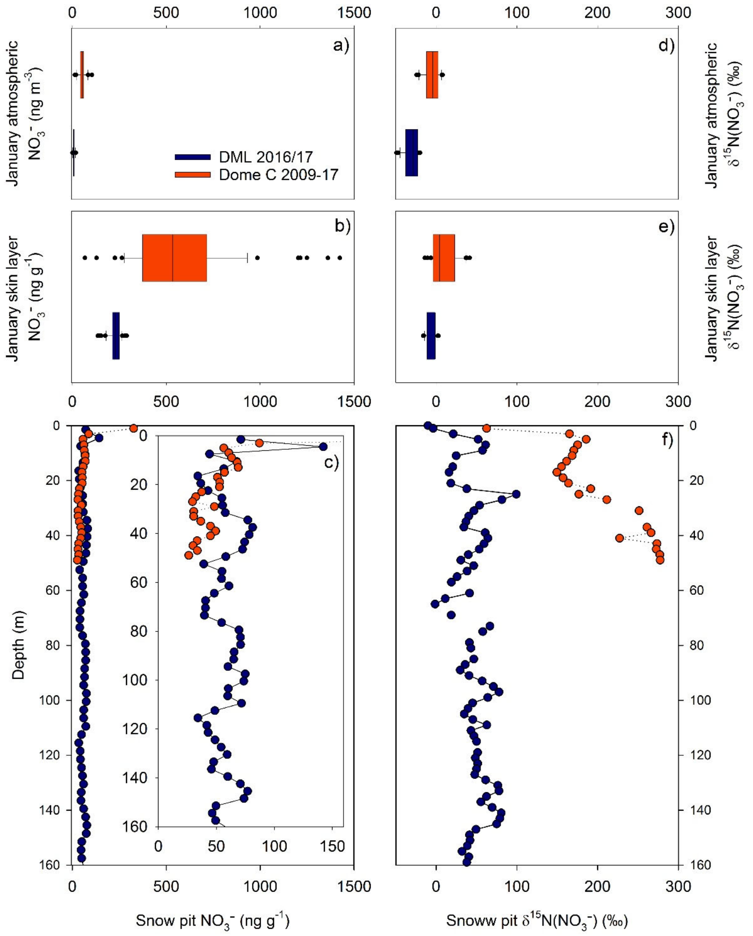
a)
b)
c)
d)
e)
f)
DML 2016/17
Dome C 2009-17
January atmospheric NO$_3^-$ (ng m^{-3})
January skin layer NO$_3^-$ (ng g^{-1})
January atmospheric δ^{15}N(NO$_3^-$) (‰)
January skin layer δ^{15}N(NO$_3^-$) (‰)
Depth (m)
Snow pit NO$_3^-$ (ng g^{-1})
Snoww pit δ^{15}N(NO$_3^-$) (‰)
0
500
1000
1500
0
100
200
300
0
20
40
60
80
100
120
140
160
0
50
100
150

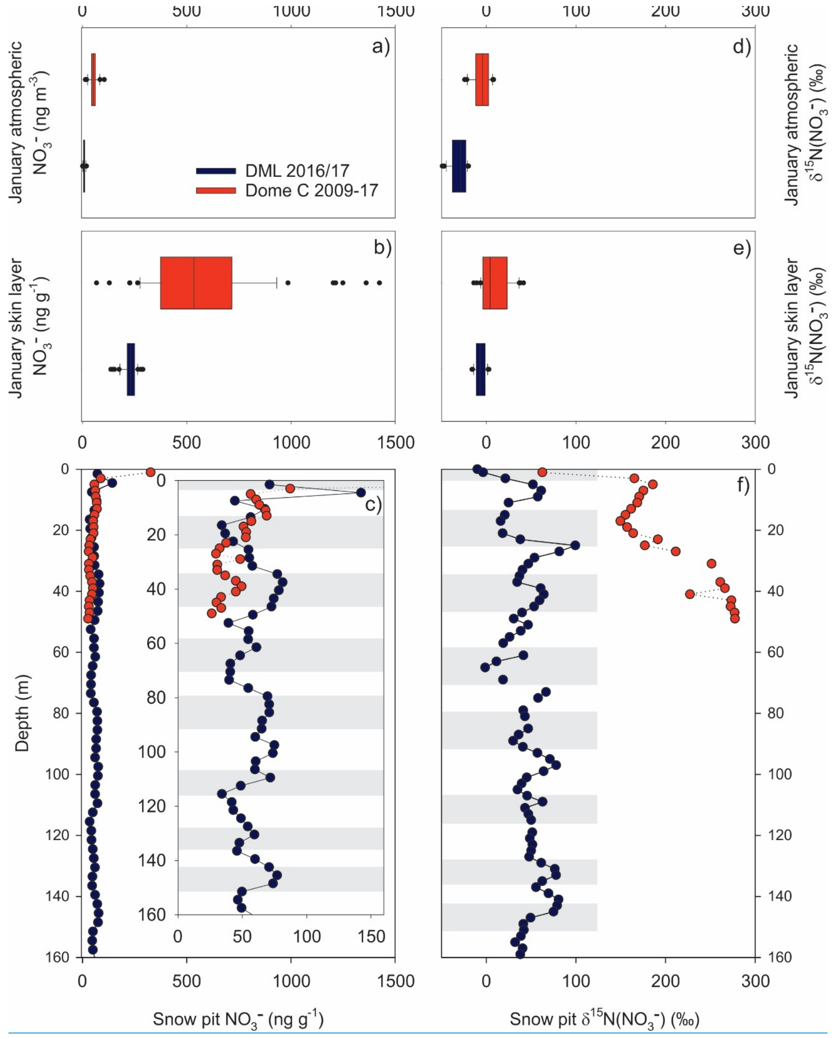

Figure 4: Comparison of NO$_3^-$ mass concentration and δ^{15}N-NO$_3^-$ at Dronning Maud Land (DML) and Dome C in January 2017. NO$_3^-$ mass concentration in a) atmosphere, b) skin layer, and c) depth profiles. Insert: Depth profile of NO$_3^-$ mass concentration highlighting seasonal variability. δ^{15}N-NO$_3^-$ in d) atmosphere, e) skin layer, and f) depth profiles. Grey bars indicate summer seasons for DML depth profiles.

Formatted: Not Superscript/ Subscript

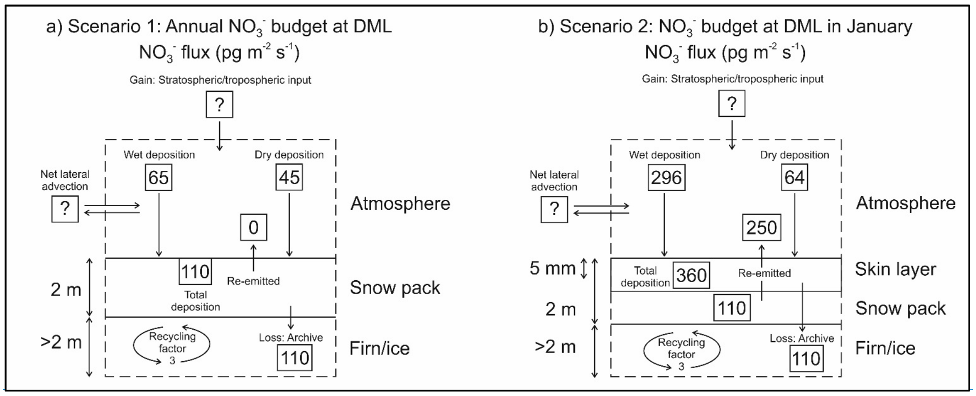

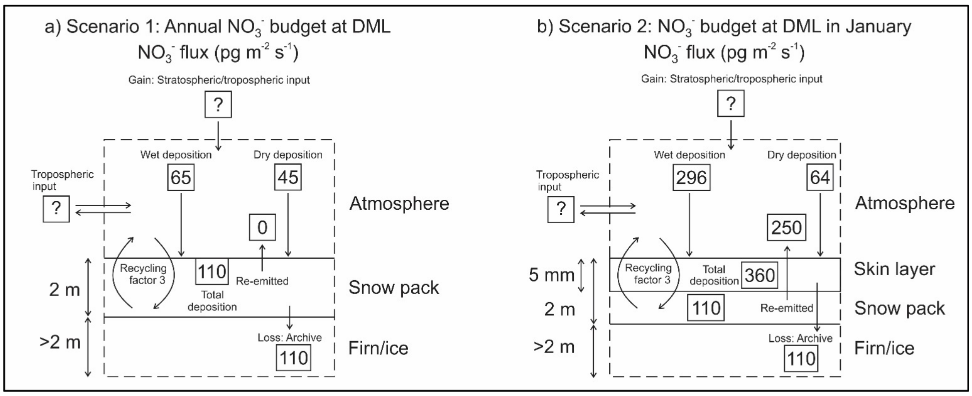

Figure 5: Schematic of NO_3^- mass fluxes at Dronning Maud Land (DML) for a) annual mean scenario and b) January scenario.

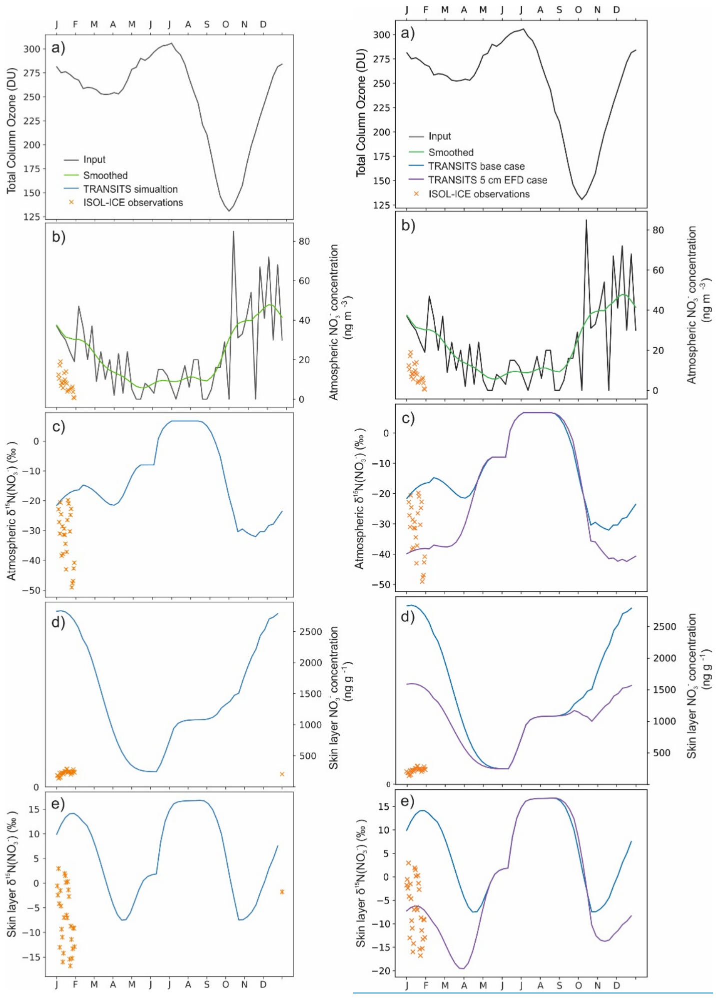

Figure 6: ISOL-ICE observations and simulated annual cycle of skin layer and atmospheric NO$_3^-$ mass concentration and δ^{15}N-NO$_3^-$ at Dronning Maud Land (DML) from the base case and 5 cm EFD case ~~the~~ TRANSITS model simulations for January 2017. a) Total column ozone: NIWA Bodeker combined dataset version 3.3 at DML averaged from 2000 to 2016 (http://www.bodekerscientific.com/data/total-column-ozone). b) Atmospheric NO$_3^-$ mass concentration~~ data~~s are observations from Kohnen Station (Weller and Wagenbach, 2007) that are used as input into the model. ISOL-ICE observations and TRANSI~~IS~~TS simulations of c) atmospheric δ^{15}N-NO$_3^-$, d) skin layer NO$_3^-$ mass concentration and e) skin layer δ^{15}N-NO$_3^-$.

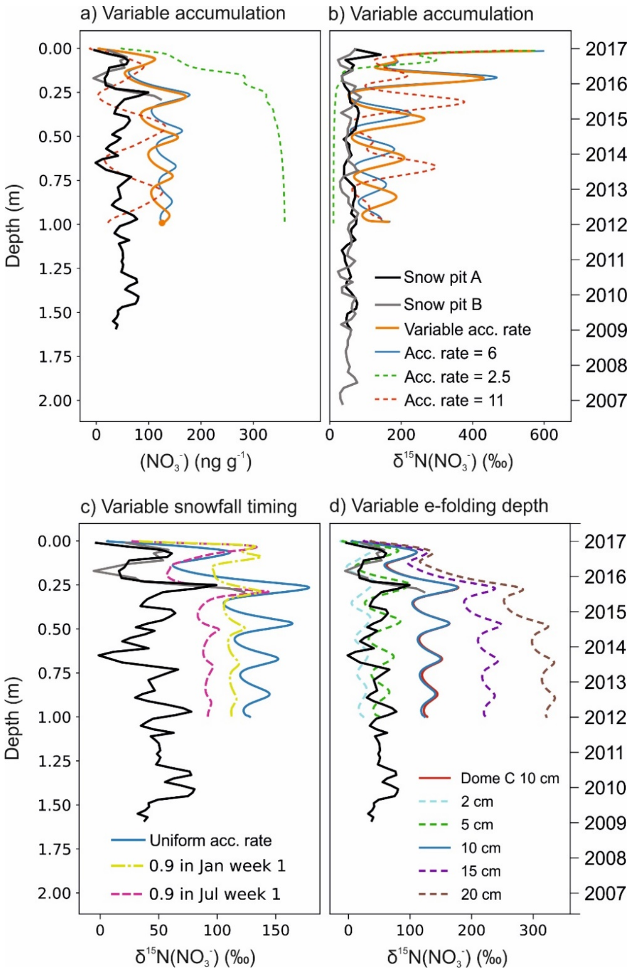
a) Variable accumulation
b) Variable accumulation
c) Variable snowfall timing
d) Variable e-folding depth
Depth (m)
0.00
0.25
0.50
0.75
1.00
1.25
1.50
1.75
2.00
0
100
200
300
(NO$_3^-$) (ng g^{-1})
0
200
400
600
δ^{15}N(NO$_3^-$) (‰)
2017
2016
2015
2014
2013
2012
2011
2010
2009
2008
2007
Snow pit A
Snow pit B
Variable acc. rate
Acc. rate = 6
Acc. rate = 2.5
Acc. rate = 11
0
50
100
150
Uniform acc. rate
0.9 in Jan week 1
0.9 in Jul week 1
Dome C 10 cm
2 cm
5 cm
10 cm
15 cm
20 cm
0
100
200
300

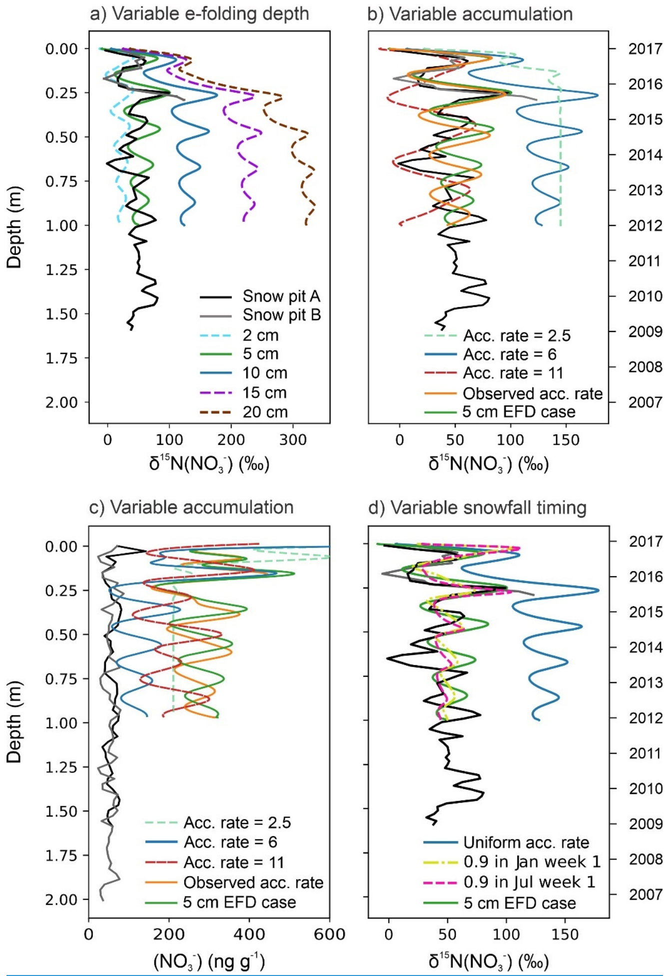

Figure 7: Snow pit depth profiles of observations and simulations from TRANSITS. ~~Sensitivity of~~ a) Sensitivity of δ^{15}N-NO$_3^-$ to the e-folding depth, b) Sensitivity of δ^{15}N-NO$_3^-$ and c~~b~~) sensitivity of NO$_3^-$ mass concentration to the upper and lower bounds of accumulation rates observed over the last thousand years at Dronning Maud Land (DML). Also shown are ~~our snow pit observations, and~~ the depth profiles of the simulated δ^{15}N-NO$_3^-$ values and NO$_3^-$ mass concentration using the observed accumulation rate in our snow pits, i.e., variable accumulation rate with depth (orange line). The observed snow accumulation rate from the snow pits varied between 3.5 and 7.1 cm yr^{-1} (w.e.). ~~Sensitivity of~~ d~~e~~) Sensitivity of δ^{15}N-NO$_3^-$ to the timing of snow accumulation~~, d) δ^{15}N-NO$_3^-$ to the~~

Formatted: Not Highlight

Formatted: Not Highlight

Formatted: Not Highlight

Formatted: Not Highlight

~~e-folding depth~~. In each panel, b~~B~~lue is the base case simulation, and green is the 5 cm EFD case simulation, which ~~in which~~ we refer to throughout the study. Note that ~~panels a-b) have the same legend, and~~ the nominal date refers to the base case simulation.

Formatted: Not Highlight

Formatted: Not Highlight

Formatted: Not Highlight

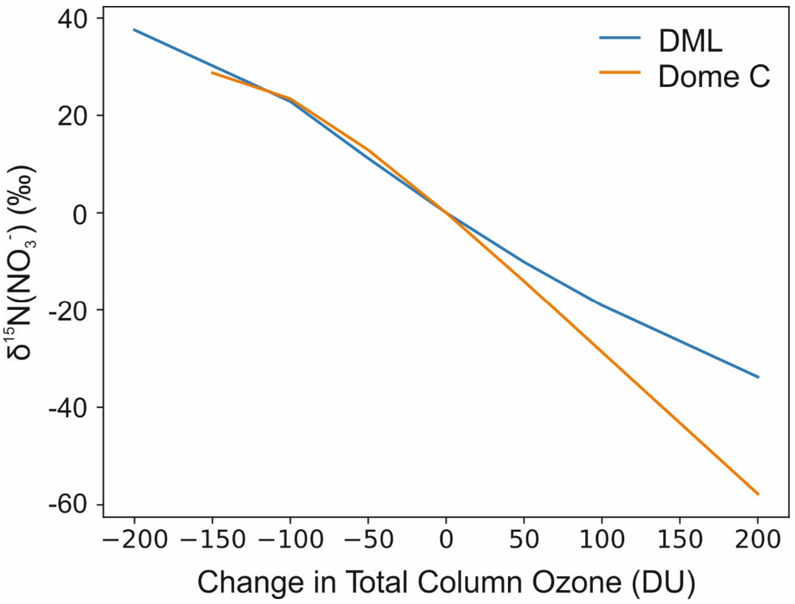

Formatted: Centered

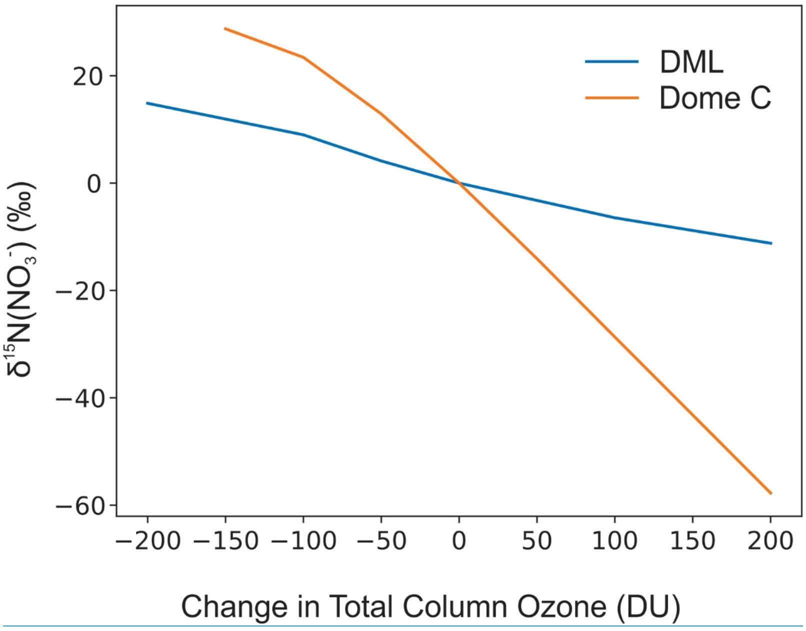

Figure 8: Expected response of archived $\delta^{15}N-NO_3^-$ to changes in total column ozone at Dronning Maud Land (DML) and Dome C. Calculated sensitives represent an upper range as the real ozone hole lasts September to November before recovery, and not as modelled using the entire sunlit season. Archived DML $\delta^{15}N-NO_3^-$ values were simulated using the observed~~a fixed~~ accumulation rate ~~of 6 cm yr^{-1} (w.e.),~~ ~~and~~ e-folding depth of ~~10~~ 5 cm (5 cm, EFD case), and present day TCO values. These TCO values, that were used in all our calculations, vary weekly and can be found in Table S3. For each week, a constant amount of ozone (e.g. 100 DU) was added or subtracted from these present day values. Dome C data source: Erbland et al. (2015).

Formatted: Not Highlight

Table 1: Site characteristics of Dronning Maud Land (DML) and Dome C ice core sites.

	DML	Dome C
Latitude (°S)	75	75
Elevation (m a.s.l.)	2892	3233
Distance from the coast (km)	550	900
Mean snow accumulation (cm y^{-1}; w.e.)	[1]6	[2]2.5
Predominate wind direction (°)	45	180-200
Mean summer temperature (°C)	[3]-28	[4]-30
Annual mean temperature (° C)	[3]-41	[4]-52
Maximum summer temperature (°C)	[3]-9	[4]-17
Minimum winter temperature (°C)	[3]-74	[4]-80
e-folding depth (cm)	[4]~~[3]~~2-5	~~[4]10~~[6]10-20
Average January nitrate mass concentration in skin layer (ng g^{-1})	[4]~~[3]~~230	~~[3]600~~[5]600
Average annual nitrate mass concentration in firn (ng g^{-1})	[4]~~[3]~~60	~~[5]50~~[7]50
Average January nitrate mass concentration in atmosphere (ng m^{-3})	[4]~~[3]~~10	~~[3]60~~[5]60

[1] Sommer et al. (2000);Hofstede et al. (2004)

[2] Le Meur et al. (2018)

[3] University of Utrecht (AWS9; DML05/Kohnen)

[4] Erbland et al. (2013)

[5] This study

~~[4]France et al. (2011)~~[6]France et al. (2011)

~~[5]Frey et al. (2009)~~[7]Frey et al. (2009)

Formatted: Superscript

Formatted: Superscript

Formatted: Font: Bold

Formatted: Superscript

Table 2: Summary of observed and simulated archived, aerosol and skin layer NO_3^- mass concentrations,~~ and~~ $\delta^{15}N$-NO_3^- composition and NO_3^- mass fluxes at Dronning Maud Land (DML) and Dome C. n.d.: no data. Base case refers to the TRANSITS simulation with a snow accumulation rate of 6 cm yr^{-1} (w.e.) and an e-folding depth of 10 cm, while the 5 cm EFD case refers to a TRANSITS simulation with an observed snow accumulation rate that varied year to year between 6.0 and 7.1 cm yr^{-1} (w.e.) and an e-folding depth of 5 cm.

Archived (≥~~<~~30 cm)	**NO_3^- (ng g^{-1})**	**$\delta^{15}N$-NO_3^- (‰)**	**Flux (pg m^{-2} s^{-1})**	**Reference**
DML Pit A	60	50	110	This study
DML Pit B	50	n.d.	120	This study
DML TRANSITS (base case)	120	130	210	This study
DML TRANSITS (5 cm EFD case)	280	50	480	This study
*DML expected	100	100	140	Erbland et al. (2015);Erbland et al. (2013)
Dome C	50	280	<140	Erbland et al. (2013)
Aerosol (January mean)	**NO_3^- (ng m^{-2})**	**$\delta^{15}N$-NO_3^- (‰)**	**Flux (pg m^{-2} s^{-1})**	**Reference**
DML	10	-30	70	This study
DML TRANSITS (base case)	30	-20	190	This study; Weller and Wagenbach (2007)
DML TRANSITS (5 cm EFD case)	30	-40	50	This study; Weller and Wagenbach (2007)
Dome C	60	-10	90	This study; Erbland et al. (2013)
Skin layer (January mean)	**NO_3^- (ng g^{-1})**	**$\delta^{15}N$-NO_3^- (‰)**	**Flux (pg m^{-2} s^{-1})**	**Reference**
DML	230	-10	360	This study
DML TRANSITS (base case)	2800	10	4800	This study
DML TRANSITS (5 cm EFD case)	1650	-10	2900	This study
Dome C	590	10	470	This study; Erbland et al. (2013)

*Expected values for a site with an accumulation rate of 6 cm yr^{-1} (w.e.) based on the spatial transect of Erbland et al. (2015).

Formatted: Not Superscript/ Subscript

Formatted: Superscript

Formatted: Not Highlight

Formatted: Not Highlight

Field Code Changed

Field Code Changed

Field Code Changed

Formatted: Not Highlight

Formatted: Not Highlight

Formatted: Not Highlight

Formatted: Not Highlight